

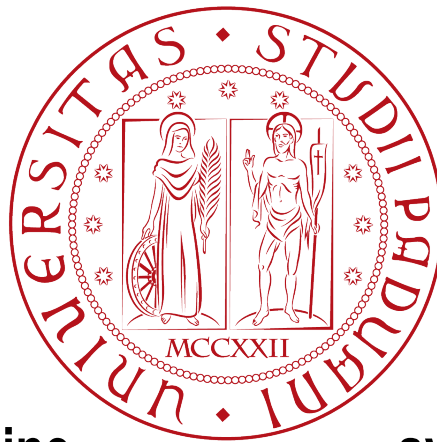
UNIVERSITA' DEGLI STUDI DI PADOVA

DIPARTIMENTO DI INGEGNERIA

DELL'INFORMAZIONE

CORSO DI LAUREA IN BIOINGEGNERIA

Tesi di Laurea Magistrale



A new telemedicine

system for Chronic

Obstructive Pulmonary Disease:

validation of the sensing wearable framework

RELATORE:

Prof. Giovanni Sparacino

CORRELATORI:

Prof. Raffele Dellacà

Ing. Leonardo Govoni

Ing. Roberto Rosso

LAUREANDA:

Francesca Peroli

A. A. 2010/2011

Ai miei genitori

Table of contents

Summary	1
Sommario	3
Introduction	5
Chapter 1: The respiratory system: anatomy, physiology and pathologies	7
1.1 Anatomy and physiology of the respiratory system	7
1.1.1 Structure of lungs	7
1.1.1.1 Blood-gas interface and airways	7
1.1.1.2 Blood vessels and flow	9
1.1.2 Pulmonary ventilation.....	13
1.1.3 Air transportation and diffusion.....	18
1.1.4 Mechanics of breathing.....	25
1.2 The Chronic Obstructive Pulmonary Disease	30
1.2.1 Diagnosis	31
1.2.2 Symptoms	32
1.2.3 Epidemiology, risk factors and natural history of COPD	34
1.2.4 Management of COPD	35
1.3 Measurements techniques for the parameters of the respiratory system	37
1.3.1 Pneumotachograph	37
1.3.2 Respiratory inductive plethysmography	41
1.3.3 Opto-Electronic Plethysmography.....	44
Chapter 2: Telemedicine for monitoring COPD patients	48
2.1 State of the art	48
2.2 Chronious: a new system for COPD patients	53
2.2.1 General description	53
2.2.2 Wearable platform	57
2.2.3 External devices	60
Chapter 3: Pre-testing phase	63
3.1 Experimental setup	63
3.2 Experimental protocol	68

3.3 Data analysis	69
3.3.1 Method 1.....	70
3.3.2 Method 2.....	73
3.4 Results	76
Chapter 4: Validation on healthy subjects	85
4.1 Experimental setup	85
4.2 Experimental protocol	88
4.3 Data analysis	89
4.3.1 Method 1.....	89
4.3.2 Method 2.....	90
4.4 Results	93
Chapter 5: Validation on COPD patients	101
5.1 Experimental setup	101
5.2 Experimental protocol	104
5.3 Data analysis	105
5.3.1 Method 1.....	105
5.3.2 Method 2.....	106
5.4 Results	109
Conclusion and future developments	119
Appendix A	122
Appendix B	141
Appendix C	159
References	171
Ringraziamenti	173

Summary

The work of this thesis is focused on the validation of the wearable framework of the Chronious platform. Chronious is a FP7 European Community project which works on an innovative system with intelligent sensors and decision support system for patients and healthcare professionals in the area of chronic diseases. For testing purposes, it focuses on the Chronic Obstructive Pulmonary Disease (COPD), but the aim is to create an easily adapted system to other chronic diseases requirements. COPD seems to be the most problematic chronic disease for the health systems, with frequent exacerbations, hospitalizations and related costs. The number of people suffering from this diseases is rising and telemedicine is a possible solution to ensure quality and cost containment. The principal reason for using remote monitoring is to identify COPD exacerbations at a point in which it might be possible to intervene successfully.

The Chronious system collected data by using intelligent sensors, mostly wearable, that control continuously patients' physiological parameters, context and environmental variables and patient motion and other activities such as drug intake and dietary habits. The system will assist health care experts and patients by providing tools for health status monitoring and decision support. The continue monitoring of many parameters, and most importantly, the generation of alarms if a potential health risks or abnormal behavior is detected makes Chronious a promising platform for the management of the chronic diseases.

The aim of this work is to develop and test the wearable system of the Chronious platform in order to improve physiological parameters acquisition on COPD patients.

The work has been developed in three successive phases characterized by the use of different hardware and software devices.

The first chapter provides a description of anatomy and physiology of the respiratory system, and of the pathophysiology of the Chronic Obstructive Pulmonary Disease (COPD). Moreover, three measurements techniques of pulmonary ventilation are described: the pneumotachograph (PNT), the respiratory inductive plethysmography (RIP) and the Opto-electronic Plethysmography (OEP).

The second chapter is an introduction of the telemedicine services for patients affected by COPD and it is described the Chronious project, a new approach for managing COPD patients at their home.

In chapter three is presented the pre-testing phase of the project in which a first prototype of the wearable device has been assembled and evaluated on five healthy subjects. This phase allowed us to develop the procedures and functions to compute the calibration of the RIP and to test the wearable system. We suggested some improvements on the hardware and we studied some design changes of the shirt in order to improve signals' quality both of the RIP and the ECG. These improvements have been introduced and a new prototype of the wearable system has been produced.

In chapter four is presented a project phase in which the new prototype have been tested on four healthy subjects in order to prepare the set-up for the clinical validation on COPD patients. Finally, in chapter five is presented the phase of the project in which the Chronious Wearable framework has been tested on nine COPD patients. In this experimental activity the accuracy of the wearable system was tested including the respiratory parameters, the pulseoximeter and the ambient temperature and humidity sensors. The measures acquired by the wearable system was compared with those acquired by gold standard devices.

These experimental activities allowed us to improve the system and the clinical validation shown that the wearable system produces reliable signals concerning the RIP and the pulseoximeter. Concerning the ambient temperature and humidity sensors we found that some improvements are still necessities.

Sommario

L'obiettivo di questa tesi consiste nella validazione del sistema indossabile del progetto Chronious. Chronious è un progetto europeo nell'ambito del 7° Programma Quadro (FP7) composto da un sistema di sensori e sistemi decisionali a supporto dei pazienti e dei clinici nel trattamento delle malattie croniche. L'obiettivo del progetto è di realizzare un sistema che sia adatto per qualsiasi malattia cronica, ma per il momento si occupa principalmente del trattamento della Bronco Pneumopatia Cronica Ostruttiva (BPCO). La BPCO sembra essere la malattia cronica più problematica per il sistema sanitario, in quanto prevede frequenti riacutizzazioni, ospedalizzazioni e alti costi. Il numero di persone che soffre di questa malattia è in aumento e la telemedicina è una possibile soluzione per assicurare una qualità migliore della cura e contenere i costi.

Chronious, infatti, sviluppa un sistema a supporto del clinico per il monitoraggio di pazienti cronici attraverso sensori, indossabili o dislocati nell'abitazione, e servizi rivolti sia al paziente stesso sia al personale medico, come supporto all'assistenza e alla cura. Inoltre, il sistema assiste il personale medico e il paziente con un monitoraggio continuo dello stato di salute e un sistema di supporto decisionale, che si basa su linee guida mediche riconosciute a livello internazionale e sulle ontologie. Il continuo monitoraggio di tanti parametri, ma più importante la generazione di allarmi, se un evento anomalo viene rilevato, rende chronious una piattaforma importante per la gestione delle malattie croniche.

L'obiettivo di questo lavoro consiste nello sviluppare e testare il sistema indossabile del progetto Chronious al fine di migliorare i parametri fisiologici acquisiti sui pazienti affetti di BPCO.

Il lavoro è stato svolto in tre successive fasi caratterizzate dall'uso di diversi strumenti hardware e software.

Il primo capitolo contiene la descrizione dell'anatomia e fisiologia del sistema respiratorio, e la fisiopatologia della Bronco Pneumopatia Cronica Ostruttiva (BPCO). Infine, sono descritte tre tecniche di misura della meccanica respiratoria: il pneumotacografo (PNT), la pletismografia respiratoria induttiva (RIP) e la pletismografia opto-elettronica (OEP).

Nel secondo capitolo sono descritti i servizi di telemedicina rivolti ai pazienti affetti da BPCO e viene presentato il progetto Chronious, un nuovo approccio per il trattamento dei pazienti affetti da BPCO a casa loro.

Nel terzo capitolo viene presentata la fase di pre-test del progetto, in cui il primo prototipo del sistema indossabile è stato assemblato e valutato. Questa attività sperimentale ci ha permesso di sviluppare le procedure di calibrazione delle bande respiratorie (RIP) e di testare il sistema indossabile.

Il capitolo quattro descrive la fase di progetto in cui sono stati apportati nuovi miglioramenti al sistema e sono stati testati su quattro soggetti sani, l'obiettivo era di preparare il set up per la successiva fase sperimentale. Infine, nel quinto capitolo viene presentata la fase di progetto in cui il sistema indossabile è stato testato su nove pazienti affetti da BPCO. In questa attività sperimentale l'accuratezza del sistema indossabile è stata testata per quanto riguarda i parametri respiratori, il pulsossimetro e il sensore per il rilevamento della temperatura ambiente e dell'umidità. Le misure acquisite dal sistema indossabile sono state confrontate con quelle acquisite da dispositivi di riferimento.

Queste attività sperimentali ci hanno permesso di migliorare il sistema e la validazione clinica ha dimostrato che il sistema Chronious produce segnali affidabili per quanto riguarda le bande respiratorie e il pulsossimetro. Invece, per quanto riguarda il sensore di temperatura ambiente e di umidità sono necessari altri miglioramenti.

Introduction

Telemedicine is the use of information and communication technologies to provide and support healthcare when distance separates two subjects, typically a patient and the caregiver or two caregivers. Diagnosis, interventions, and treatment decisions are based on information transmitted through telecommunication technologies^[13]. The number of people suffering from chronic diseases is rising and so are the costs for their care; telemedicine is a possible solution to ensure quality and cost containment. In particular, the chronic obstructive pulmonary disease (COPD) is an important but under-recognized cause of morbidity and mortality worldwide: it has been estimated that in 2020 COPD will move from the sixth to the third most common cause of death worldwide, while rising from fourth to third in terms of morbidity in the same time-frame. COPD is characterized by chronic airflow limitation and a range of pathological changes in the lung, some significant extra-pulmonary effects, and important co-morbidities, which may contribute to the severity of the disease in individual patients. COPD is usually a progressive disease but it has variable natural history and not all individuals follow the same clinical course over time^[17]. COPD seems to be the most problematic chronic disease for the health systems, with frequent exacerbations, hospitalizations and related costs. The principal reason for using remote monitoring is to identify COPD exacerbations at a point in which it might be possible to intervene successfully, that is, to reduce the risk of hospital admission by using appropriate therapy as soon as possible. Furthermore, the need to rationalize healthcare costs has prompted the development of new technologies for home assistance.

CHRONIOUS - An Open, Ubiquitous and Adaptive Chronic Disease Management Platform for COPD and Renal Insufficiency is a FP7 European Community project which developed an innovative system with intelligent sensors and decision support systems for patients and healthcare professionals in the area of chronic diseases. This platform is focused to realize simple, customized and adaptive interfaces that take into account the user's profile, medical history and relating HCI (human-computer interaction) factors. The system integrates state of the art sensors and services. The intention is covering both patients and healthcare professional's needs in the area of chronic diseases. Data is collected by using intelligent sensors, mostly wearable, that control continuously patients' physiological parameters, context and environmental variables and patient motion and

other activities such as drug intake and dietary habits. The system will assist health care experts and patients by providing tools for health status monitoring and decision support. The continue monitoring of many parameters, and most importantly, the generation of alarms if a potential health risks or abnormal behavior is detected makes Chronious a promising platform for the management of the chronic diseases. The Chronious objectives are very innovative taking into account the current state of the art in monitoring Chronic Obstructive Pulmonary Disease (COPD) patients. Chronious suggests the implementation of generic system architecture to be easily adapted to any chronic disease management program. For testing purposes, it focuses on COPD, but the aim is to create an easily adapted system to other chronic diseases requirements.

The work of this thesis is focused on the validation of the wearable framework of the Chronious platform. Three phases of test are performed to assess accuracy and reliability of the whole wearable platform. In particular, the thesis is focused on respiration and the devices used to collect respiratory parameters.

The wearable system of the Chronious project is composed of a shirt made of washable stretch-material into which are sewn several sensors: two-respiratory bands (RIP), 4 ECG electrodes, a reflectance pulseoximeter, a sensor for the skin temperature and a sensor for the ambient temperature and humidity. All sensors are connected to the Data Handler (DH), a microcontroller-based acquisition system devoted to data collection able to send acquired data to a PDA via a Bluetooth wireless connection.

The two respiratory bands (RIP) inserted in the shirt allow to measure non-invasively the thoracic and the abdominal volume displacement signals; but these data are not calibrated. One of the main objectives of this thesis are the development and validation of appropriate procedures and functions to compute the calibration of the RIP. In order to achieve these objectives we developed and implemented the algorithms that performed the calibration procedure and performed the testing on the data collected during several experimental sessions. The experimental activities were conducted on healthy subjects at the Biomedical Engineering Department of the Politecnico di Milano and on COPD patients during ambulatory visits at the University Hospital of Careggi – Firenze, Dipartimento di Fisiopatologia Toracica. Furthermore, in part of the experimental activities we also tested the reliability and the accuracy of the electrocardiographic signals, the pulseoximeter and the ambient temperature and humidity sensors.

Chapter 1

The respiratory system: anatomy, physiology and pathologies

This chapter contains the description of anatomy and physiology of the respiratory system. It presents also the pathophysiology of the Chronic Obstructive Pulmonary Disease (COPD). Lastly three measurements techniques of pulmonary ventilation are described.

1.1 Anatomy and physiology of the respiratory system

The goals of respiration are to provide oxygen to the tissue and to remove carbon dioxide. To achieve these goals, respiration can be divided into four major topics: (1) *structure of lungs*, how the architecture of the lung subserves its functions; (2) *ventilation*, how gas gets to the alveoli; (3) *diffusion*, how gases are exchanged within blood; and (4) *mechanics of breathing*, how the lungs are supported and move.

1.1.1 Structure of lungs

The lung is for gas exchange; its prime function is to allow oxygen to move from the air into the venous blood and carbon dioxide to move in the opposite direction. The lung also metabolizes some compounds, filter toxic materials from the circulation, and acts as a reservoir for blood. But its cardinal function is to exchange gas.

1.1.1.1 Blood-gas interface and airways

Oxygen and carbon dioxide move between air and blood by simple diffusion, that is, from an area of high to low partial pressure, much as water runs downhill. Fick's law of diffusion states that the amount of gas that moves across a sheet of tissue is proportional to the area of the sheet but inversely proportional to its thickness. The blood-gas barrier is exceedingly thin and has an area of between 50 and 100 square meters. It is therefore well suited to its function of gas exchange.

It's possible to obtain such a prodigious surface area for diffusion inside the limited thoracic cavity because the small blood vessels (capillaries) are wrapping around an enormous number of small air sacs called *alveoli*.

Gas is brought to one side of the blood-gas interface by airways and blood to the other side by blood vessels.

The airways consist of a series of branching tubes which become narrower, shorter, and more numerous as they penetrate deeper into the lung (Figure 1.1).

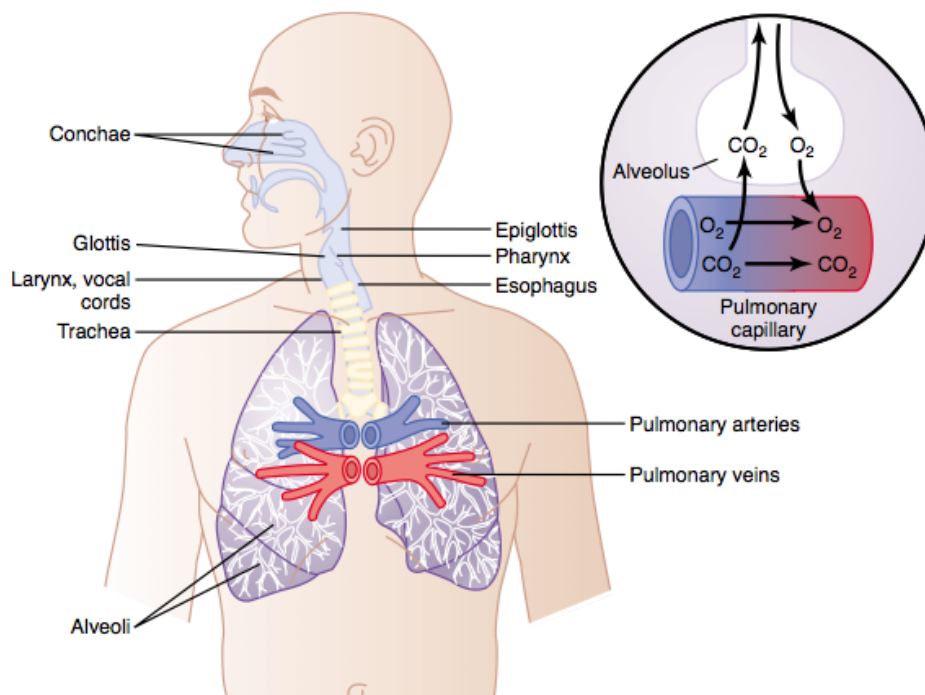


Figure 1.1: Respiratory passages, the air is distributed to the lungs by way of the trachea, bronchi, and bronchioles [1].

The *trachea* divides into right and left main bronchi, which in turn divide into lobar, then segmental bronchi. This process continues down to the *terminal bronchioles*, which are the smallest airways without alveoli. All these bronchi make up the conducting airways. Their function is to lead inspired air to the gas exchanging regions of the lung (Figure 1.2). Since the conducting airways contain no alveoli and therefore take no part in gas exchange, they constitute the *anatomic dead space*; its volume is about 150 ml.

The terminal bronchioles divide into respiratory bronchioles, which have occasional alveoli budding from their walls. Finally, we come to the *alveolar ducts*, which are completely lined with alveoli. This alveolated region of the lung where the gas exchange occurs is known as the

respiratory zone. The portion of lung distal to a terminal bronchiole forms an anatomical unit called the *acinus* or *lobule* ^[3].

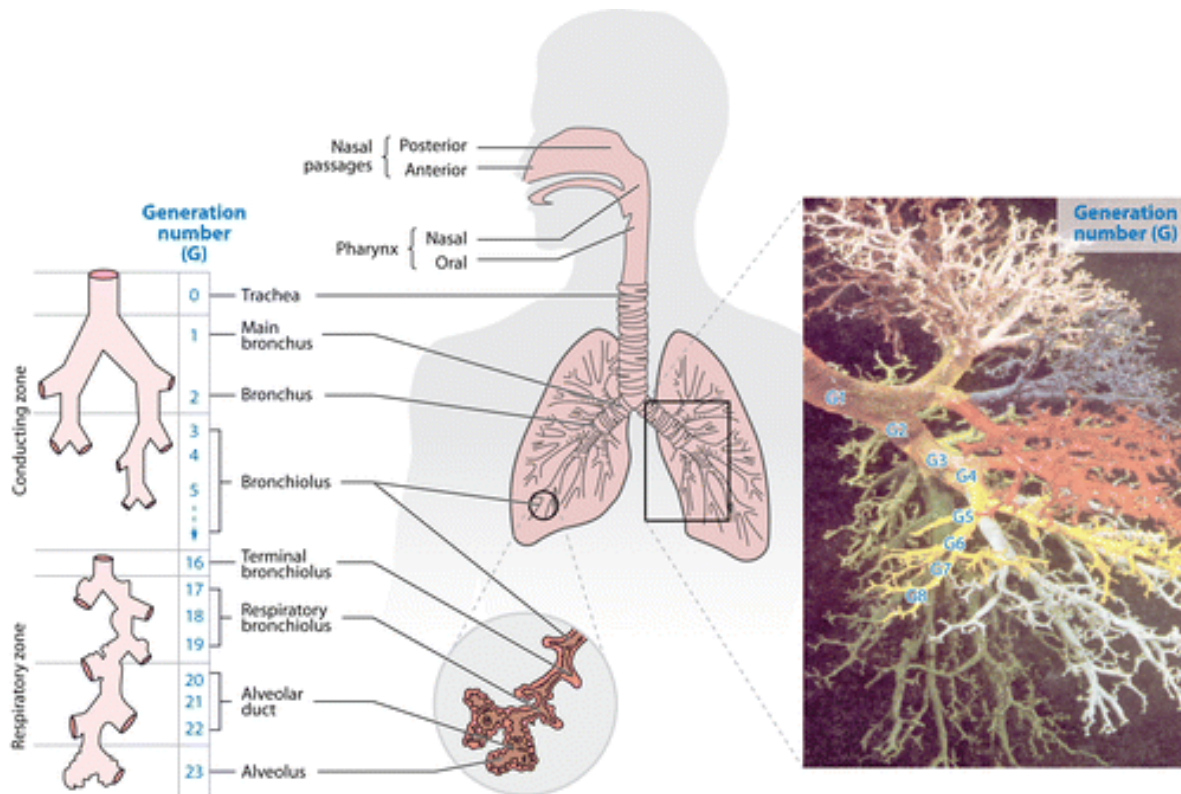


Figure 1.2: Idealization of the human airways according to Weibel ^[2]

1.1.1.2 Blood vessels and flow

The pulmonary blood vessels form a series of branching tubes from the pulmonary artery to the capillaries and back to the pulmonary veins. Initially, the arteries, veins, and bronchi run close together, but toward the periphery of the lung, the veins move away to pass between the lobules, whereas the arteries and bronchi travel together down the centers of the lobules. The capillaries form a dense network in the walls of the alveoli. The diameter of a capillary segment is about 10 μm , just large enough for a red blood cell. The lengths of the segments are so short that the dense network forms an almost continuous sheet of blood in the alveolar wall, a very efficient arrangement for gas exchange.

The pulmonary circulation begins at the main pulmonary artery, which receives the mixed venous blood pumped by the right ventricle. This artery then branches the system of airways and the blood is oxygenated. Successively, this blood is collected from the capillary bed by the small pulmonary

veins, which drain in the left atrium. The pressures in the pulmonary circulation are remarkably low. The mean pressure in the main pulmonary artery is only about 15mmHg; the systolic and diastolic pressures are about 25 and 8mmHg, respectively (Figure 1.3). The pressure is therefore very pulsatile. By contrast, the mean pressure in the aorta is about 100mmHg – about six times more than in the pulmonary artery. The pressures in the right and left atriums are not very dissimilar – about 2 and 5mmHg, respectively. Thus, the pressure differences from inlet to outlet of the pulmonary and systemic systems are about $(15 - 5) = 10\text{mmHg}$ and $(100 - 2) = 98\text{mmHg}$, respectively.

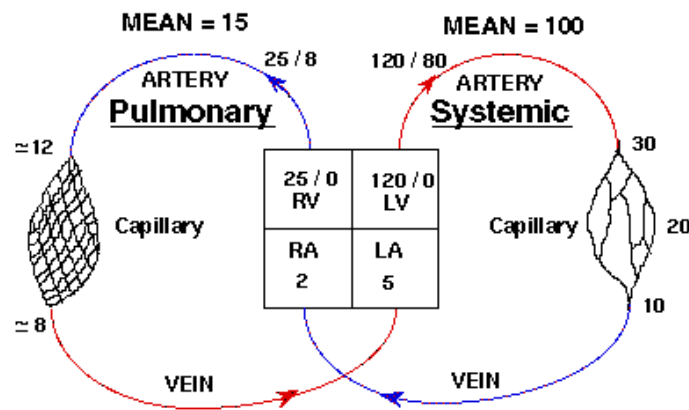


Figure 1.3: Comparison of pressures (mmHg) in the pulmonary and systemic circulations^[3].

In keeping with these low pressures, the walls of the pulmonary artery and its branches are remarkably thin and contain relatively little smooth muscle. This is in striking contrast to the systemic circulation where the arteries generally have thick walls, and the arterioles in particular have abundant smooth muscle. The reasons for these differences lie in the functions of the two circulations. The systemic circulation regulates the supply of blood to various organs, including those, which may be far above the level of the heart. By contrast, the lung is required to accept the whole of the cardiac output at all times.

The pressure within the pulmonary capillaries is uncertain. The pulmonary capillaries are unique in that they are virtually surrounded by gas. There is a very thin layer of epithelial cells lining the alveoli, but the capillaries receive little support from this and, consequently, they are liable to collapse or distend, depending on the pressures within and around them. The latter is very close to alveolar pressure. Under some special conditions, the effective pressure around the capillaries is reduced by the surface tension of the fluid lining the alveoli. But usually, the effective pressure is

alveolar pressure, and when this rises above the pressure inside the capillaries, they collapse. The pressure difference between the inside and outside of the vessels is often called the *transmural pressure*.

Instead, the pressure around the pulmonary arteries and veins is considerably less than alveolar pressure. As the lung expands, these larger blood vessels are pulled open by the radial traction of the elastic lung parenchyma, which surrounds them. Consequently, the effective pressure around them is low; in fact there is some evidence that this pressure is even less than the pressure around the whole lung (*intrapleural pressure*).

The behavior of the capillaries and the larger blood vessels is so different they are often referred to as *alveolar* and *extra-alveolar* vessels. Alveolar vessels are exposed to alveolar pressure and include the capillaries and the slightly larger vessels in the corners of the alveolar walls. Their caliber is determined by the relationship between alveolar pressure and the pressure within them. Extra-alveolar vessels include all the arteries and veins that run through the lung parenchyma. Their caliber is greatly affected by lung volume since this determines the expanding pull of the parenchyma on their walls. The very large vessels near the hilum are outside the lung substance and are exposed to intrapleural pressure.

It is also useful to describe the resistance of a system of blood vessels as follows:

$$\text{Vascular resistance} = \frac{\text{input pressure} - \text{output pressure}}{\text{blood flow}}$$

This number is certainly not a complete description of the pressure flow properties of the system. For example, the number usually depends on the magnitude of the blood flow. Nevertheless, it often allows a helpful comparison of different circulations, or the same circulations under different conditions.

We have seen that the total pressure drop from pulmonary artery to left atrium in the pulmonary circulation is only some 10mmHg against about 100mmHg for the systemic circulation. Since the blood flows through the two circulation are virtually identical, it follows that the pulmonary vascular resistance is only one-tenth that of the systemic circulation. The high resistance of the systemic circulation is largely caused by the muscular arterioles, which allow the regulation of blood flow to various organ of the body. The pulmonary circulation has non such vessels and although its resistance is extraordinary small, it has a remarkable facility for becoming even smaller as the pressure within it rises. Two mechanisms are responsible for this. Under normal conditions,

some capillaries are either closed, or open but with no blood flow. As the pressure rises, these vessels begin to conduct blood, thus lowering the overall resistance. This is termed *recruitment* (Figure 1.4) and is apparently the chief mechanism for the fall in pulmonary vascular resistance that occurs as the pulmonary artery pressure is raised from low levels. At higher vascular pressure, widening of individual capillary segments occurs. This increase in caliber, or *distension*, is hardly surprising in view of the very thin membrane, which separates the capillary from the alveolar space. Distension is probably chiefly a change in shape of the capillaries from near-flattened to more circular. There is evidence that the capillary wall strongly resist stretching. Distension is apparently the predominant mechanism for the fall in pulmonary vascular resistance at relatively high vascular pressure ^[3].

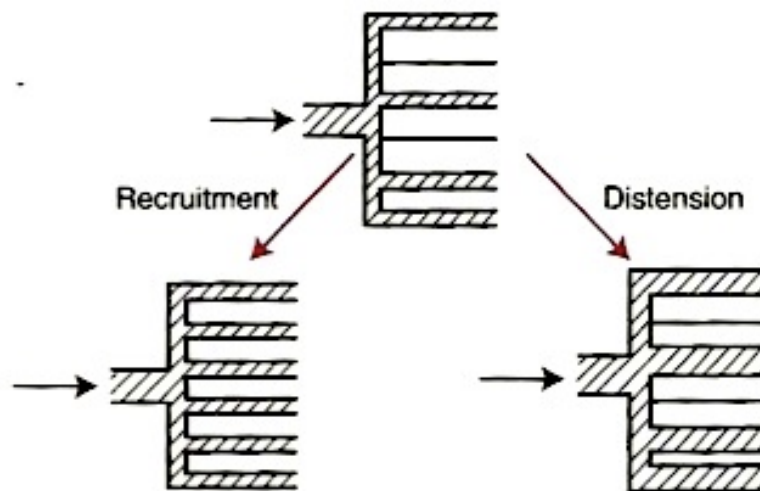


Figure 1.4: Recruitment (opening of previously closed vessels) and distension (increase in caliber vessels). These are two mechanisms for the decrease in pulmonary vascular resistance that occurs as vascular pressures are raised ^[3].

Another important determinant of pulmonary vascular resistance is *lung volume*. The caliber of the extra-alveolar vessels is determined by a balance between various forces. As we have seen, they are pulled open as the lung expands. As a result, their vascular resistance is low at large lung volumes. On the other hand, their walls contain smooth muscle and elastic tissue, which resist distension and tend to reduce their caliber. Consequently they have a high resistance when lung volume is low (Figure 1.5). Indeed, if the lung is completely collapsed, the smooth muscle tone of these vessels is so effective that the pulmonary artery pressure has to be raised several centimeters of water above downstream pressure before any flow at all occurs. This is called a *critical opening pressure* ^[3].

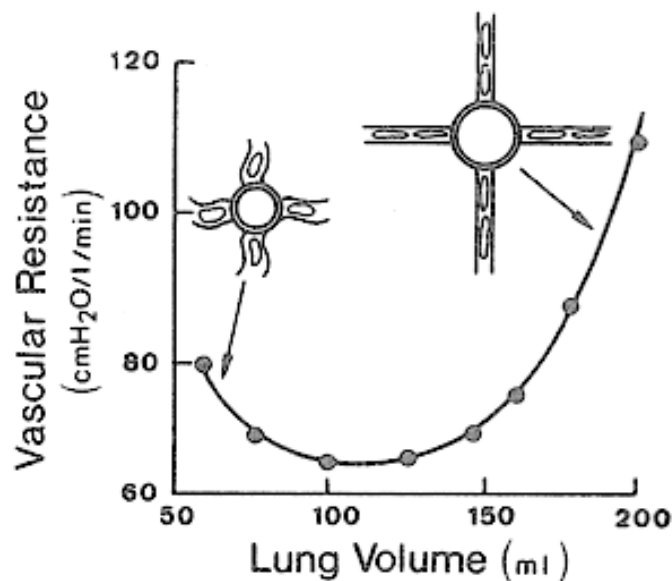


Figure 1.5: Effect of lung volume on pulmonary vascular resistance when the transmural pressure of the capillaries is held constant. At low lung volumes, resistance is high because the extra-alveolar vessels become narrow. At high volumes, the capillaries are stretched, and their caliber is reduced. (Data from a dog lobe preparation) ^[3].

1.1.2 Pulmonary ventilation

The lungs can be expanded and contracted in two ways: (1) by downward and upward movement of the diaphragm to lengthen or shorten the chest cavity, and (2) by elevation and depression of the ribs to increase and decrease the anteroposterior diameter of the chest cavity. Figure 1.6 shows these two methods.

Normal quiet breathing is accomplished almost entirely by the first method, that is, by movement of the diaphragm. During inspiration, contraction of the diaphragm pulls the lower surfaces of the lungs downward. Then, during expiration, the diaphragm simply relaxes, and the *elastic recoil* of the lungs, chest wall, and abdominal structures compresses the lungs and expels the air. During heavy breathing, however, the elastic forces are not powerful enough to cause the necessary rapid expiration, so that extra force is achieved mainly by contraction of the *abdominal muscles*, which pushes the abdominal contents upward against the bottom of the diaphragm, thereby compressing the lungs.

The second method for expanding the lungs is to raise the rib cage. This expands the lungs because, in the natural resting position, the ribs slant downward, as shown on the left side of Figure 1.6, thus allowing the sternum to fall backward toward the vertebral column. But when the rib cage is elevated, the ribs project almost directly forward, so that the sternum also moves forward, away from the spine, making the anteroposterior thickness of the chest about 20 per cent greater during

maximum inspiration than during expiration. Therefore, all the muscles that elevate the chest cage are classified as muscles of inspiration, and those muscles that depress the chest cage are classified as muscles of expiration. The most important muscles that raise the rib cage are the external intercostals, but others that help are the *sternocleidomastoid muscles*, which lift upward on the sternum; *anterior serrati*, which lift many of the ribs; and *scaleni*, which lift the first two ribs.

The muscles that pull the rib cage downward during expiration are mainly the *abdominal recti*, which have the powerful effect of pulling downward on the lower ribs at the same time that they and other abdominal muscles also compress the abdominal contents upward against the diaphragm, and *internal intercostals* [1].

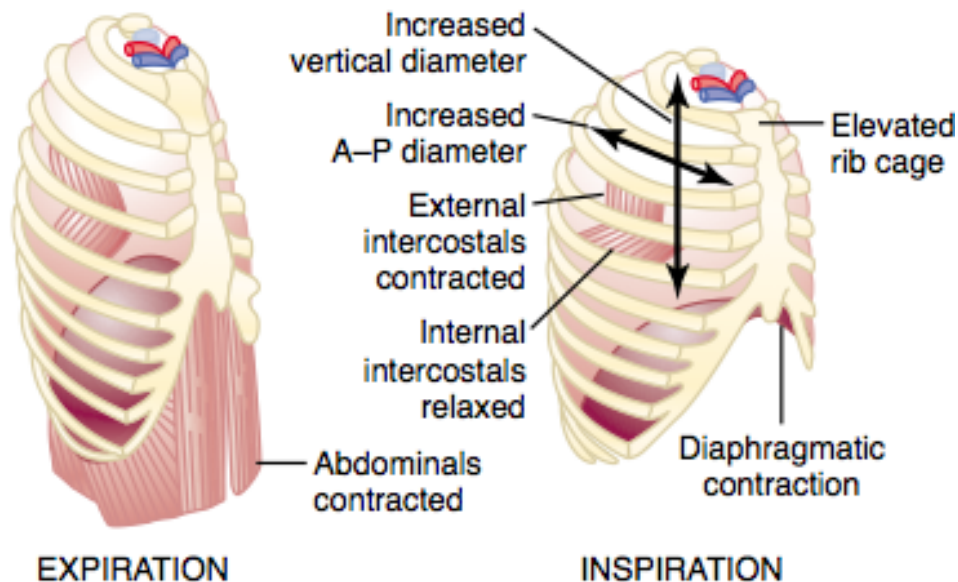


Figure 1.6: Contraction and expansion of the thoracic cage during expiration and inspiration, demonstrating diaphragmatic contraction, function of the intercostal muscles, and elevation and depression of the rib cage [1].

Figure 1.6 also shows the mechanism by which the external and internal intercostals act to cause inspiration and expiration. To the left, the ribs during expiration are angled downward, and the external intercostals are elongated forward and downward. As they contract, they pull the upper ribs forward in relation to the lower ribs, and this causes leverage on the ribs to raise them upward, thereby causing inspiration. The internal intercostals function exactly in the opposite manner, functioning as expiratory muscles because they angle between the ribs in the opposite direction and cause opposite leverage.

The lung is an elastic structure that collapses like a balloon and expels all its air through the trachea whenever there is no force to keep it inflated. Also, there are no attachments between the

lung and the walls of the chest cage, except where it is suspended at its hilum from the mediastinum. Instead, the lung “floats” in the thoracic cavity, surrounded by a thin layer of pleural fluid that lubricates movement of the lungs within the cavity. Further, continual suction of excess fluid into lymphatic channels maintains a slight suction between the visceral surface of the lung pleura and the parietal pleural surface of the thoracic cavity. Therefore, the lungs are held to the thoracic wall as if glued there, except that they are well lubricated and can slide freely as the chest expands and contracts.

The pressures that cause the movements of air in and out of the lungs during normal breathing are (1) pleural pressure; (2) alveolar pressure; and (3) transpulmonary pressure.

Pleural pressure is the pressure of the fluid in the thin space between the lung pleura and the chest wall pleura. This is normally a slight suction, which means a slightly negative pressure. The normal pleural pressure at the beginning of inspiration is about -5 centimeters of water, which is the amount of suction required to hold the lungs open to their resting level. Then, during normal inspiration, expansion of the chest cage pulls outward on the lungs with greater force and creates more negative pressure, to an average of about -7.5 centimeters of water.

These relationships between pleural pressure and changing lung volume are demonstrated in Figure 1.7, showing in the lower panel the increasing negativity of the pleural pressure from -5 to -7.5 during inspiration and in the upper panel an increase in lung volume of 0.5 liter. Then, during expiration, the events are essentially reversed ^[1].

Alveolar pressure is the pressure of the air inside the lung alveoli. When the glottis is open and no air is flowing into or out of the lungs, the pressures in all parts of the respiratory tree, all the way to the alveoli, are equal to atmospheric pressure, which is considered to be zero reference pressure in the airways - that is, 0 centimeters water pressure. To cause inward flow of air into the alveoli during inspiration, the pressure in the alveoli must fall to a value slightly below atmospheric pressure (below 0). The second curve (labeled “alveolar pressure”) of Figure 1.7 demonstrates that during normal inspiration, alveolar pressure decreases to about -1 centimeter of water. This slight negative pressure is enough to pull 0.5 liter of air into the lungs in the 2 seconds required for normal quiet inspiration. During expiration, opposite pressures occur: the alveolar pressure rises to about +1 centimeter of water, and this forces the 0.5 liter of inspired air out of the lungs during the 2 to 3 seconds of expiration.

Finally, the difference between the alveolar pressure and the pleural pressure is called the *transpulmonary pressure*. It is the pressure difference between that in the alveoli and that on the

outer surfaces of the lungs, and it is a measure of the elastic forces in the lungs that tend to collapse the lungs at each instant of respiration, called the *recoil pressure*.

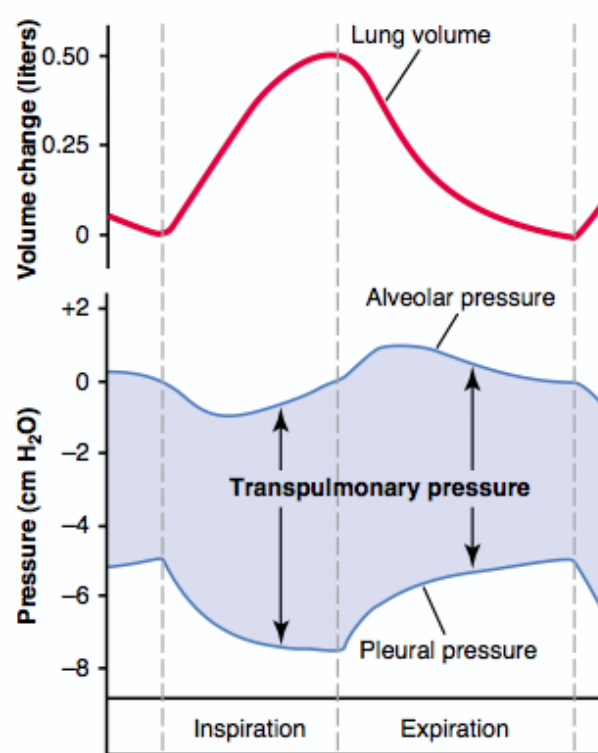


Figure 1.7: Changes in lung volume, alveolar pressure, pleural pressure, and transpulmonary pressure during normal breathing ^[1].

The extent to which the lungs will expand for each unit increase in transpulmonary pressure (if enough time is allowed to reach equilibrium) is called the *lung compliance*. The total compliance of both lungs together in the normal adult human being averages about 200 milliliters of air per centimeter of water transpulmonary pressure. That is, every time the transpulmonary pressure increases 1 centimeter of water, the lung volume, after 10 to 20 seconds, will expand 200 milliliters.

A simple method for studying pulmonary ventilation is to record the volume movement of air into and out of the lungs, a process called spirometry. Figure 1.8 shows a spirogram indicating changes in lung volume under different conditions of breathing. For ease in describing the events of pulmonary ventilation, the air in the lungs has been subdivided in this diagram into four volumes and four capacities, which are the average for a young adult man. To the left in Figure 1.8 are listed four pulmonary lung volumes, when added together, equal the maximum volume to which the lungs can be expanded ^[1].

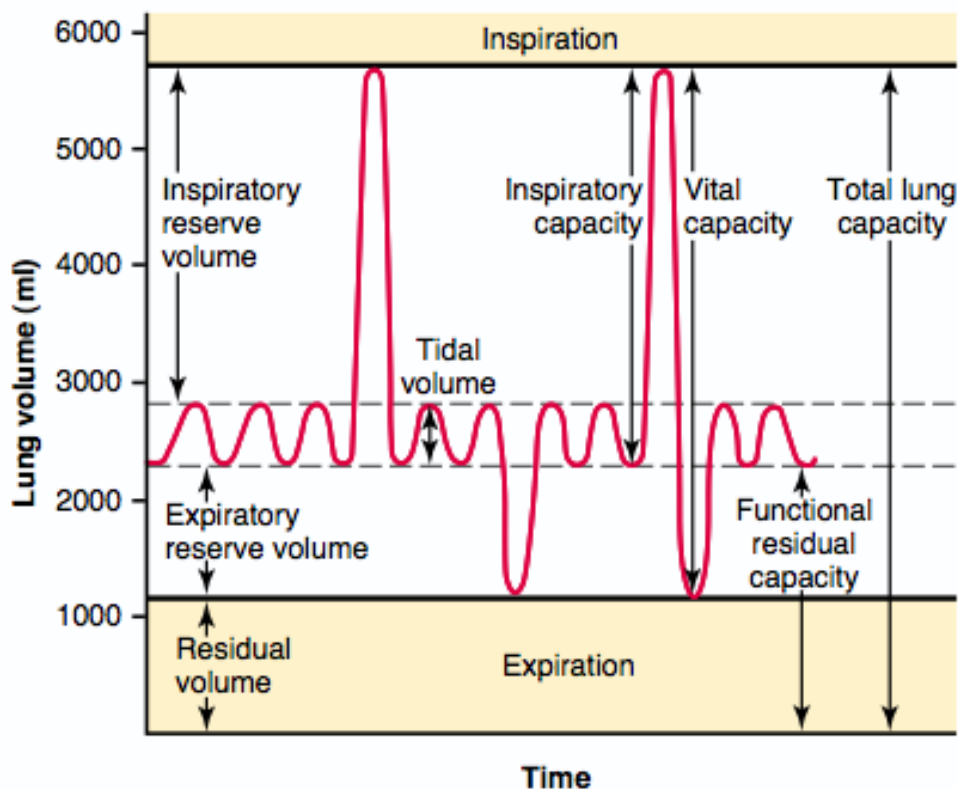


Figure 1.8: Diagram showing respiratory excursion during normal breathing and during maximal inspiration and maximal expiration ^[1].

The meaning of each of these volumes is the following:

- The *tidal volume* (V_T) is the volume of air inspired or expired with each normal breath; it amounts to about 500 milliliters in the adult male.
- The *inspiratory reserve volume* (IRV) is the extra volume of air that can be inspired over and above the normal tidal volume when the person inspires with full force; it is usually equal to about 3000 milliliters.
- The *expiratory reserve volume* (ERV) is the maximum extra volume of air that can be expired by forceful expiration after the end of a normal tidal expiration; this normally amounts to about 1100 milliliters.
- The *residual volume* (RV) is the volume of air remaining in the lungs after the most forceful expiration; this volume averages about 1200 milliliters.

In describing events in the pulmonary cycle, it is sometimes desirable to consider two or more of the volumes together. Such combinations are called *pulmonary capacities*. To the right in Figure 1.8

are listed the important pulmonary capacities, which can be described as follows:

- The *inspiratory capacity* (IC) equals the tidal volume plus the inspiratory reserve volume. This is the amount of air (about 3500 milliliters) a person can breathe in, beginning at the normal expiratory level and distending the lungs to the maximum amount.
- The *functional residual capacity* (FRC) equals the expiratory reserve volume plus the residual volume. This is the amount of air that remains in the lungs at the end of normal expiration (about 2300 milliliters).
- The *vital capacity* (VC) equals the inspiratory reserve volume plus the tidal volume plus the expiratory reserve volume. This is the maximum amount of air a person can expel from the lungs after first filling the lungs to their maximum extent and then expiring to the maximum extent (about 4600 milliliters).
- The *total lung capacity* (TLC) is the maximum volume to which the lungs can be expanded with the greatest possible effort (about 5800 milliliters); it is equal to the vital capacity plus the residual volume.

All pulmonary volumes and capacities are about 20 to 25 per cent less in women than in men, and they are greater in large and athletic people than in small and asthenic people ^[1].

1.1.3 Air transportation and diffusion

After the alveoli are ventilated with fresh air, the next step in the respiratory process is diffusion of oxygen from the alveoli into the pulmonary blood and diffusion of carbon dioxide in the opposite direction, out of the blood. The process of diffusion is simply the random motion of molecules intertwining their way in all directions through the respiratory membrane and adjacent fluids.

All the gases of concern in respiratory physiology are simple molecules that are free to move among one another, which is the process called *diffusion*. This is also true of gases dissolved in the fluids and tissues of the body.

For diffusion to occur, there must be a source of energy. This is provided by the kinetic motion of the molecules themselves. Except at absolute zero temperature, all molecules of all matter are continually undergoing motion. For free molecules that are not physically attached to others, this means linear movement at high velocity until they strike other molecules. Then they bounce away

in new directions and continue until striking other molecules again. In this way, the molecules move rapidly and randomly among one another.

If a gas chamber or a solution has a high concentration of a particular gas at one end of the chamber and a low concentration at the other end *net diffusion* of the gas will occur from the high-concentration area toward the low-concentration area.

Pressure is caused by multiple impacts of moving molecules against a surface. Therefore, the pressure of a gas acting on the surfaces of the respiratory passages and alveoli is proportional to the summated force of impact of all the molecules of that gas striking the surface at any given instant. This means that the pressure is directly proportional to the concentration of the gas molecules.

In respiratory physiology, one deals with mixtures of gases, mainly of *oxygen*, *nitrogen*, and *carbon dioxide*. The rate of diffusion of each of these gases is directly proportional to the pressure caused by that gas alone, which is called the *partial pressure* of that gas. The concept of partial pressure can be explained as follows. Consider air, which has an approximate composition of 79 per cent nitrogen and 21 per cent oxygen. The total pressure of this mixture at sea level averages 760 mm Hg. It is clear from the preceding description of the molecular basis of pressure that each gas contributes to the total pressure in direct proportion to its concentration. Therefore, 79 per cent of the 760 mm Hg is caused by nitrogen (600 mm Hg) and 21 per cent by oxygen (160 mm Hg). Thus, the “partial pressure” of nitrogen in the mixture is 600 mm Hg, and the “partial pressure” of oxygen is 160 mm Hg; the total pressure is 760 mm Hg, the sum of the individual partial pressures. The partial pressures of individual gases in a mixture are designated by the symbols P_{O_2} , P_{CO_2} , P_{N_2} , P_{H_2O} , and so forth.

The partial pressure of a gas in a solution is determined not only by its concentration but also by the *solubility coefficient* of the gas. That is, some types of molecules, especially carbon dioxide, are physically or chemically attracted to water molecules, whereas others are repelled. When molecules are attracted, far more of them can be dissolved without building up excess partial pressure within the solution. Conversely, in the case of those that are repelled, high partial pressure will develop with fewer dissolved molecules. These relations are expressed by the following formula, which is *Henry’s law*:

$$\text{Partial Pressure} = \frac{\text{Concentration of dissolved gas}}{\text{Solubility Coefficient}}$$

When partial pressure is expressed in atmospheres (1 atmosphere pressure equals 760 mm Hg) and

concentration is expressed in volume of gas dissolved in each volume of water, the solubility coefficients for important respiratory gases at body temperature are the following:

Oxygen	0.024
Carbon dioxide	0.570
Carbon monoxide	0.018
Nitrogen	0.012
Helium	0.008

From this table, one can see that carbon dioxide is more than 20 times as soluble as oxygen. Therefore, the partial pressure of carbon dioxide (for a given concentration) is less than one twentieth that exerted by oxygen.

The partial pressure of each gas in the alveolar respiratory gas mixture tends to force molecules of that gas into solution in the blood of the alveolar capillaries. Conversely, the molecules of the same gas that are already dissolved in the blood are bouncing randomly in the fluid of the blood, and some of these bouncing molecules escape back into the alveoli. The rate at which they escape is directly proportional to their partial pressure in the blood.

The direction of the net diffusion is determined by the difference between the two partial pressures. If the partial pressure is greater in the gas phase in the alveoli, as is normally true for oxygen, then more molecules will diffuse into the blood than in the other direction. Alternatively, if the partial pressure of the gas is greater in the dissolved state in the blood, which is normally true for carbon dioxide, then net diffusion will occur toward the gas phase in the alveoli.

From the preceding discussion, it is clear that when the partial pressure of a gas is greater in one area than in another area, there will be net diffusion from the high-pressure area toward the low-pressure area. Therefore, the net diffusion of gas from the area of high pressure to the area of low pressure is equal to the number of molecules bouncing in this forward direction minus the number bouncing in the opposite direction; this is proportional to the gas partial pressure difference between the two areas, called simply the *pressure difference for causing diffusion*.

In addition to the pressure difference, several other factors affect the rate of gas diffusion in a fluid. They are (1) the solubility of the gas in the fluid, (2) the cross-sectional area of the fluid, (3) the distance through which the gas must diffuse, (4) the molecular weight of the gas, and (5) the temperature of the fluid. In the body, the last of these factors, the temperature, remains reasonably constant and usually need not be considered.

The greater the solubility of the gas, the greater the number of molecules available to diffuse for any given partial pressure difference. The greater the cross-sectional area of the diffusion pathway, the greater the total number of molecules that diffuse. Conversely, the greater the distance the molecules must diffuse, the longer it will take the molecules to diffuse the entire distance. Finally, the greater the velocity of kinetic movement of the molecules, which is inversely proportional to the square root of the molecular weight, the greater the rate of diffusion of the gas. All these factors can be expressed in a single formula, as follows:

$$D \propto \frac{\Delta P \times A \times S}{d \times \sqrt{MW}}$$

in which D is the diffusion rate, ΔP is the partial pressure difference between the two ends of the diffusion pathway, A is the cross-sectional area of the pathway, S is the solubility of the gas, d is the distance of diffusion, and MW is the molecular weight of the gas.

It is obvious from this formula that the characteristics of the gas itself determine two factors of the formula: solubility and molecular weight. Together, these two factors determine the diffusion coefficient of the gas, which is proportional to S/\sqrt{MW} . That is, the relative rates at which different gases at the same partial pressure levels will diffuse are proportional to their diffusion coefficients.

Once oxygen has diffused from the alveoli into the pulmonary blood, it is transported to the peripheral tissue capillaries almost entirely in combination with hemoglobin. The presence of hemoglobin in the red blood cells allows the blood to transport 30 to 100 times as much oxygen as could be transported in the form of dissolved oxygen in the water of the blood.

In the body's tissue cells, oxygen reacts with various foodstuffs to form large quantities of carbon dioxide. This carbon dioxide enters the tissue capillaries and is transported back to the lungs. Carbon dioxide, like oxygen, also combines with chemical substances in the blood that increase carbon dioxide transport 15- to 20-fold.

We have already pointed out that gases can move from one point to another by diffusion and that the cause of this movement is always a partial pressure difference from the first point to the next. Thus, oxygen diffuses from the alveoli into the pulmonary capillary blood because the oxygen partial pressure (P_{O_2}) in the alveoli is greater than the P_{O_2} in the pulmonary capillary blood. In the other tissues of the body, a higher P_{O_2} in the capillary blood than in the tissues causes oxygen to diffuse into the surrounding cells.

Conversely, when oxygen is metabolized in the cells to form carbon dioxide, the intracellular

carbon dioxide pressure (P_{CO_2}) rises to a high value, which causes carbon dioxide to diffuse into the tissue capillaries. After blood flows to the lungs, the carbon dioxide diffuses out of the blood into the alveoli, because the P_{CO_2} in the pulmonary capillary blood is greater than that in the alveoli. Thus, the transport of oxygen and carbon dioxide by the blood depends on both diffusion and the flow of blood.

Normally, about 97 per cent of the oxygen transported from the lungs to the tissues is carried in chemical combination with hemoglobin in the red blood cells. The remaining 3 per cent is transported in the dissolved state in the water of the plasma and blood cells. Thus, under normal conditions, oxygen is carried to the tissues almost entirely by hemoglobin.

The hemoglobin is a protein composed of four protein chains, two alpha chains and two beta chains, each with a ring-like *heme* group containing an *iron* atom. Oxygen binds reversibly to these iron atoms and is transported through blood (Figure 1.9).

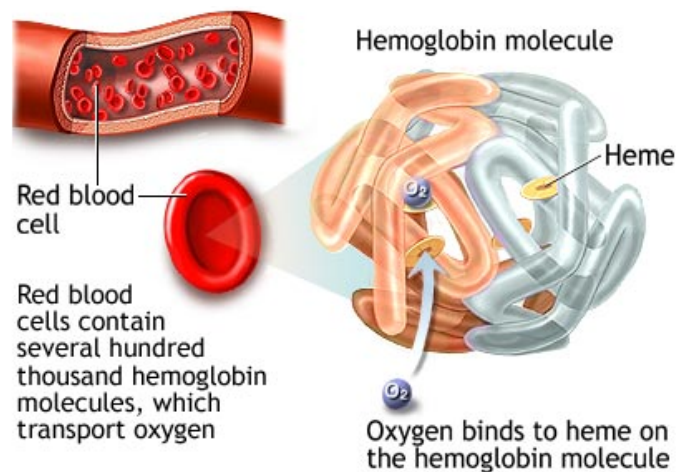


Figure 1.9: The oxygen molecule combines loosely and reversibly with the heme portion of hemoglobin.

When P_{O_2} is high, as in the pulmonary capillaries, oxygen binds with the hemoglobin, but when P_{O_2} is low, as in the tissue capillaries, oxygen is released from the hemoglobin. This is the basis for almost all oxygen transport from the lungs to the tissues.

Figure 1.10 shows the *oxygen-hemoglobin dissociation curve*, which demonstrates a progressive increase in the percentage of hemoglobin bound with oxygen as blood P_{O_2} increases, which is called the *per cent saturation of hemoglobin*. Because the blood leaving the lungs and entering the systemic arteries usually has a P_{O_2} of about 95 mm Hg, one can see from the dissociation curve that the usual oxygen saturation of systemic arterial blood averages 97 per cent. Conversely, in normal venous blood returning from the peripheral tissues, the P_{O_2} is about 40 mm Hg, and the saturation of

hemoglobin averages 75 per cent ^[1].

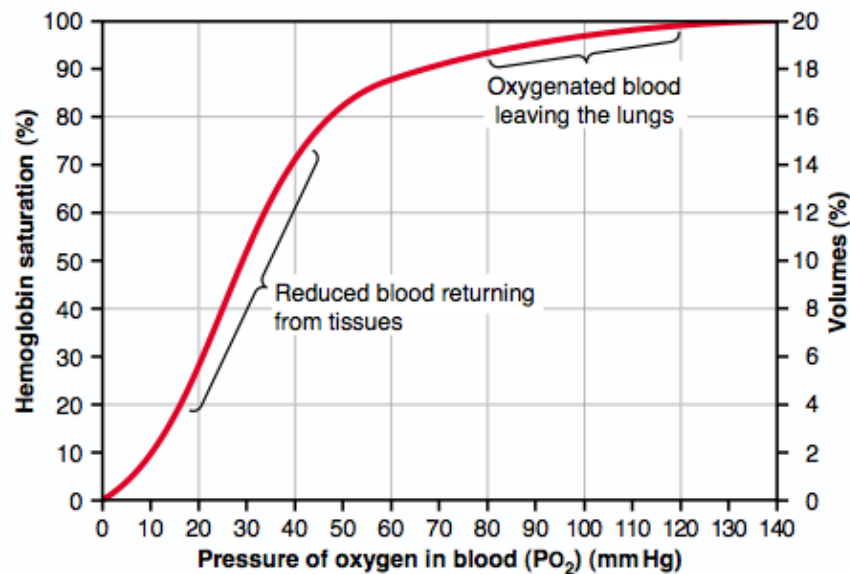


Figure 1.10: Oxygen-hemoglobin dissociation curve ^[1].

The blood of a normal person contains about 15 grams of hemoglobin in each 100 milliliters of blood, and each gram of hemoglobin can bind with a maximum of 1.34 milliliters of oxygen (1.39 milliliters when the hemoglobin is chemically pure, but impurities such as methemoglobin reduce this). Therefore, 15 times 1.34 equals 20.1, which means that, on average, the 15 grams of hemoglobin in 100 milliliters of blood can combine with a total of almost exactly 20 milliliters of oxygen if the hemoglobin is 100 per cent saturated. This is usually expressed as 20 volumes per cent. The oxygen-hemoglobin dissociation curve for the normal person can also be expressed in terms of volume per cent of oxygen, as shown by the far right scale in Figure 1.10, instead of per cent saturation of hemoglobin.

The total quantity of oxygen bound with hemoglobin in normal systemic arterial blood, which is 97 per cent saturated, is about 19.4 milliliters per 100 milliliters of blood. On passing through the tissue capillaries, this amount is reduced, on average, to 14.4 milliliters (PO₂ of 40 mm Hg, 75 per cent saturated hemoglobin). Thus, under normal conditions, about 5 milliliters of oxygen are transported from the lungs to the tissues by each 100 milliliters of blood flow.

During heavy exercise, the muscle cells use oxygen at a rapid rate, which, in extreme cases, can cause the muscle interstitial fluid PO₂ to fall from the normal 40 mm Hg to as low as 15 mm Hg. At this low pressure, only 4.4 milliliters of oxygen remain bound with the hemoglobin in each 100

milliliters of blood, as shown in Figure 1.12. Thus, 19.4 – 4.4, or 15 milliliters, is the quantity of oxygen actually delivered to the tissues by each 100 milliliters of blood flow. Thus, three times as much oxygen as normal is delivered in each volume of blood that passes through the tissues. Furthermore, the cardiac output can increase to six to seven times normal in well-trained marathon runners. Thus, multiplying the increase in cardiac output (six- to sevenfold) by the increase in oxygen transport in each volume of blood (threefold) gives a 20-fold increase in oxygen transport to the tissues ^[1].

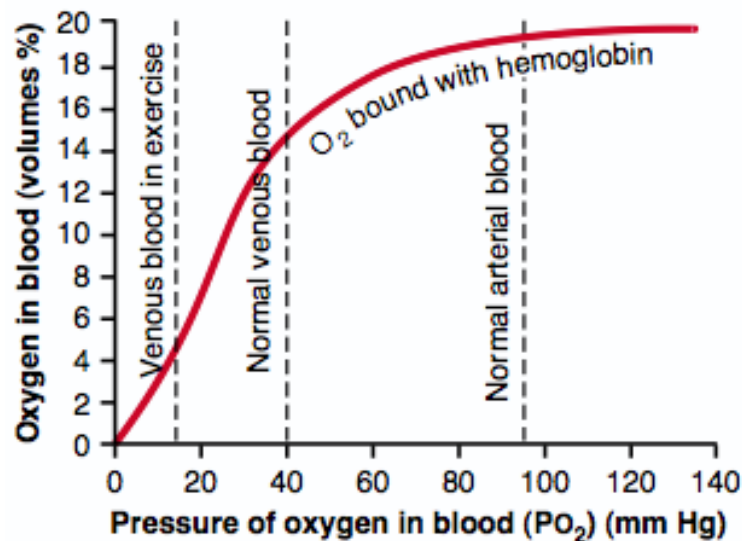


Figure 1.11 Effect of blood P_{O_2} on the quantity of oxygen bound with hemoglobin in each 100 millimeters of blood ^[1].

The oxygen-hemoglobin dissociation curves of Figures 1.10 and 1.11 are for normal, average blood. However, a number of factors can displace the dissociation curve in one direction or the other in the manner shown in Figure 1.12. This figure shows that when the blood becomes slightly acidic, with the pH decreasing from the normal value of 7.4 to 7.2, the oxygen-hemoglobin dissociation curve shifts, on average, about 15 per cent to the right. Conversely, an increase in pH from the normal 7.4 to 7.6 shifts the curve a similar amount to the left.

In addition to pH changes, several other factors are known to shift the curve. Three of these, all of which shift the curve to the right, are (1) increased carbon dioxide concentration, (2) increased blood temperature, and (3) increased 2,3-biphosphoglycerate (BPG), a metabolically important phosphate compound present in the blood in different concentrations under different metabolic conditions.

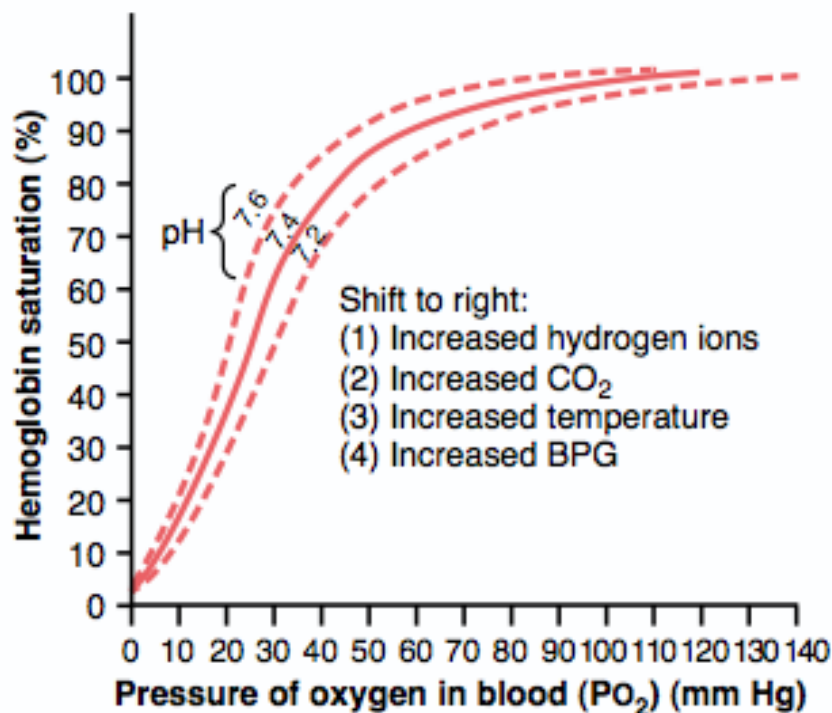


Figure 1.12: Shift of the oxygen-hemoglobin dissociation curve to the right caused by an increase in hydrogen ion concentration (decrease in pH) ^[1].

Although hemoglobin is necessary for the transport of oxygen to the tissues, it performs another function essential to life. This is its function as a “tissue oxygen buffer” system. That is, the hemoglobin in the blood is mainly responsible for stabilizing the oxygen pressure in the tissues ^[1].

1.1.4 Mechanics of breathing

Earlier we have seen the muscles of respiration, now we are going to discuss the pressure-volume curve and the airways resistance. Suppose we take an excised animal lung, cannulate the trachea, and place it inside a jar (Figure 1.13). When the pressure within the jar is reduced below atmospheric pressure, the lung expands and its change in volume can be measured with a spirometer. The pressure is held at each level, as indicated by the points, for a few seconds to allow the lung to come to rest. In this way, the pressure-volume curve of the lung can be plotted.

In Figure 1.13, the expanding pressure around the lung is generated by a pump, but in humans it is developed by an increase in volume of the chest cage. The fact that the intrapleural space between the lung and chest wall is much smaller than the space between the lung and the bottle in Figure 1.13 makes no essential difference. The intrapleural space contains only a few milliliters of fluid. This figure also shows that the curves which the lung follows during inflation and deflation

are different. This behavior is known as *hysteresis*. Note that the lung volume at any given pressure during deflation is larger than during inflation. Note also that the lung without any expanding pressure has some air inside it. In fact, even if the pressure around the lung is raised above atmospheric pressure, little further air is lost because small airways close, trapping gas in the alveoli. This *airway closure* occurs at higher lung volumes with increasing age and also in some types of lung disease.

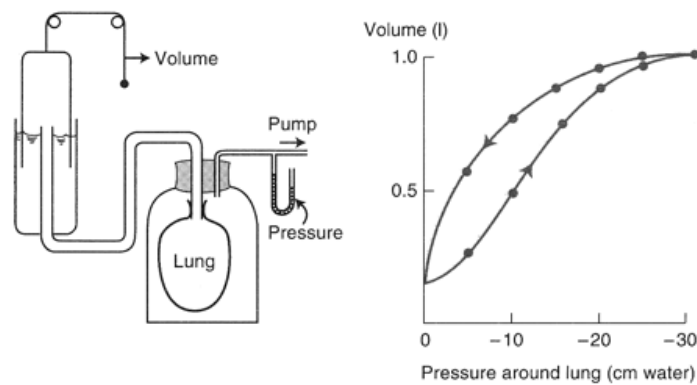


Figure 1.13: Measurements of the pressure-volume curve of excised lung. The lung is held at each pressure for a few seconds while its volume is measured. The curve is nonlinear and becomes flatter at high expanding pressures. Note that the inflation and deflation curves are not the same; this is called hysteresis^[3].

In Figure 1.13 the pressure inside the airways and alveoli of the lung is the same as atmospheric pressure, which is zero on the horizontal axis. Thus, this axis also measures the difference in pressure between the inside and outside of the lung. This is known as *transpulmonary pressure* and is numerically equal to the pressure around the lung when the alveolar pressure is atmospheric. It is also possible to measure the pressure-volume of the lung shown in Figure 1.13 by inflating it with positive pressure and leaving the pleural surface exposed to the atmosphere. In this case, the X axis could be labeled “airway pressure”, and the values would be positive. The curve would be identical to those shown in Figure 1.13.

The slope of the pressure-volume curve, or the volume change per unit pressure change, is known as the *compliance*. In the normal range (expanding pressure of about – 5 to -10 cm water) the lung is remarkably distensible or very compliant. The compliance of the human lung is about 200 ml/cm water. However, at high expanding pressures, the lung is stiffer, and its compliance is smaller, as shown by the flatter slope of the curve.

The compliance of lung depends on its size. Clearly, the change in volume per unit change of

pressure will be larger for a human lung than, say a mouse lung. For this reason, the compliance per unit volume of lung, or *specific compliance*, is sometimes measured if we wish to draw conclusions about the intrinsic elastic properties of the lung tissue.

The pressure surrounding the lung is less than atmospheric in Figure 1.13 (and in the living chest) because of the elastic recoil of the lung. The responsible for the lung's elastic behavior, that is, its tendency to return to its resting volume after distension is the elastic tissue, which is visible in histological sections. Fibers of elastin and collagen can be seen in the alveolar walls and around vessels and bronchi. Probably the elastic behavior of the lung has less to do with simple elongation of these fibers than it does with their geometrical arrangement. The changes in elastic recoil that occur in the lung with age and in emphysema are presumably caused by changes in this elastic tissue.

Another very important factor in the pressure-volume behavior of lung is the surface tension of the liquid film lining the alveoli. Surface tension is the force acting across an imaginary line 1 cm long in the surface of the liquid (Figure 1.14A). It arises because the attractive forces between adjacent molecules of the liquid are much stronger than those between the liquid and gas, with the result that the liquid surface area becomes as small as possible. This behavior is seen clearly in a soap bubble blown on the end of a tube (Figure 1.14B). The surfaces of the bubble contract as much as they can, forming a sphere (smallest surface area for a given volume) and generating a pressure that can be predicted from Laplace's law: pressure = (4 x surface tension)/radius. When only one surface is involved in a liquid-lined spherical alveolus, the numerator has the number 2 rather than 4.

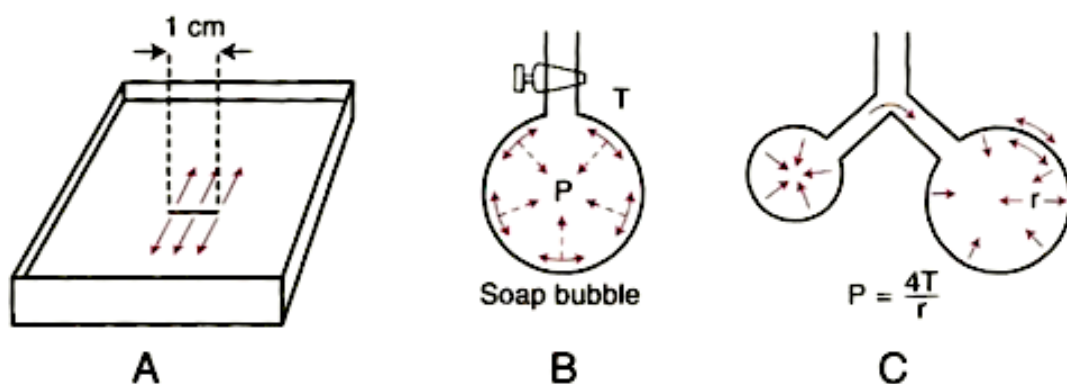


Figure 1.14: (A) Surface tension is the force acting across an imaginary line 1 cm long in a liquid surface. (B) Surface forces in a soap bubble tend to reduce the area of the surface and generate a pressure within the bubble. (C) Because the smaller bubble generates a larger pressure, it blows up the large bubble^[3].

The first evidence that surface tension might contribute to the pressure-volume behavior of the lung was obtained by early physiologists when they showed that lungs inflated with saline have a much larger compliance (are easier to distend) than air-filled lungs (Figure 1.15). Because the saline abolished the surface tension forces but presumably did not affect the tissue forces of the lung, this observation meant that surface tension contributed a large part of the static recoil force of the lung. Some time later, workers studying edema foam coming from the lungs of animals exposed to noxious gases noticed that the tiny air bubbles of the foam were extremely stable. They recognized that this indicated a very low surface tension, an observation which led to the remarkable discovery of pulmonary *surfactant* ^[3].

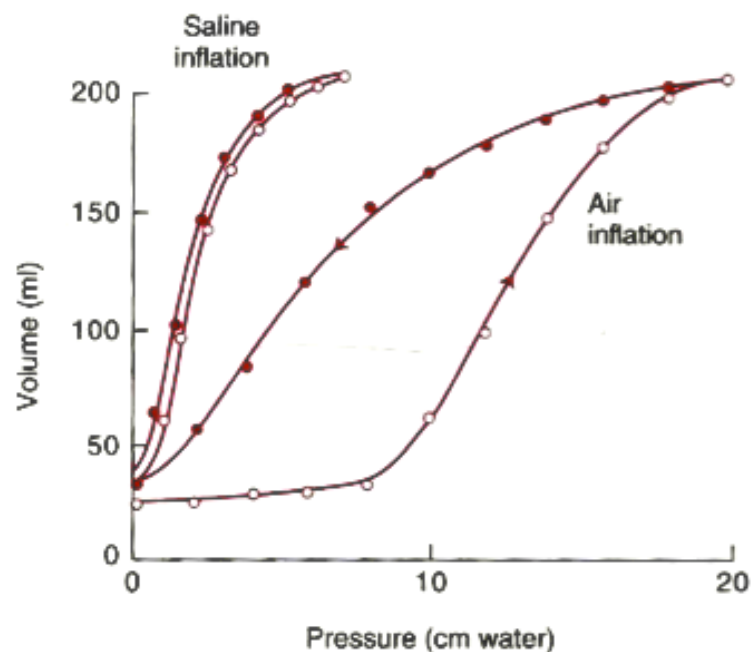


Figure 1.15: Comparison of pressure-volume curves of air-filled and saline-filled lungs (cat). Open circles, inflation; closed circles, deflation. Note that the saline-filled lung has a higher compliance and also much less hysteresis than the air-filled lung ^[3].

Just as the lung is elastic, so is the thoracic cage. This can be illustrated by putting air into the intrapleural space (pneumothorax). Figure 1.16 shows that the normal pressure outside the lung is subatmospheric just as it is in the jar of Figure 1.13. When air is introduced into the intrapleural space, raising the pressure to atmospheric, the lung collapses inward, and the chest wall springs outward.

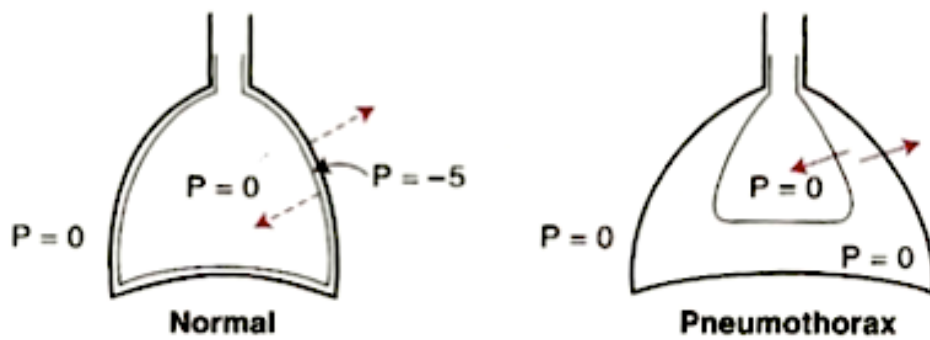


Figure 1.16: The tendency of the lung to recoil to its deflated volume is balanced by the tendency of the chest cage to bow out. As a result, the intrapleural pressure is subatmospheric. Pneumothorax allows the lung to collapse and the thorax to spring out ^[3].

This shows that under equilibrium conditions, the chest wall is pulled inward while the lung is pulled outward, the two pulls balancing each other.

These interactions can be seen more clearly if we plot a pressure-volume curve for the lung and chest wall (Figure 1.17). For this, the subject inspires or expires from a spirometer and then relaxes the respiratory muscles while the airway pressure is measured (“relaxation pressure”). Incidentally, this is difficult for an untrained subject. Figure 1.18 shows that at functional residual capacity (FRC), the relaxation pressure of the lung and chest wall is atmospheric. Indeed, FRC is the equilibrium volume when the elastic recoil of the lung is balanced by the normal tendency for the chest wall to spring out. At volume above this, the pressure is positive, and at smaller volumes, the pressure is subatmospheric.

Figure 1.17 also shows the curve for the lung alone. This is similar to that shown in Figure 1.13, except that for clarity no hysteresis is indicated and the pressures are positive instead of negative. They are the pressures that would be found from the experiment of Figure 1.13 if, after the lung had reached a certain volume, the line to the spirometer were clamped, the jar opened to the atmosphere (so that the lung relaxed against the closed airway), and the airway pressure measured. Note that at zero pressure the lung is at its minimal volume, which is below residual volume (RV).

The third curve is for the chest wall only. We can imagine this being measured on a subject with a normal chest wall and no lung. Note that at FRC the relaxation pressure is negative. In other words, at this volume the chest cage is tending to spring out. It is not until the volume is increased to about 75% of the vital capacity that the relaxation pressure is atmospheric, that is, that the chest wall has found its equilibrium position. At every volume, the relaxation pressure of the lung plus chest wall is the sum of the pressures for the lung and the chest wall measured separately. Because the pressure (at a given volume) is inversely proportional to compliance, this implies that the total

compliance of the lung and chest wall is the sum of the reciprocals of the lung and chest wall compliances measured separately, or $1/C_T = 1/C_L + 1/C_{CW}$ [3].

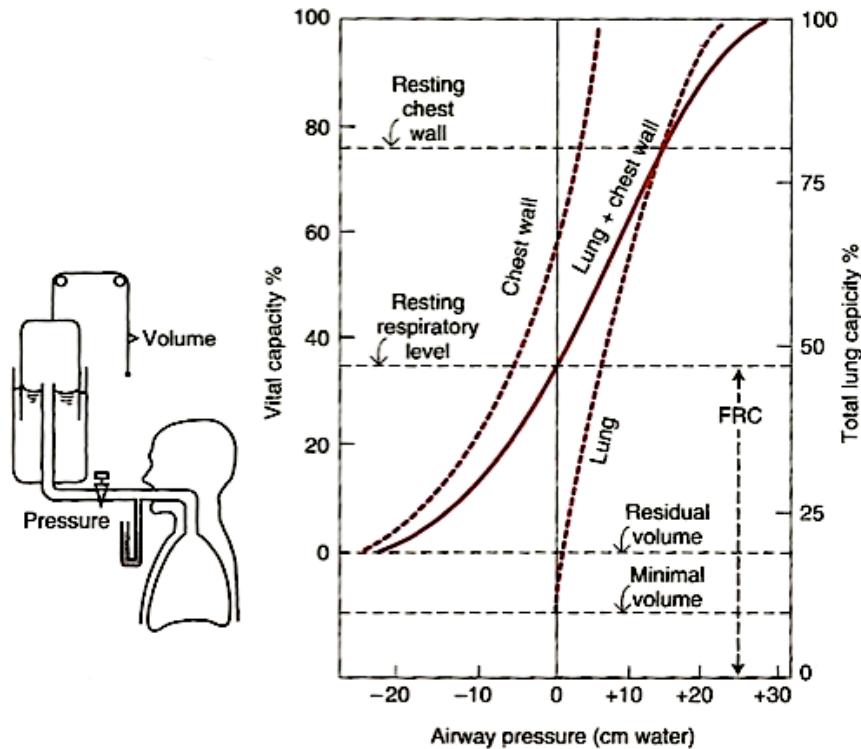


Figure 1.17: Relaxation pressure-volume curve of the lung and the chest wall. The subject inspires (or expires) to a certain volume from the spirometer, the tap is closed, and he then relaxes his respiratory muscles. The curve for lung + chest wall can be explained by the addition of the individual lung and chest wall curves [3].

1.2 The Chronic Obstructive Pulmonary Disease

Chronic obstructive pulmonary disease (COPD) is characterized by the presence of emphysema and chronic bronchitis. The airflow limitation caused by the narrowing of the small airways is associated with an abnormal inflammatory response of the lungs to noxious particles or gases, primarily caused by cigarette smoking. The obstruction is generally progressive, may be accompanied by airway hyperactivity, and may be partially reversible.

Emphysema is defined pathologically as an abnormal permanent enlargement of the air space distal to the terminal bronchioles, accompanied by destruction of their walls, without fibrosis. In most patients both processes coexist simultaneously. The disease does not affect all portions of the lung to the same degree. This uneven distribution influences the physiological behavior of different parts of the lung [4]. Chronic bronchitis is a disease characterized by excessive mucus production in

the bronchial tree, sufficient to cause excessive expectoration of sputum. In practice, criteria for “excessive” expectoration are often laid down, for example, expectoration on most days for at least 3 months in the year for at least 2 successive years ^[5].

1.2.1 Diagnosis

According to guidelines, COPD should be suspected in any patient aged 40 years or more with symptoms of cough, sputum production, or breathlessness and/or a history of exposure to risk factors, in particular smoking. Smoking is well known for causing COPD but the list of risk factors for developing COPD is long and include both host factors and environmental exposures, most often interacting. This should especially be taken into account outside Europe and the USA where exposure to risk factor other than smoking seems to play a larger role.

Guidelines usually state that a suspected diagnosis of COPD is confirmed by spirometry with the well-known – but perhaps still questioned – post-bronchodilator ratio (FEV_1/FVC) of <0.7 .

The most difficult clinical problem will often be distinguishing COPD from persistent poorly reversible asthma, especially in older patients. In general, it is easy to distinguish asthma from COPD, in particular in young and middle-aged patients where history will often suffice and where demonstration of a significant bronchodilator response is diagnostic of asthma. However, in older patients with significant previous cigarette exposure and only modest reversibility to a bronchodilator, the diagnosis can be difficult.

For most of the other differential diagnoses, the combination of a good clinical assessment together with simple investigations will usually resolve any uncertainty; often a chest radiograph will be helpful.

When differential diagnoses have been excluded, a post-bronchodilator FEV_1/FVC ratio <0.7 confirms the diagnosis of COPD. Again, caution is required when using this fixed cut-off value. The normal value for the FEV_1/FVC ratio is age-dependent and whereas a ratio <0.7 is clearly abnormal in a 40-year old it is close to the expected value for an 80-year old. Thus, COPD is likely to be under-diagnosed in younger adults and “over-diagnosed” in the elderly; whether this is truly over-diagnosis or actually abnormality associated with excess risk (like arterial hypertension associated with age) is currently unknown.

Once a diagnosis of COPD is established it is recommended that staging takes place. According to guidelines, classification of the severity of the disease is based on FEV_1 expressed in per cent of predicted value as shown in Table 1.1. In addition to problems arising from the use of different

reference values, or lack of locally derived reference values in certain ethnic population groups, it is well-known that composite scores including lung function, symptoms, body weight and exercise tolerance have better predictive value than FEV₁ alone; a good example of such a score is the BODE index [6].

Stage I:	Mild FEV ₁ /FVC < 0.70	FEV ₁ ≥ 80% predicted
Stage II:	Moderate FEV ₁ /FVC < 0.70	50% ≤ FEV ₁ < 80% predicted
Stage III:	Severe FEV ₁ /FVC < 0.70	30% ≤ FEV ₁ < 50% predicted
Stage IV:	Very severe FEV ₁ /FVC < 0.70	FEV ₁ < 30% predicted or FEV ₁ < 50% predicted plus chronic respiratory failure

Table 1.1: Severity grading of chronic obstructive pulmonary disease (COPD) according to GOLD.

1.2.2 Symptoms

The most common symptoms seen in COPD are breathlessness, cough and fatigue. There is no good correlation between lung function and symptoms of COPD, not even the standardized scoring of breathlessness correlates well with FEV₁; but a simple physiological measure can never substitute a symptom history.

Breathlessness is the most significant symptom in COPD and it is associated with significant disability, poor quality-of-life and poor prognosis. Breathlessness is defined as an awareness of increased or inappropriate respiratory effort and is assumed to relate to an awareness of the motor command to breathe. The terms used to describe breathlessness may vary with the stimulus used to provoke it and despite the increased time for expiration many COPD patients describe the sensation of breathlessness as one of inspiratory difficulty. The intensity of breathlessness is best related to changes in end-expiratory lung volumes during exercise and this fact probably explains the need to look at changes in measurements other than FEV₁ and FVC for characterizing COPD patients disability or for assessing effects of treatment. For this purpose, measurements of inspiratory capacity (IC) may be better suited.

In early stages of COPD, patients often modify their behavior in order to cope with the sensation of breathlessness; with increasing severity of COPD, breathlessness becomes an unavoidable symptom and in severe and very severe COPD there is rarely any time when patients are

asymptomatic. In very severe COPD, the patient is usually breathless on minimal exertion but due to the poor correlation between FEV₁ and breathlessness some patients may have surprisingly high levels of activity, even in late-stage COPD.

The degree of breathlessness can be measured using a number of different scales and questionnaires. The simple Medical Research Council (MRC) dyspnea scale is a useful tool but as it was originally developed for assessing breathlessness in epidemiological surveys in the workplace, it is relatively insensitive to changes. However, a slightly modified version of the MRC Questionnaire is shown in Table 1.2.

Grade	Description
0	Not troubled with breathlessness except with strenuous exercise
1	Troubled by shortness of breath when hurrying or walking up a slight hill
2	Walks slower than people of the same age due to breathlessness or has to stop for breath when walking at own pace on the level
3	Stops for breath after walking 100 m or after a few minutes on the level
4	Too breathless to leave the house or breathless when dressing or undressing

Table 1.2: The Medical Research Council dyspnea scale (Modified) ¹⁶.

The Borg category scale, as shown in Table 1.3, often used in the exercise laboratory as it measures short-term changes in perceived intensity during a particular task, e.g., during shuttle walk testing. It is simple and easy to explain. As an alternative, visual analogue scales can be used; however, like the Borg scale, this approach is for use in task-specific situations and cannot be used for assessing the degree of breathlessness associated with usual daily tasks.

Cough is a respiratory defense mechanism protecting the airways and it is the major method of clearing excess mucus production. In COPD patients, cough as a symptom is almost as common as breathlessness and may actually precede the onset of breathlessness. Cough is usually worse in the morning but seldom disturbs the patient's sleep; it can, nevertheless, be disabling because of the embarrassment felt by many patients when they have bursts of productive cough on social occasions and may contribute to the isolation often imposed on patients due to breathlessness.

Cough is difficult to measure. Questionnaires exist but their validity is questionable and devices for direct measurement of cough are still in the development stage.

Wheezing is generally seen as an asthma symptom but frequently occurs in COPD as well.

However, nocturnal wheeze is uncommon in COPD and suggests the presence of asthma and/or heart failure.

0	Nothing at all
0.5	Very, very slight (just noticeable)
1	Very slight
2	Slight (light)
3	Moderate
4	Somewhat severe
5	Severe (heavy)
6	
7	Very severe
8	
9	
10	Very, very severe (almost maximal)
	Maximal

Table 1.3: The Borg Scale ^[6].

Fatigue is frequently reported by COPD patients. It is a ubiquitous and multifactorial symptom not to be confused with simple physical exhaustion due to breathlessness but is more an awareness of a decreased capacity for physical and mental activity due to lack of resources needed to perform the activity in question. Fatigue has been identified as a serious consequence in a number of chronic conditions and will undoubtedly be a focus of attention in the future characterization of COPD. No standardized measurement scales for fatigue in COPD exist ^[6].

1.2.3 Epidemiology, risk factors and natural history of COPD

COPD is a leading cause of morbidity and mortality worldwide, and results in an economic and social burden that is both substantial and increasing. The prevalence and morbidity data greatly underestimate the total burden of COPD because the disease is usually not diagnosed until it is clinically apparent and moderately advanced. In people aged 25–75 yrs in the USA, the estimated prevalence of mild COPD was 6.9% and of moderate COPD was 6.6%, according to National Health and Nutrition Examination Survey (NHANES). COPD is the fourth-leading cause of death in the USA and Europe, and COPD mortality in females has more than doubled over the last 20 yrs. Currently, COPD is a more costly disease than asthma and, depending on country, 50–75% of the

costs are for services associated with exacerbations. Tobacco smoke is by far the most important risk factor for COPD worldwide. Other important risk factors are occupational exposures, socio-economic status and genetic predisposition.

COPD has a variable natural history and not all individuals follow the same course. The often-quoted statistic that only 15–20% of smokers develop clinically significant COPD may underestimate the toll of COPD.

It is increasingly apparent that COPD often has its roots decades before the onset of symptoms. Impaired growth of lung function during childhood and adolescence, caused by recurrent infections or tobacco smoking, may lead to lower maximally attained lung function in early adulthood. This abnormal growth will, often combined with a shortened plateau phase in teenage smokers, increase the risk of COPD.

The risk factors for COPD are shown in table 1.4 and they are separated into host factors and exposures ^[7].

Host factors	Exposures
Genetic factors	Smoking
Sex	Socio-economic status
Airway hyperreactivity, IgE and asthma	Occupation
	Environmental pollution
	Perinatal events and childhood illness
	Recurrent bronchopulmonary infections
	Diet

Table 1.4: Risk factors for COPD ^[7]. Ig: immunoglobulin.

1.2.4 Management of COPD

Effective medications for COPD are available and all patients who are symptomatic merit a trial of drug treatment. The medications for COPD currently available can reduce or abolish symptoms, increase exercise capacity, reduce the number and severity of exacerbations, and improve health status. At present, no treatment has modified the rate of decline in lung function. The inhaled route is preferred.

The change in lung function after brief treatment with any drug does not help in predicting other clinically related outcomes. Changes in FEV₁ following bronchodilator therapy can be small but are often accompanied by larger changes in lung volumes, which contribute to a reduction in perceived breathlessness. Combining different agents produces a greater change in spirometry and symptoms

than single agents alone.

Supplemental long-term oxygen therapy (LTOT) improves survival, exercise, sleep and cognitive performance in hypoxaemic. Reversal of hypoxaemia supersedes concerns about carbon dioxide (CO₂) retention.

Arterial blood gas (ABG) assessment is the preferred method to determine oxygen need because it includes acid- base information. Arterial oxygen saturation as measured by pulse oximetry (S_pO₂) is adequate for trending. Physiological indications for oxygen include a arterial oxygen tension (P_aO₂) < 7.3 kPa (55 mmHg). The therapeutic goal is to maintain S_pO₂>90% during rest, sleep and exertion. If oxygen is prescribed during an exacerbation, ABG should be rechecked in 30–90 days. Withdrawal of oxygen because of improved P_aO₂ in patients whose need for oxygen was determined when in a stable state may be detrimental.

Active patients require portable oxygen. Oxygen sources include gas, liquid and concentrator; while oxygen delivery methods include nasal continuous flow, pulse demand, reservoir cannula and transtracheal catheters. Patient education improves compliance.

Pulmonary rehabilitation is defined as "a multidisciplinary programme of care for patients with chronic respiratory impairment that is individually tailored and designed to optimize physical and social performance and autonomy". Pulmonary rehabilitation results in improvements in multiple outcome areas of considerable importance to the patient, including dyspnea, exercise ability, health status and healthcare utilization. These positive effects occur no specific pulmonary function inclusion criteria that indicate the need for pulmonary rehabilitation, since symptoms and functional limitations direct the need for pulmonary rehabilitation.

The pulmonary rehabilitation programmer includes exercise training, education, psychosocial/behavioral intervention, nutritional therapy, outcome assessment and promotion of long-term adherence to the rehabilitation recommendations.

Weight loss, as well as a depletion of fat-free mass (FFM), may be observed in stable COPD patients, irrespective of the degree of airflow limitation, and being underweight is associated with an increased mortality risk.

Nutritional screening is recommended in the assessment of COPD. Simple screening can be based on measurements of BMI and weight change. Patients are considered:

- underweight: BMI <21 kg · m⁻²; age >50 yrs,
- normal weight: BMI 21–25 kg · m⁻²,

- overweight: BMI 25–30 kg · m⁻²,
- obese: BMI ≥30 kg · m⁻².

Criteria to define weight loss are weight loss >10% in the past 6 months or >5% in the past month. Weight loss and particularly muscle wasting contribute significantly to morbidity, disability and handicap in COPD patients. Weight loss and loss in fat mass is primarily the result of a negative balance between dietary intake and energy expenditure, while muscle wasting is a consequence of an impaired balance between protein synthesis and protein breakdown. In advanced stages of COPD, both energy balance and protein balance are disturbed. Therefore, nutritional therapy may only be effective if combined with exercise or other anabolic stimuli ^[7].

1.3 Measurements techniques for the parameters of the respiratory system

In this section we are going to see two techniques for the measurements of pulmonary ventilation, which we used for the objectives of this thesis: the pneumotachograph, the respiratory inductive plethysmography (RIP) and the Opto-electronic Plethysmography (OEP). The OEP is an optical device able to non-invasively measure chest wall volumes changes and the RIP is another non-invasive technique designed to measure the thorax and the abdomen volume displacement signals. The pneumotachograph, with a mouthpiece and a noseclip, measures the flow at the mouth, and it can provide volume changes of the lungs.

1.3.1 Pneumotachograph

The basis of flow measurement in respiratory physiology is the pneumotachograph, which is a calibrated resistance (R) across which a differential pressure is measured (Fig. 1.18). When gas flows through the pneumotachograph, there is a pressure drop (ΔP) from the upstream side of the resistance to the downstream side that increases as flow (\dot{V}) increases:

$$\Delta P = R\dot{V}$$

If R is independent of \dot{V} over the range of flows of interest, then the pneumotachograph is said to be linear. Linearity is generally achieved only within a range of flow values, and therefore it is necessary to invert the previous equation to calculate flow from a measurement of ΔP .

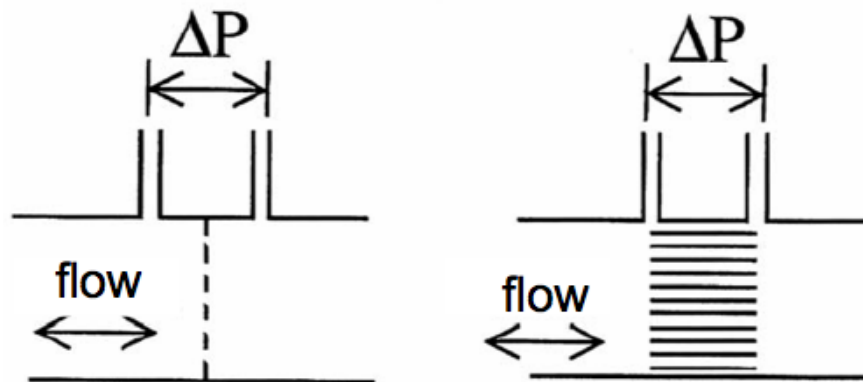


Figure 1.18: The pneumotachograph (longitudinal view). Flow-resistive elements can consist of either wire screen (*left*) or a honeycomb arrangement of conduits (*right*)^[8].

The frequency response of a pneumotachograph depends on the construction of its resistive element, which may have a honeycomb arrangement of conduits or consist of a wire screen. The honeycomb type is less likely to become partially blocked by secretions but has a poorer frequency response than the screen type, as ΔP become dependent on a second term proportional to the derivative of the flow time through the inertia of the gas (which in turn is proportional to gas density and to the volume of the resistive element). Either type should be heated to above body temperature during prolonged use to avoid breath condensate from settling on the resistive element and changing its resistance (and hence altering the calibration of the device). Pneumotachographs can have a good frequency response above 20 Hz with a resonance occurring at around 70 Hz, provided that the associated differential transducer has a response at least that good and is connected with the shortest possible lengths of tubing. The frequency response of a pneumotachograph degrades rapidly as the tubing connecting the transducer to the lateral taps either side of the resistance element increases in length.

As concern the integration of flow a simple method for numerical integration is to calculate the area under the curve defined by the series of measured data (Figure 1.19). The key problem is that the sampling frequency should be high enough so that the errors involved in approximating the true curve between points are negligible.

Another important problem is integration drift. When flow is integrated to yield volume, an upward or downward drift in the volume baseline is invariably seen. Some degree of drift is expected for purely physiological reasons. For example, the respiratory exchange ratio (i.e. carbon dioxide production/oxygen consumption) is usually ~ 0.8 , i.e. the volume of O_2 absorbed by the lungs is 20% greater than the volume of CO_2 excreted. This is reflected in a slightly greater volume

of gas being inspired than expired with each breath. Also, if the inspired air is not warmed to body temperature and pre-humidified, the volume of gas expired with each breath can be increased by up to 5%, relative to that inspired, by a gain in water-vapour content. These physiological effects contribute to a gradually increasing or decreasing volume measured at the mouth, but not to a real change in baseline lung volume. In addition to the physiological factors discussed above, the following methodological factors also contribute to volume drift:

1. *Temperature changes between inspired and expired gas.* If the inspired air is not warmed to body temperature before passing through the pneumotachograph, it has a different viscosity and density than expired air, which causes the pneumotachograph to register the transit of an equal number of molecules differently between inspiration and expiration. Variations in temperature may also affect the physical dimensions of the pneumotachograph due to the coefficients of thermal expansion of its components.
2. *Changes in gas composition between inspiration and expiration.* Inspired and expired gases differ in their partial pressures of O₂ and CO₂. This leads to slight differences in the viscosities of the gas mixtures, with concomitant effects on the flows registered during inspiration and expiration by the pneumotachograph.
3. *Leaks.* Any leaks between the airway opening and the pneumotachograph, whether through the mask seal or around a tracheal tube, cause a discrepancy between the volume registered by the apparatus and that entering or leaving the lungs, and hence a drift in volume. This problem is most likely to occur immediately after mask displacement, such as if an infant patient moves, or in a pressurised system (e.g. during artificial ventilation).
4. *Zero offset in flow calibration.* If the true zero flow is registered as some finite value, then integration of this offset over time results in a linear drift in volume with a slope equal to the offset. Accurate delineation of the zero flow point is more difficult as the sensitivity of the pneumotachograph decreases, which generally occurs as the linear range increases. The resolution of the A/D converter used to sample the flow also sets a limit on how accurately the zero flow point can be identified. Therefore, perfect offset compensation is never possible. To prevent this volume drift, a dead band around the zero flow, in which all values are set to zero, is used in some devices. However, a dead band can hamper breath detection, especially when flow is very low; thus its use and the flow thresholds of the dead band should be described by the manufacturer of the

equipment.

5. *Imperfections in the pneumotachometer response.* If the transducer for measuring flow does not function as a perfect measuring instrument (which is always the case to some degree and may be significantly so under dynamic conditions), it is unlikely that the inspiratory and expiratory flows are measured equally. This produces asymmetries in the recorded flow. Such asymmetry can often be seen in measurements from infants intubated with small endotracheal tubes, due to the geometric differences on either side of the pneumotachograph.

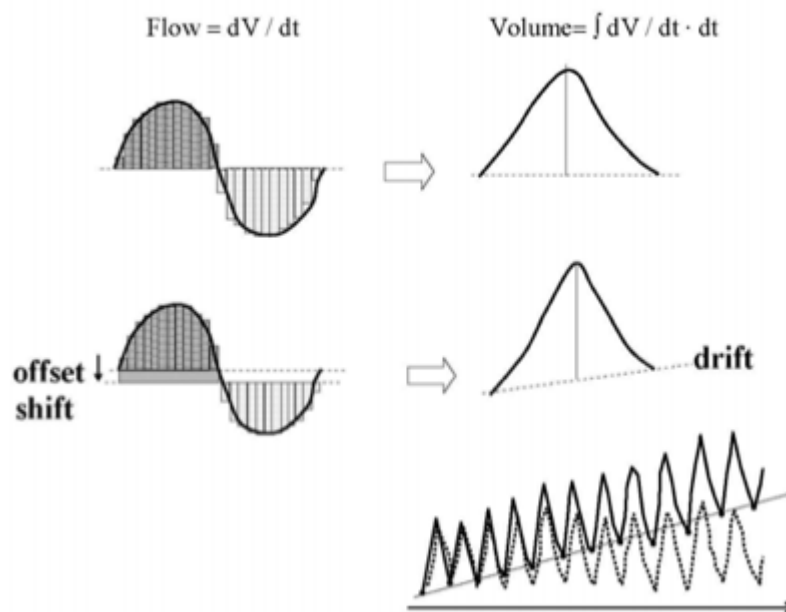


Figure 1.19: *Top panel*, volume is obtained by numeric integration of flow signal. *Middle panel*, different physiological and methodological factors (see text) contribute to an offset shift in the flow signal, which determines a drift in its numeric integration. *Bottom panel*, example of volume drift correction. The oscillating volume signal drifting upwards (*solid line*) has a straight line that characterises its drift. Subtracting this line from the volume yields a drift-corrected signal that oscillates about a stable baseline (*dotted line*)^[8].

As concern the correction of drift, it might be possible to avoid drift in volume in this type of data record by pre-conditioning the inspired gas to body temperature pressure saturated (BTPS) conditions, continuously monitoring gas partial pressures in both the alveoli and the pulmonary arterial and venous blood to correct for respiratory-exchange ratios not equal to unity and eliminating all the methodological factors discussed above. However, this is extremely difficult, if not impossible, in practice. Consequently, it is never known how much of the baseline drift in volume is due to drift and how much represents a true change in absolute lung volume. Also, because the subject is assumed to be in the physiological steady state when data are recorded, the

assumption is generally made that Functional Residual Capacity (FRC) remains more or less constant throughout the study period. Such a situation is thus forced on the measured volume signal by some kind of drift correction algorithm that first assesses the drift and then removes it. This does not, of course, mean that FRC must be identical from one breath to the next, but merely that there is no net upward or downward trend in FRC over a period containing many breaths.

Although the resistive pneumotachograph is the principal device used to measure flow in respiratory applications, other devices have been proposed. Ultrasonic transducers based on differences in time-of-flight of sound propagating into the direction of flow versus away from it have an excellent frequency response and avoid the problems of a resistive element becoming clogged with secretions. Devices based on the rate of cooling of a heated wire are also used ^[8].

1.3.2 Respiratory inductive plethysmography

Respiratory Inductive Plethysmography (RIP) is a technique that is able to measure lung volume changes. It is composed of two inductive coils of insulated electric wire sewn into the shirt and placed around the thorax and abdomen. Each coil is connected to an oscillator module that produces a sine wave of approximately 20mV of amplitude and at a frequency of 930 kHz and 850 kHz, respectively for thorax and abdomen's coil. This module is in turn connected to a demodulator unit which outputs signals proportional to the cross-sectional area of each coil. In fact changes in cross-sectional area of each compartment produce variations in self-inductance of the wire, thereby changing frequency. This frequency change is demodulated to produce an analog voltage corresponding to waveforms of ribcage and abdomen compartmental volumes as they change during respiration ^[10]. A microcontroller performs the acquisition of the volume traces continuously and an analysis software can be used to calculate volume changes and breathing rate. (Figure 1.20).

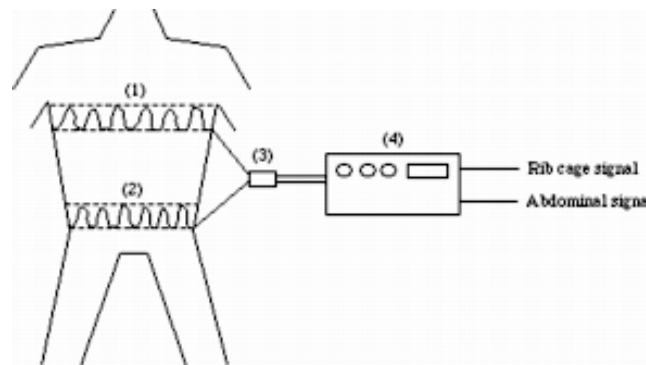


Figure 1.20: The respiratory inductive plethysmography system including the rib cage (1) and abdominal (2) sensor bands, the oscillator (3), and the signal demodulator (4).

The weighted sum of the ribcage and abdomen is therefore proportional to the tidal volume (V_T). Whereas uncalibrated RIP is a valuable means of assessing both respiratory timing and various qualitative aspects of ribcage and abdomen asynchrony, calibration is essential if quantitative changes in ventilation are to be assessed. Such calibration, involves a two-stage process of determining the relative contributions of ribcage and abdomen to each breath and then ascertaining a proportionality coefficient in order to scale the weighted sum to actual tidal volume.

Five main methods of calibration have been proposed:

- 1) The ribcage (RC) and abdomen (ABD) signals are compared with simultaneous recordings of V_T from a PNT, according to the equation:

$$V_T = K (V_{RC} + V_{ABD}) \quad (1)$$

where V_{RC} is the amplitude of the RC signal expressed in V and V_{ABD} is that of the ABD signal. Providing V_T is measured over a large enough number of breaths, a proportionality coefficient K can then be derived using a least squares or graphical solution to the equation. However, since this always requires the simultaneous use of a PNT, the advantages of RIP are at least partially lost ^[12].

- 2) In 1987 it was described the isovolume maneuver, as a means of determining the relative contribution of RC and ABD without a PNT. This requires the subject to shift gas gently between the RC and ABD during a breath hold or airway occlusion, thereby producing paradoxical movements of the two compartments. Since V_T does not change, equation (1) can be rewritten as:

$$K = -V_{ABD}/V_{RC} \quad (2)$$

This is, however, unsuitable for infants and young children since it requires the subject's cooperation. In an attempt to overcome this problem, various modifications of the isovolume technique have been proposed for use in infants and children, including the use of different patterns of ventilation, due to changes in body posture, sleep state or airway occlusion, to derive the relative contribution of the RC and ABD to the tidal volume and thereby assign appropriate calibration coefficients. Nevertheless, these methods generally remain too

complex for wide- spread use ^[12].

- 3) In 1989 it was described a computerized method of calibration termed Qualitative Diagnostic Calibration (QDC). This allows calibration to be performed during natural, quiet breathing by taking advantage of spontaneous variations in the relative contributions of the RC and ABD to different breaths to solve equation (1). This method is based on the assumption that, if the subject breathes with a constant tidal volume, the variability of RC and ABD displacements, as reflected by their standard deviation, can be used to solve for the proportionality constant K , such that:

$$K = - SD(V_{ABD})/SD (V_{RC}) \quad (3)$$

The QDC method is based on the same assumptions as those outlined by the second method, but requires two additional assumptions. The first is that of a constant V_T , which is approximated by collecting 5 min of tidal breathing and excluding breaths which differ by >1 SD from the mean sum ($V_{RC} + V_{ABD}$). The second assumption is that there is intrinsic variability in the relative contribution of the RC and ABD to tidal breathing. These additional assumptions allow the derivation of qualitative calibration coefficients from the breath-to-breath variance of the uncalibrated RC and ABD signals, using specialized software. While this method only provides information about the relative contribution of the RC and ABD, the simultaneous use of a PNT allows derivation of the volumetric scaling factors, thus allowing derivation of quantitatively calibrated values for the QDC V_T if so desired ^[12].

- 4) In this thesis, the RC and ABD signals are compared with simultaneous recordings of V_T from a Pneumotachograph (PNT) or a Opto-Electronic Plethysmography (OEP) or a Spirometer (SP), according to the equation:

$$\Delta V_T \cong M [K(\Delta uV_{RC}) + \Delta uV_{ABD}] \quad (4)$$

Where ΔuV_{RC} is the changes of uncalibrated RC, ΔuV_{ABD} the changes of uncalibrated and ΔV_T the change of volume measured by OEP or PNT or SP. This method is based on the assumption that the subject breathes with a constant tidal volume and providing V_T is

measured over a large enough number of breaths. The calibration coefficients K and M are derived using a Linear Least Squares method.

- 5) Finally, we introduced an improvement of the previous method, the RC and ABD signals are compared with simultaneous recordings of V_T from a Spirometer (SP), according to the equation:

$$\Delta V_T \cong M[K(\Delta V_{RC}) + \Delta V_{ABD}] + Q \quad (5)$$

Where ΔV_{RC} and ΔV_{ABD} are the ribcage and abdominal signals, and ΔV_T is the signal measured by a Spirometer. This method is based on the assumption that the subject breathes with a constant tidal volume and providing V_T is measured over a large enough number of breaths. The calibration coefficients K , M and Q are derived using a Linear Least Squares method.

1.3.3 Opto-Electronic Plethysmography

As shown in Figure 1.21, OEP is based on an automatic motion analyser that detects passive markers composed of a thin film of retro-reflective paper on plastic hemispheres (5–10 mm diameter). The markers are placed on the skin by bio-adhesive hypoallergenic tape. Special TV cameras (solid-state CCDs) operate up to 120 frames per second synchronised with coaxial infrared flashing LEDs. A dedicated software processes in real time the images coming from the different cameras (six in the typical configuration,) to compute their 3D co-ordinates by stereo-photogrammetric techniques. From the 3D co-ordinates of the points belonging to the chest-wall surface, the volume enclosed by any surface described by proper geometrical models can be computed at each frame. Different geometrical descriptions of the chest wall can be achieved in order to obtain the volume enclosed by the whole chest wall surface or those of its different compartments.

In the first studies based on OEP measurements, the chest wall was modelled as being composed of three different compartments: the pulmonary rib cage (RCp), i.e. the part of the rib cage apposed to the lung; the abdominal rib cage (RCa), i.e. the part of the rib cage apposed to the diaphragm, and the abdomen (Ab). Thus, the total chest-wall volume is the sum of V_{RCp} , V_{RCa} and V_{Ab} .

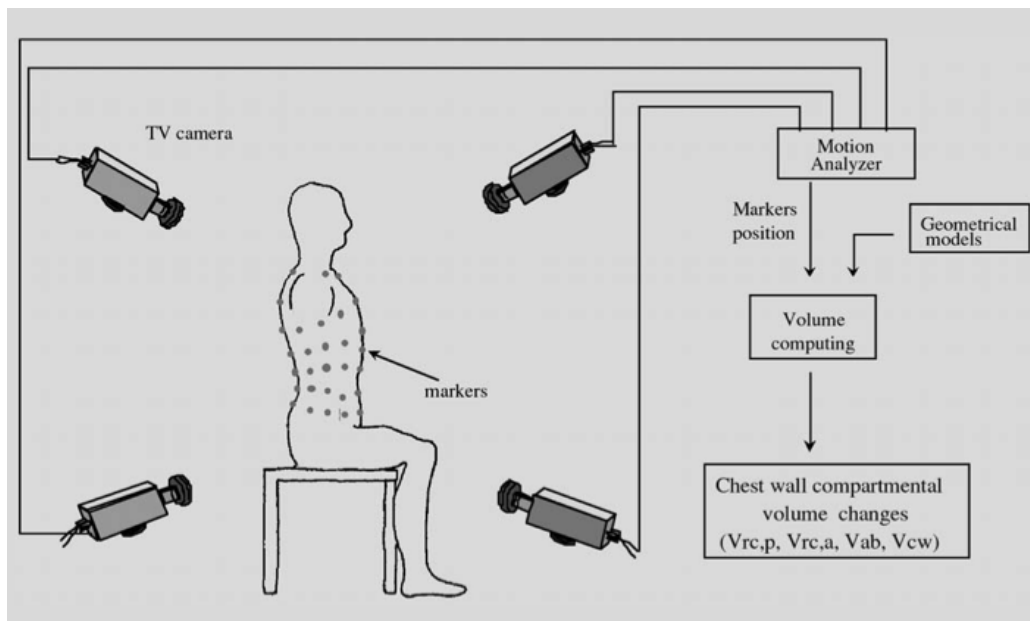


Figure 1.21: Opto-electronic Plethysmography: principle of measurements ^[8].

One of the most useful characteristics of OEP is that the subdivision of the chest-wall volume into different compartments is totally free and, in this context, the ability of the OEP to measure the subdivision between right and left chest wall expansion is particularly useful when asymmetries of respiratory muscle action and chest wall compliance are being considered.

OEP has been used following various measurement protocols specifically developed for different applications and different experimental and clinical situations. In the arrangement designed for the analysis of subjects in sitting and standing positions, 89 markers are arranged at different levels on the anterior and posterior surfaces of the chest wall. OEP has been successfully used also in constrained postures, such as supine and prone positions. In these situations, the analysis is performed by placing the markers only on the visible part of the trunk surface, while the inferior part should be fixed to the support (e.g. the bed) ^[8].

Once the 3D coordinates of the points belonging to the chest wall surface have been acquired, the next step is to compute the volume of the closed surface obtained by connecting the points to form triangles. Starting from the measured points a special geometrical modelling of the chest wall was developed to describe the surface of the whole chest wall and its different compartments (Figure 1.22).

The definition of the geometry of the model allows the computation of the enclosed volume and its variations determined by movement by integrating over the surface using Gauss's theorem to obtain a volume integral. In detail, the analytical expression of the theorem is:

$$\int_S \mathbf{F} \cdot \mathbf{n} dS = \int_V \nabla \mathbf{F} dV \quad (1)$$

where S is the surface, V is the volume enclosed by S , \mathbf{F} is an arbitrary vector, \mathbf{n} is the normal unit vector at the different points of S , and ∇ is the divergence operator.

If we choose an arbitrary vector with a unit divergence, Eq. (1) becomes:

$$\int_S \mathbf{F} \cdot \mathbf{n} dS = \int_V dV = V \quad (2)$$

and the volume integral is computed by means of an easier surface integral. Passing from continuous to discrete form, Eq. (2) becomes:

$$\sum_{i=1}^K \mathbf{F} \cdot \mathbf{n}_i A_i = V$$

where K is the total number of the triangles, A_i is the area of the i^{th} triangle, and \mathbf{n}_i is the normal unit vector of the i^{th} triangle.

Considering the geometric model of the whole trunk surface it is thus possible to obtain total chest wall volume variations, and, in addition, the contributions of different chest wall compartments to the total volume change.

After several experimental iterations the model has been optimized to obtain a satisfactory trade off between accuracy and clinical feasibility. The best arrangement consisted of 89 markers in the seated, 45 markers in the supine and 52 in the prone position ^[9].

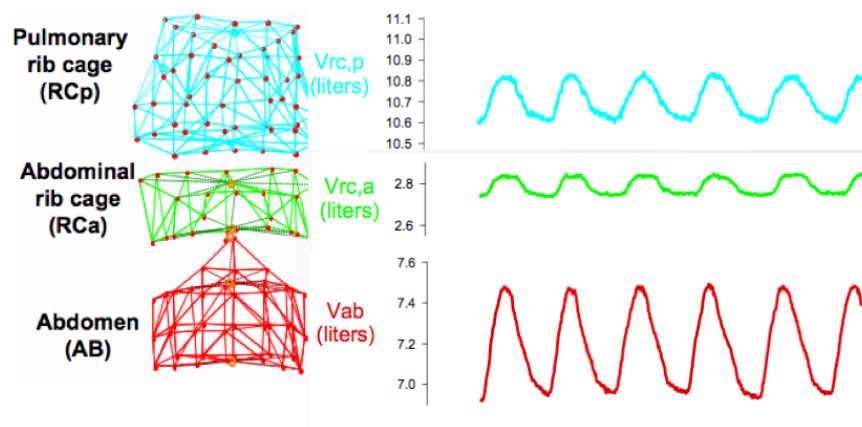


Figure 1.22: Geometrical models of the three chest wall compartments: pulmonary rib cage (RCp), abdominal rib cage (RCa), and abdomen (AB); (left) their volumes changes during quiet spontaneous breathing.

OEP has the great advantage that it can measure breathing patterns in any conditions (e.g. rest, exercise, phonation, sleep) where the chest wall can be visualized totally noninvasively. It can be used to study respiratory kinematics and, if combined with pressure measurements, statics, dynamics, and energetics. It is highly accurate in the measurements of total chest wall volume variations, allowing partitioning of the complex shape of the chest wall into different compartments. In addition to being non-invasive it requires no connection to the patient. Furthermore, it is not based upon any subject-specific calibration, because it provides a direct measurement of the volumes in a three-dimensional reference frame ^[4].

Chapter 2

Telemedicine for monitoring COPD patients

In this chapter is presented an introduction of the telemedicine services for patients affected by COPD and it is shown a new approach for managing COPD patients at their home.

2.1 State of the art

Telemedicine is the use of information and communication technologies to provide and support healthcare when distance separates two subjects, typically a patient and the caregiver or two caregivers. Diagnosis, interventions, and treatment decisions are based on information transmitted through telecommunication technologies. Telemedicine is not a new type of medical treatment it only changes the care delivery process.

In telemedicine usually two participants are involved, the caregivers and patients. Four common uses of telemedicine are identified:

- Teleassistance: physician assists a patient who is geographically isolated.
- Telemonitoring: transmission of medical information for monitoring purposes.
- Teleconsultation (patient-caregiver): patients seeking for medical advice.
- Teleconsultation (caregiver-caregiver): one caregiver helps the other one.

Telemedicine is not new, the first telemedicine system was introduced by Einthoven in 1905, analogic telephone lines were used to transfer electrocardiograms (ECGs) from a hospital to a laboratory. Ever since a wide variety of telemedicine applications have been developed, varying from remote asthma monitoring to real-time monitoring of vital signs of astronauts in space.

A mistake that can be made is that telemedicine involves using the most edge cutting and sophisticated technologies; for example, simple telephone consult is also an example of telemedicine.

Telemedicine encompasses both health telematics services and the systems that make use of the

telematics services. Telemedicine is focused on the delivery of care and is a subset of telehealth. *Telehealth* encompasses not only clinical applications, but also educational, research and administrative applications. More recently the term *e-health* has been introduced. E-health relates to the delivery of online electronic health information, products and (direct) services, offered by professionals, non-professionals, businesses and consumers ^[13].

The number of people suffering from chronic diseases is rising and so are the costs for their care. These and other facts create significant challenges to the current healthcare systems, which were mainly designed to look after acute episodes, and therefore, are not adapted to the kind of care required by chronic diseases. The management of chronic patients has become a key area of research and telemedicine is a possible way of solution for ensures quality and cost containment.

Home care should focus on a patient-centered perspective and patient and family satisfaction: reduction of complications resulting from hospitalization; maintaining an acceptable quality of life; and enabling a comfortable and dignified death have been proposed as major end-points. Chronic obstructive pulmonary disease (COPD) seems to be the most problematic chronic disease for all the health systems, with frequent exacerbations, hospitalizations and related costs. Various follow-up models to prevent hospitalizations and exacerbations have been proposed: these include self-management, home care and dedicated chronic care model with or without support via information technologies. The need to rationalize healthcare costs has prompted the development of new technologies for home assistance ^[14]. In the 1990s, electronic diary and spirometer systems were mostly used for telemonitoring, while recent studies introduced more sophisticated technologies such as handheld devices, digital technology, and wireless networks. Some technologies used for telemonitoring may have important effects on patient behavior. The use of complicated procedures for data transfer that involve video transmission or non-user-friendly monitors for recording symptoms is associated with poor compliance, as opposed to applications with reminders and prompts, which are associated with good patient adherence. Overall, ease of use and friendliness of the technology and monitoring equipment may contribute to good compliance among patients and their acceptance of the telemonitoring systems ^[15].

In a recent systematic review of home monitoring for COPD six studies were analyzed. The effectiveness of telemonitoring interventions was evaluated in the patient's medical condition and quality of life, reductions in health service utilization and economic savings. The specific findings of each study are summarized in Table 2.2 ^[16].

Four of the six studies had an educational component to their intervention programme; the others provided ongoing information throughout the course of the intervention on disease management and

illness education via a web-based computerized programme. The frequency of telemonitoring assessments or contact with the health care provider over the course of the follow-up period varied greatly across the included studies. Five of the six studies required the patients to record physiological indices of their health status (e.g. arterial oxygen saturation, pulmonary functioning); four of the six studies relied on the patients’ subjective report or their symptoms and vital signs. In these studies, the staff of a call center recorded the patient’s responses to a set of questions that assessed the likelihood of an exacerbation given the severity of the patient’s symptoms. Table 2.1 summarizes the telemonitoring components used in the included studies. The studies were composed of multiple components and it is not clear whether the educational strategies, the increased professional contact or the monitoring technologies had the most impact. It is likely that there is a synergistic effect of the different components.

The outcomes of a telemonitoring intervention are therefore: exacerbations (recognized and unrecognized) and their eventual outcome in terms of treatment, and its eventual impact on service use. Four of the six studies examined whether participation in telemonitoring intervention reduced the number of COPD exacerbations and two of these reported a statistically significant reduction. Two of the six studies examined the patients’ self-reported quality of life, only one of these observed a significant improvement. Only one of the six studies reported mortality as an outcome and did not find any reduction in mortality rate with intervention. All these studies are positive about their results, but the benefit of telemonitoring for COPD is not yet proven, for the lack of heterogeneous population and because the telemonitoring intervention is generally poorly described

Reference	Measurement parameters				Recording of biomarkers		Call/web centre access*	Data transmission			Assessment process		
	Spirometer	Pulse oximeter	Peak flow	Symptom report	Nurse	Patient		Auto	Video	Verbal	Auto alert	Lay person	Clinician
Dang (2006) [18]				•			•	•		•	•	•	
Koff (2009) [13]	•	•		•		•		•				•	
Maiolo (2003) [17]		•		•		•		•		•		•	
Pare (2006) [15]			•	•		•	•	•		•		•	
Trappenburg (2008) [16]				•		•		•		•		•	
Vitacca (2009) [14]		•		•		•	•			•		•	

[16]

Table 2.1: The components of the telemonitoring intervention in the six studies [16]. *Patients could contact these centres with a health-related query when required. Typically, call centers were staffed for 8 hours a day, 5 days a week. Outside of these hours, an automated service was provided.

These studies shown that the principal motive for using remote monitoring is to identify COPD exacerbations at a point in which it might be possible to intervene successfully, that is, to reduce the risk of hospital admission by using appropriate therapy as soon as possible. For the success of the home telemonitoring, it is important consider the patient’s condition, the type of telemonitoring

service and duration, and the frequency, type, and amount of transferred data. The integration of reminders and alarms into monitoring devices might improve patient compliance, and is also essential the development of user-friendly interfaces that can be used by patients of all ages. With these objectives Chronious, an innovative project with intelligent sensors and a decision support system, has been developed. This platform is focused on realize simple, customized and adaptive interfaces that take into account the user's profile, medical history and relating HCI (human-computer interaction) factors. Emphasis is placed on designing interfaces appropriate for each user category (patients, healthcare professionals). The system integrates state of the art sensors and services. The intention is covering in the area of chronic diseases both patients and healthcare professional's needs. Data is collected by using intelligent sensors, mostly wearable, that control continuously vital signals, dietary habits and plans, drug intake, environmental parameters, biochemical parameters, activity and social context. In addition, wearable context monitoring allows long-term recording of patient activity and situations to which has been exposed. All the information collected is fundamental for evaluating disease signs, patients' behavior and activity, and their contextual situations. Another important feature of this project is its intelligence, which is devoted to patients' monitoring data analysis and understanding, able to provide clinicians with filtered information and advices for their decision making. The aim of such services are: analyze collected data for identifying worrying conditions, alert clinicians when an acute event is happening and combines patients' information for providing suggestion on possible changes of therapeutic plans. The continue monitoring of many parameters, and most importantly, the generation of alarms if a potential health risks or abnormal behavior is detected makes Chronious a promising platform for the management of the chronic diseases.

First author (year)	Design (evidence score)	Included patients, sample and power calculation	Intervention	Follow-up months	Economic evaluation	Results
Dang (2006) [18]	UBA (4)	Overall sample 59 [†] (COPD, DM and CHF). COPD n = 17 male veterans aged ≥60 years. Power calculation not performed.	Automated system logged patients' self-reported symptoms and provided illness education. Referral alerts were generated if patients' status changed.	6	No	No significant differences in the number of bed days of care, outpatient visits, hospital admissions or emergency department visits.
Koff (2009) [13]	RCT (2b)	COPD GOLD Stage 3 or 4. Intervention: n = 19, 55% female, mean age = 67 years. Control: n = 19, 50% female, mean age = 65 years. Power calculation reported.	Intervention: patients transmitted self-reported symptoms, oximetry and spirometry readings to a central record system. Daily completion of illness education and disease management modules. Contact with coordinator via mobile phone. Control: usual care.	3	RC	Significant difference in St George's Respiratory Questionnaire scores between groups. Data on exacerbations in control group not collected. No savings in medical costs reported; no adjustment for intervention costs.
Maiolo (2003) [17]	UBA (4)	n = 20 [†] , with COPD and on long-term oxygen, 9% female, mean age = 73 years. No power calculation reported.	Twice weekly nocturnal pulse oximetry readings sent via telephone line to a central storage system. Scheduled calls by doctor to patient after analysing the oximetry data.	12	RC	Significant decrease in the number of hospital admissions (2.15 vs. 1.21 admissions), in Phase 1 versus Phase 2 respectively. (P < 0.01).
Pare (2006) [15]	NCBA (4)	Patients with respiratory failure, emphysema and asthma. intervention: n = 19, 37% female, mean age = 69 years. Control: n = 10, 50% female, mean age = 72 years. No power calculation reported.	Intervention: Patients transmitted peak flow symptoms and medication data. Control: usual homecare. Both groups had access to a nurse-led telephone service.	6	CMA	Significantly fewer hospital admissions in the intervention group than the control in the 6-month study, 2 versus 6, (P < 0.05). However, when the intervention patients were admitted, the duration was significantly longer, 13.5 versus 7.3 days (P < 0.01). Reported cost saving of \$355 per person.
Trappenburg (2008) [16]	NCBA (4)	COPD patients GOLD 3 and 4: Intervention: n = 59, 54% female, mean age = 69 years. Control: n = 56, 39% female, mean age = 70 years. No power calculation reported.	Intervention: patients transmitted symptoms and medication data. Illness education and disease management training was provided. Control: usual care.	6	No	Reported statistical difference in number of exacerbations (P < 0.004) and hospital admission in intervention group compared to control group (P < 0.02) but the numbers of events are low. No significant differences in quality of life scores, number of inpatient days or outpatient visits.
Vitacca (2009) [14]	RCT (2b)	Patients on home mechanical ventilation or on long term oxygen therapy. Intervention: n = 57. Control: n = 44. * No other details by diagnosis. Power calculation not performed.	Intervention: regular telephone appointments with a nurse where patients gave oximetry readings and reported their symptoms. Access to call centre. Control: usual care.	3-12	CMA	Significant decrease in the average number of hospital admissions in the intervention group (P < 0.02). Patients in the intervention group showed a greater probability of remaining free of emergency visits (P < 0.001), general practitioner calls (P < 0.02) and exacerbations (P < 0.001). No differences in mortality rates. Telemonitoring costs 50% cheaper per patient.

Table 2.2: Characteristics of six studies on home telemonitoring in patients with COPD [16]. CMA, cost minimization analysis; CMF, congestive heart failure; COPD, chronic obstructive pulmonary disease; DM, diabetes mellitus; GOLD, global initiative for chronic obstructive lung disease; NCBA, non-randomized controlled before and after study; RC, reported costs; RCT, randomized clinical trial; UBA, uncontrolled before and after study.

2.2 Chronious: a new system for COPD patients

The Chronious project aims to create a platform that evolves in monitoring patient's health status: the idea is to develop an ubiquitous system that can extract clinical knowledge in a highly personalized level developed by the analysis of health status' collected data.

The Chronious objectives are very innovative taking into account the current state of the art in monitoring Chronic Obstructive Pulmonary Disease (COPD) patients and in corresponding ontology platforms.

Chronious suggests the implementation of generic system architecture to be easily adapted to any chronic disease management program. For testing purposes, it focuses on two major chronic conditions, but the aim is to create an easily adapted system to other chronic diseases requirements.

By such an approach quality of life can be raised and highly qualified and efficient healthcare services to the citizens can be provided (e.g. through disease prevention, ubiquitous and seamless to the user monitoring, adaptive interaction based on user characteristics and context of activity, reduction of unnecessary visits to hospitals and complexity of self-care especially for patients with chronic diseases). An advanced disease prediction and diagnosis tools and the exploitation of the vast pool of monitored parameters are provided (e.g. vital signs recorded for various users groups under diverse contexts and conditions) for the production of new diagnostic models and protocols. Thus some formal care burdens are reduced, and some others are improved. For example it is reduced the number of patients' visits for routine examinations, it is improved the prevention, diagnosis and in some cases prognosis of diseases, and is facilitated the immediate intervention in emergency or time-critical situations.

The approach addresses mainly two categories of users: patients, the real final users, which have to wear and interact with the system and healthcare providers, which have to use the system to monitor remotely the health conditions of the patients^[17].

2.2.1 General description

The system design is flexible. It integrates state of the art sensors and services. Data is collected by using intelligent sensors, mostly wearable, that control continuously vital signals, dietary habits and plans, drug intake, environmental parameters, biochemical parameters, activity and social context.

In Figure 2.1 there is a general scheme for the design and the development of Chronious healthcare systems and applications employed in patient monitoring and medical diagnosis. The main characteristic of this scheme is the ability of configuration and remote control by medical

experts or clinicians.

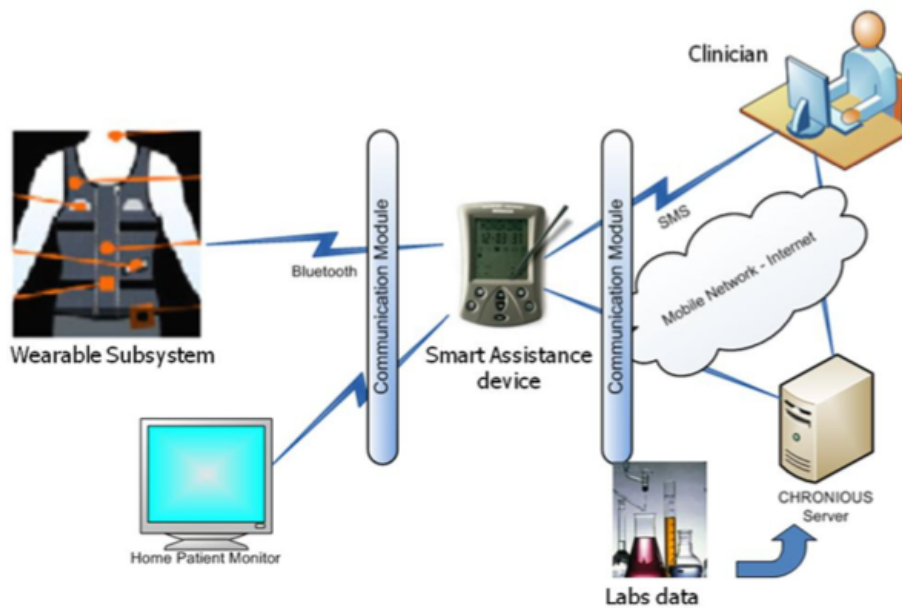


Figure 2.1 Architectural diagram of Chronious systems.

The integrated platform aimed here covers seven primary functional blocks:

1. Sensing infrastructure
2. Communication and security infrastructure
3. Data handler
4. Home patient monitor
5. Smart assistant device
6. Chronious central system
7. Clinician framework

A particular attention is paid to *sensing* capabilities and to sensor networks, which play a key role in the design, performance and acceptance of the wearable system. The choice of the localization of non-invasive devices has to satisfy several criteria and limitations like monitoring the most significant signals for the identified diseases, obtaining the best signal/noise ratio, fixing and ergonomic aspects as well as unobtrusiveness. Additional external devices will be used measuring blood glucose, body weight and blood pressure and interacting with the smart assistant device in order to provide additional clinical information.

Allowing the user maximal mobility requires wearable sensors. These sensors are a subsystem of a Wearable Platform. There are four types of sensors (subsystems) required that set up the sensing

infrastructure:

- a) *Medical*: dedicated to health checking parameters
- b) *Motion*: for activities monitoring
- c) *Environmental*: to control the quality of patients living environment
- d) *Social-Context*: to monitor the quality of life

An essential part of a wearable system is the design and construction of the *communication and security infrastructure* that connects the different components, maintaining interoperability and efficiency in a safe environment.

Sensors located on various parts of the patient body use to be connected to the data handler via cables, which are minimized by embedding them in clothing.

The data captured by the sensing infrastructure is preprocessed and forwarded by the data handler to the patient's smart assistant device using wireless technologies such as Bluetooth protocols. The data handler resides on the wearable system worn by the patient and connects wirelessly to the smart device, in order to avoid cables. The data handler will be responsible for raw data collection from the sensors and compression, when possible. It will also be responsible for performing sensor monitoring by periodically checking the status of the sensors along with their remaining battery levels. Moreover, events will be generated under certain circumstances that will enable the smart assistant device to proceed to according actions. The central role in the system holds the smart assistant device that is responsible for accepting input from the patient through an efficient interface along with gathering real time information from the patient's sensing infrastructure. The *home patient monitor* is to display the data of the smart assistant device on a larger screen and will allow the patient and caretakers to interact with the application in a comfortable and user-friendly way (Figure 2.2).

This information is processed locally and then transmitted to the *Chronious central system* for further manipulation and long-term storage. Therefore the smart device acts as a bridge between the patient's environment and the Chronious framework central infrastructure. When the smart device is set on a low power mode, during periods of a patient's inactivity the data handler will store the amount of collected data and after specific time intervals or in an emergency episode it will generate an event to set the smart device back to normal mode transferring the more resent monitoring data.

The data about a case must be adequate for making an informed decision, but they must not be

excessive. Indeed, a major challenge occurs when decision-makers are bombarded with so much information that they cannot process and synthesize the information intelligently and rapidly. Thus, it is important to know when additional data will confuse rather than clarify and when it is imperative to use tools (computational or otherwise) that permit data to be summarized for easier cognitive management. By profiling the *clinical framework* adapts to the patient's habits by intelligence mechanisms. In this way, the decisions made by the system become more personalized, flexible, adjustable, and in a sense more accurate. Most chronic diseases are greatly affected by *dietary and nutrition habits*. Also the importance of particular nutrition facts from foods and the impacts that these have to patient's health is different for each chronic disease. Therefore, it is necessary to have a nutritional planner module that manages patient's nutrition individually based on their characteristics and preferences, as well as their health situation and disease stage, especially for chronic diseases, which have great dependence on nutrition plans. The implementation of this is considered to be very complicated due to the enormous variety of food types and categories, as well as different national food recipes and various traditional cuisines. Another critical module is the *drug intake monitoring*. Here a patient input is required as the acknowledgement to an alert or reminder generated automatically from the platform based on a pre-setup schedule imported by the health professionals as part of the disease medication plan. Coupled with the pervasive communication, healthcare personnel can use internet technology to access vital signs information, review patient data and update patient charts. The design of an efficient and flexible interface for the clinician could improve the effectiveness in reviewing the patients' collected data during a longer period. The identification of health status variations will help in a better understanding the patients' pathology. Any trait of abnormal health status is recognized by the severity estimation component and actions (alerts, reminders) are formed and send to the appropriate recipients (patient, health professional, call center). The system generates alerts in case of invalid medical data or if current activity and behavior lay outside the well-established activity pattern and locomotion behavior. The Alert module provides with an intelligent "messenger" that sends alerts to the user interface of the device in a voice or display format while alerting the supervisor health professional of potential health risks or abnormal behavior. Alerts may be appeared wherever the context measurements exceed some given thresholds (vital signs or audio and locomotors events). Additionally, through the utilization of the GSM network, the clinician can be informed automatically about possible emergency episodes of a patient. The feedback of the clinician might be an alteration to the patient's treatment plan or a proposal for an alternative pharmaceutical schedule.

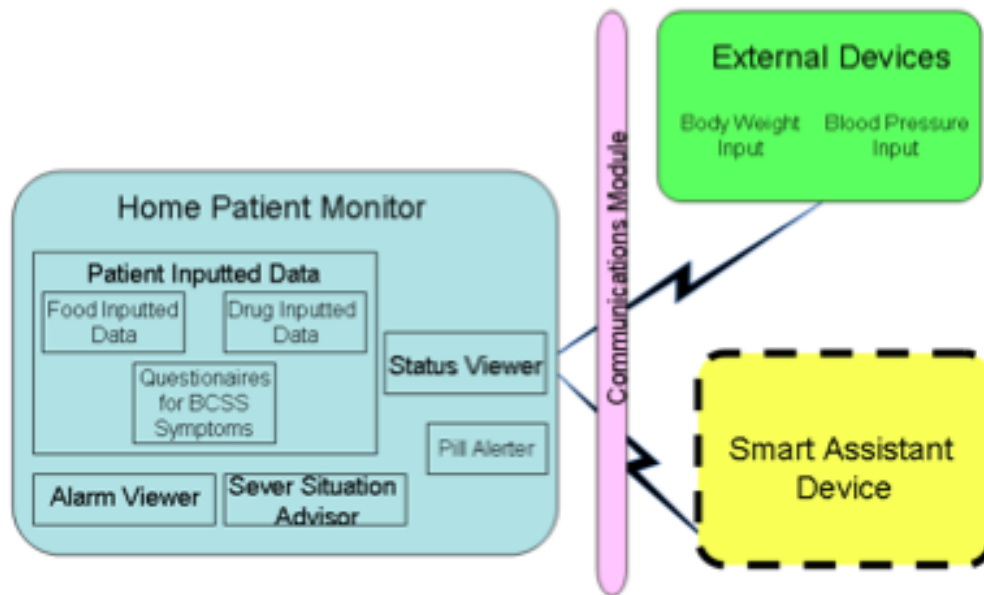


Figure 2.2: Managing and displaying the patient data.

Chronious also uses *ontologies* for knowledge management and information retrieval. The ontology is a hierarchically structured set of terms to describe the domain that can be used as a skeletal foundation for a knowledge base (in this case knowledge for COPD and renal insufficiency). In ontology, concepts, their properties and relationships, constraints and rules are described in a formal language, which makes ontologies interpretable to a computer program. Domain medical ontology provides a vocabulary for representing and communicating knowledge in that domain and a set of relationships among the terms in that vocabulary. When integrated into a broader telemedicine system, this has the potential of a revolution in medical research by data mining the literature resources and clinical information ^[17].

2.2.2 Wearable platform

The Wearable Module is an integration of different sensors and a T-Shirt; the aim is to infer complex information about the user's actions, the situation around him, and his interactions with the environment. These unobtrusive wearable sensors will allow monitoring of physiological parameters to be conducted over a period of time and, most important, in patient's natural environment. The wearable system is composed of a shirt made of washable stretch-material into

which are sewn several sensors (Figure 2.3) for the simultaneous measurement of the following parameters:

- Body temperature
- Ambient temperature and humidity
- Electrocardiographic activity and heart rate
- Respiratory activity and respiration parameters
- Arterial oxygen saturation
- Cough and snoring detection
- Motion and fall detection

The data coming from the sensors are collected and transmitted via wireless connection by the Data Handler, a microcontroller-based acquisition system. The data handler device is placed on a belt just below it, and is utilized for the collection and the transmission of the signals from the wearable network to the Smart Assistant Device through the Bluetooth protocol.

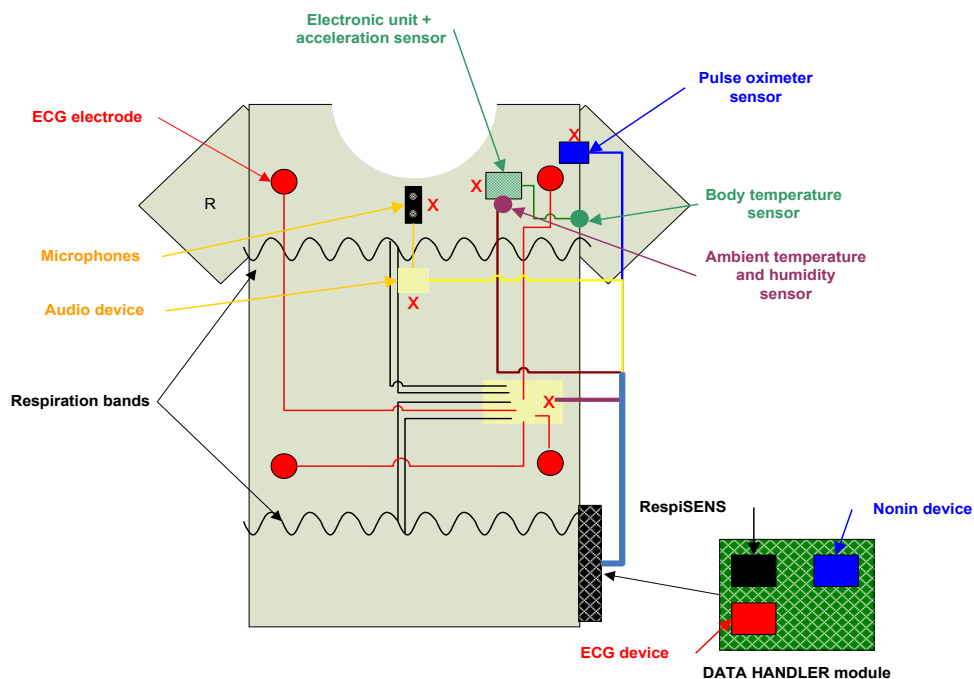


Figure 2.3: Draft of the T-shirt with integrated sensors and Data Handler module.

The electrocardiographic signal (ECG) is acquired by means of four dry electrodes that are a part

of the T-Shirt. They are woven directly on the internal side of the textile, precisely next to the right and left shoulder and next to the vertebral ribs, allowing the acquisition according to the Einthoven's triangle. They are made of silver fibres sewed on the internal side of the T-Shirt; the same material is used as “wearable wire” to conduct the ECG signal (Figure 2.4).

The arterial oxygen saturation and the heart rate are measured through the pulseoximetry technique. A pulseoximeter reflectance sensor (NONIN 8000R) is applied on the left shoulder (blue square on Figure 2.3).



Figure 2.4: Silver ECG electrode (left) and silver wires (right) used to conduct the ECG signal inside the T-Shirt.

The respiratory activity and the respiratory parameters are measured by means of two inductive bands placed around the rib cage under the armpits and around the abdomen over the belly bottom (Figure 2.5). The two respiratory bands are designed to measure the thorax and the abdomen volume displacement signal by means of the respiratory inductive plethysmography technique^[18].

The respiratory inductive plethysmography (RIP) technique can be non-invasively measured the independent motion of the rib cage and the abdomen using two wired elastic cloth-bands encircling the rib cage and the abdomen^[19] (See section 1.3.2).

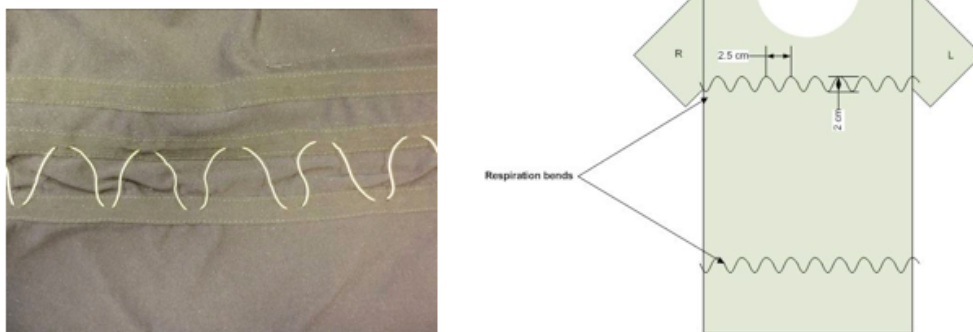


Figure 2.5: Inductive bands integration (left) and position inside the T-Shirt (right).

The body temperature is measured by means of the digital temperature sensor (IST AG, Wattwil, Switzerland), placed on the internal side of the T-Shirt near the left armpit.

The ambient temperature and humidity is measured by the temperature/humidity sensor (SENSIRION AG, Staefa, Switzerland) placed on the external side of the T-Shirt over the electronic unit (Green square on Figure 2.3).

The sensors used to detect the cough and snoring events are two miniature condenser microphones placed on the external side of the T-Shirt as shown on the figure 2.3 (black square).

Finally, the motion and fall detection is provided by analysing the output of a digital tri-axial acceleration sensor (Bosch Sensortec). The sensor is integrated inside the electronic unit (green square) as shown in Figure 2.3.

The spirometer (DATOSPIR MICRO, Sibelmed, Barcelona, Spain) is an external device and is part of the wearable module since it is the only one that forwards its measurement to the Wearable Platform. This spirometer must be able to send the flow tracing continuously during the calibration procedure. The comparison of spirometric flow and the bands signals over a period of few minutes provides, if appropriately processed by the calibration algorithms, the calibration coefficients for the RespiSENS^[18].

2.2.3 External devices

The external devices are some independent apparatuses, which communicate mainly with the Smart Assistant Device via Bluetooth. These devices collect data in some specific time periods, in a maximum frequency of 2-3 times per day. Since their recordings are collected, they are transmitted to the Smart Assistant Device for further processing and analysis. The external devices selected within the Chronious platform are five:

- The environmental monitoring system
- The spirometer
- The body weight scale
- The glucometer
- The blood pressure device

The *Environmental Monitoring System* provides measurements of the environmental parameters, which directly affect the health of the patient (Figure 2.6). It controls:

- In-door/out-door air quality of the environment in which the patient lives and acts.
- The presence of smoke or (chemical) particles.

Values acquired from this module are directly passed to the Home Patient Monitor (HPM); the HPM is the basic module of the Chronious Monitoring Framework.



Figure 2.6: The Environmental Monitoring System.

The *Spirometer* is an external handheld device, being used for the calibration of the signals extracted from the respiratory bands in Tidal Volume measurement. Data acquired by the Spirometer are passed directly to the smart assistant device (PDA) in order to compute the calibration coefficients of the Respiratory procedure (Figure 2.7).



Figure 2.7: The spirometer (DATOSPIR MICRO, Sibelman, Barcelona, Spain).

The *Blood Glucose Meter* is an external device, used by the patient in order to measure the glucose levels in blood (Figure 2.8). The measurements, which are quite important for chronic diseases, like COPD and especially CKD, can provide useful information about the effect of nutrition and drugs used in diabetes medication. The glucose meter module passes the data acquired to the HPM.

The *Blood Pressure Meter* is an external device, being used to measure the arterial blood pressure of the patient providing an accurate state of the patient's blood pressure levels (Figure 2.8). The blood pressure values acquired are passed directly from blood pressure meter to the HPM for further observation and analysis.

The *Weight Scale* external device is being used for body weight monitoring (Figure 2.8). For patients with CKD or COPD, the body weight monitoring procedure may indicate very important information for the patient's health state. As most external devices, the weight scale transmits its data acquired to the HPM ^[20].

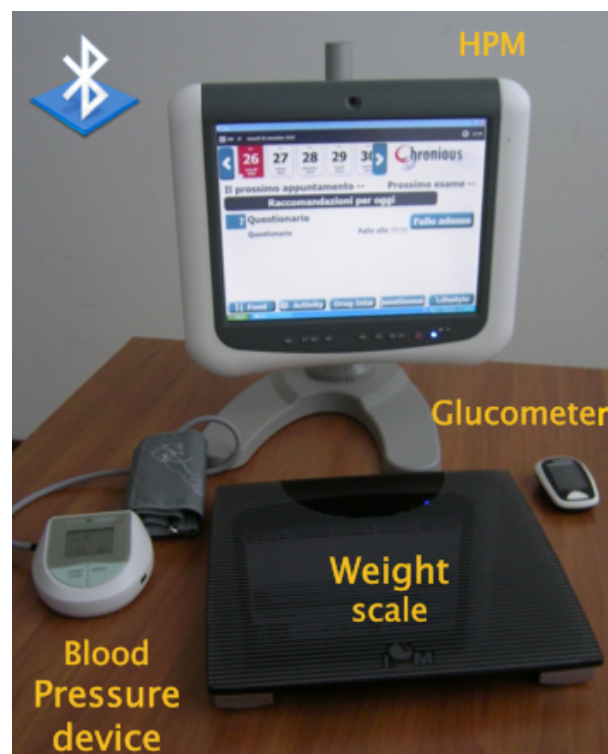


Figure 2.8: HPM, Blood Glucose Meter, Blood Pressure Meter, Weight Scale.

Chapter 3

Pre-testing phase

In this chapter is presented the pre-testing phase of the project in which a first prototype of the wearable device has been assembled and evaluated.

As we have seen in the previous chapters the Chronious platform is quite ample and complex, as it involves a lot of measuring and monitoring devices. The work of this thesis is focused on the respiration aspects and the devices used to collect respiration parameters. In this phase, the respiratory parameters are evaluated on five healthy subjects by comparing the data collected from the acquisition system with the measurements provided by the opto-electronic plethysmography (OEP) and a pneumotachograph (PNT) as references.

3.1 Experimental setup

The wearable system is composed of a T-shirt into which are sewn 4 ECG electrodes, two bands for respiratory inductive plethysmography (RIP) and a reflectance pulseoximeter. The T-shirt is made up by 8% of elastane and 92% of polyamide. It is machine washable at 30°, however the electronic unit and the sensors attached via the hook and loop fasteners must be removed before washing. The T-shirt is also realized tight enough in order to permit the measurement of the vital parameters and included a lateral zip to make elderly users easier the wearing of. Moreover, a back-lateral pocket is provided in order to host the prototype of the Data Handler device. Due to the high extensibility of the T-Shirt only two different sizes are provided (S/M and L/XL).

Into the shirt are sewn two bands for respiratory inductive plethysmography (RIP) for the measurements of rib cages and abdominal volumes. The electronic unit (RespiSENS) used to measure the changes in the bands inductance has been developed by the Fraunhofer Institute for Integrated Circuits IIS (Erlangen, Germany). RespiSENS is an embedded system based on a microcontroller (Texas Instruments) and is designed to measure thoracic and abdominal volume displacement signal sensed from the two integrated coils. The RespiSENS hardware includes two

LC oscillator circuits, an analogue to digital converter (ADC) and the microcontroller unit (Figure 3.1).

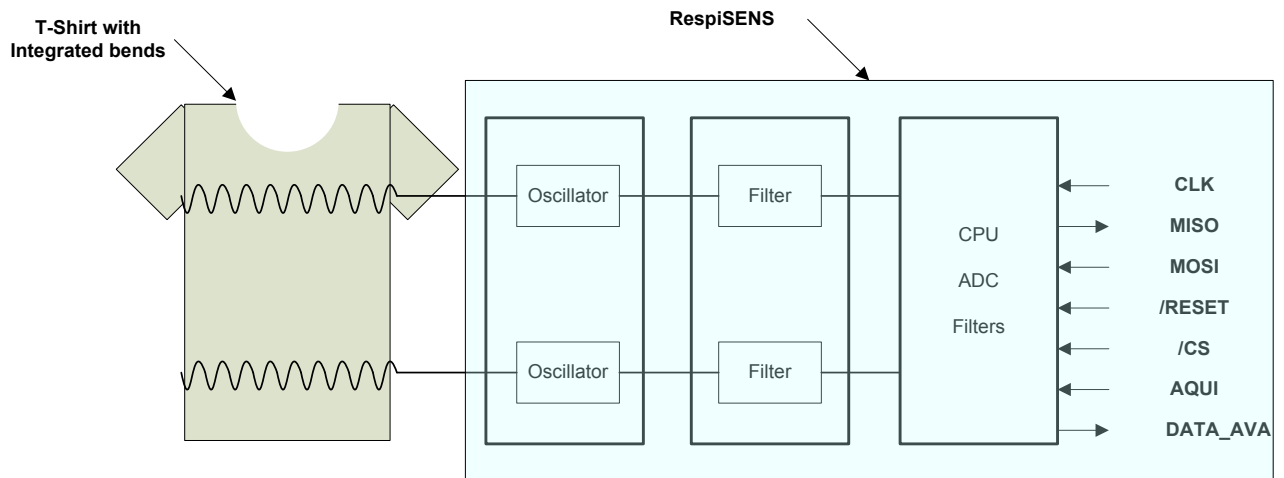


Figure 3.1: RespiSENS block diagram.

In this experimental activity the RespiSENS is placed on a developing platform powered by an external power supply of 5V and connected to a computer through a micro-usb cable. The RespiSENS is also connected at the shirt with a special connector with four pins (Figure 3.2). The microcontroller sent a continuous stream of data of thorax and abdominal volume displacements at a sampling rate of 16 Hz to a software provided by Fraunhofer institute.



Figure 3.2: RespiSENS electrical connector.

The electrocardiographic device (CardioSENS) for the acquisition of the ECG signals is an embedded system based on a microcontroller of the Texas Instruments. CardioSENS acquire data from four electrodes sewn into the shirt placed to gain a total of three ECG derivations (see Figure 3.3).

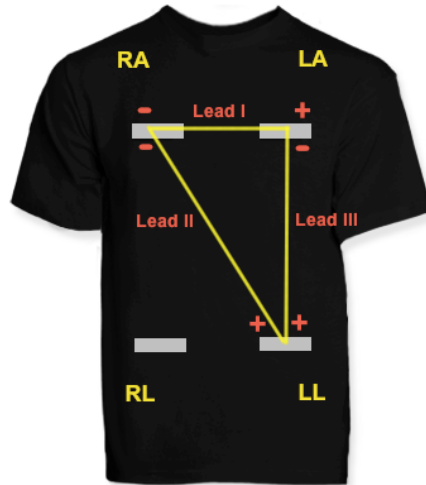


Figure 3.3: T-shirt with the Einthoven triangle and its leads.
 Lead I: LA – RA, Lead II: LL – RA, Lead III: LL – LA.

The CardioSENS hardware includes an analog signal conditioning stage, a feedback loop system, three filtering stages, an analogue to digital converter (ADC) and the microcontroller unit (Figure 3.4). It acquires three-lead electrocardiographic signals by means of four electrodes placed on the skin of the patient and transmits data to a Computer. The transferred data to the microcontroller unit are the three electrocardiographic derivations signals. The microcontroller sent a continuous stream of these data at a sampling rate of 128 Hz to a software provided by Fraunhofer institute. The CardioSENS is placed on a second developing platform connected with a shirt by a special connector with 4 contacts, and to a computer through a micro-usb cable. The device is powered by an external power supply of 5V.

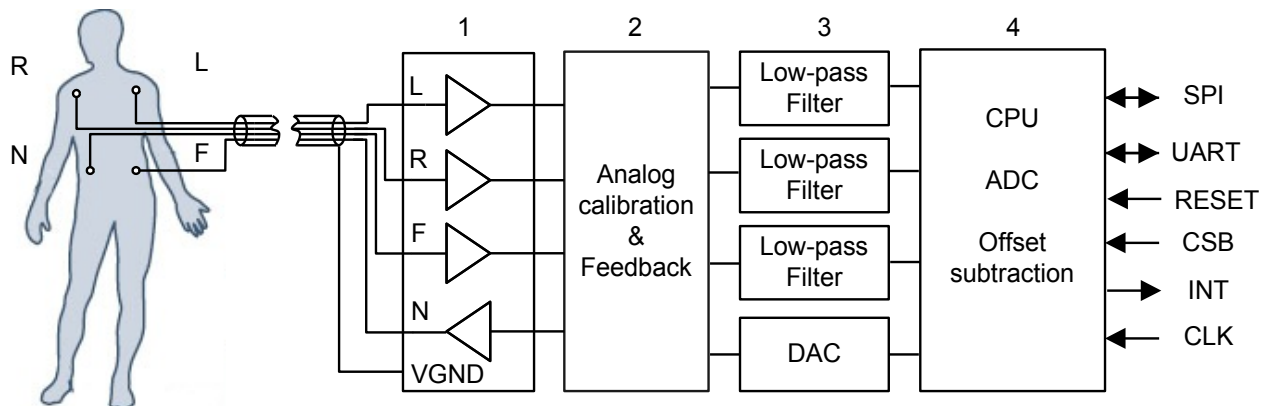


Figure 3.4: The ECG device block diagram.

The reflectance pulseoximeter (Nonin, 8000R) measures the oxygen saturation and the heart rate of the subject. The pulseoximeter module is connected to a third developing platform powered by an external power supply of 5V and connected to a computer through a micro-usb cable. The device sent a continuous stream of data of the oxygen saturation and the heart rate at a sampling rate of 1 Hz to software provided by Nonin.

The accuracy of the respiratory parameters is evaluated by comparing the data measured by the Chronious wearable with a high-accuracy chest-wall volume measurement provided by two gold standard devices, the opto-electronic plethysmography (OEP) and a pneumotachograph (PNT).

The OEP is an automatic motion analyser (Elite® system, BTS, Milano, Italy) that detects passive markers (see Section 1.3.3). We applied the markers on each subjects upon the shirt. For the seated position 89 markers are arranged on the anterior and posterior surfaces of the chest wall and abdomen of the subjects using the following scheme: 42 markers in the front and 47 on the back (Figure 3.5). While for the supine position 52 markers are arranged on the anterior surface of the chest wall and abdomen of the subjects (Figure 3.6).

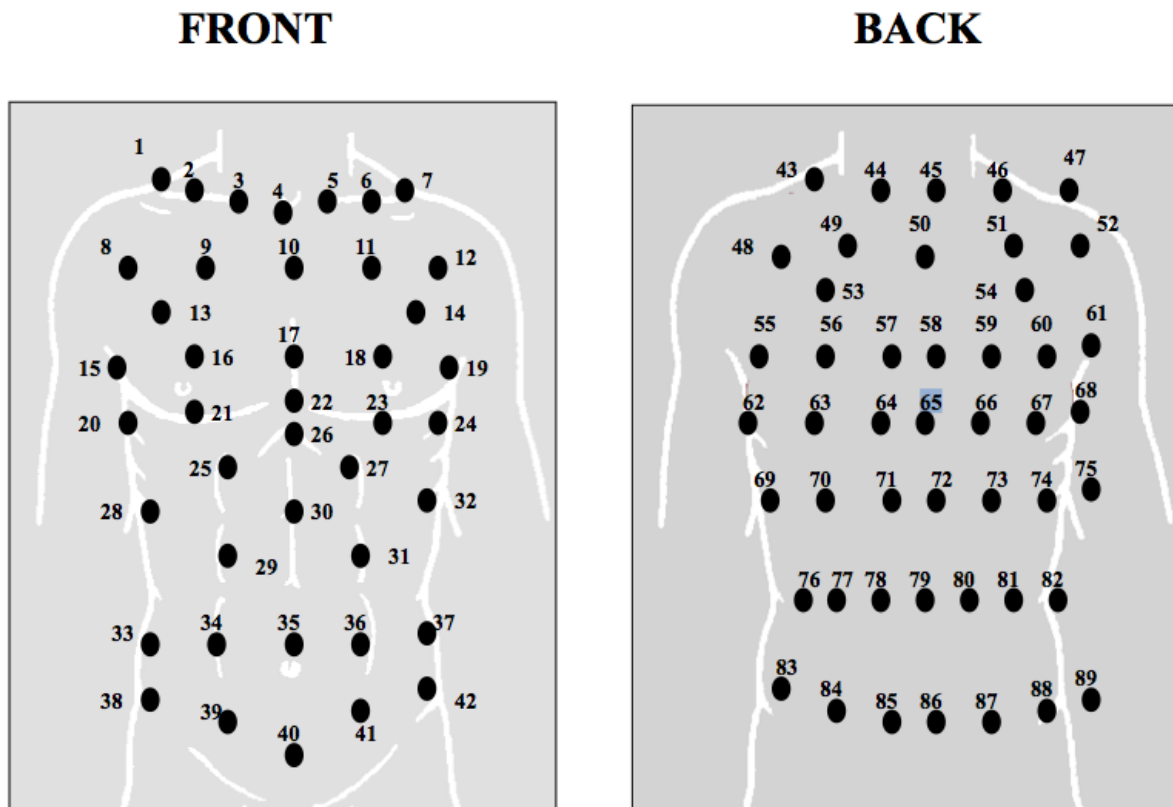


Figure 3.5: Arrangement of the marker for the seated position.

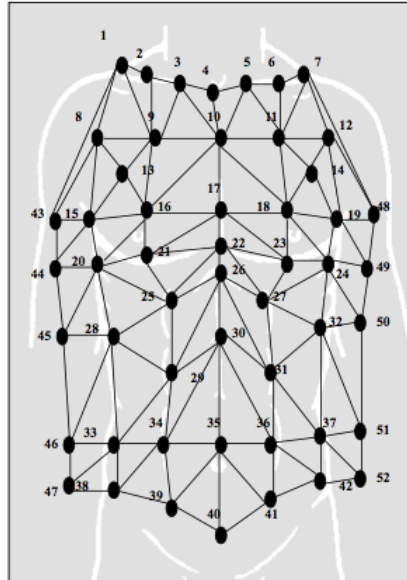


Figure 3.6 Arrangement of the marker for the supine position.

A parallel processors system provided by BTS executed real-time pattern recognition algorithms from the eight cameras and computed, with high accuracy, the three-dimensional (3D) coordinates of the different markers. Thus it was possible to continuously collect data of the absolute volume changes of the three compartments, pulmonary rib cage, abdominal rib cage and abdomen. Simultaneously the BTS system acquired the flow at the mouth of the subject measured by the PNT. The sampling rate of both OEP and PNT was set at 30 Hz.

In the following figure is shown the block diagram of the experimental setup, and in figure 3.8 is shown an example of sitting position acquisition.

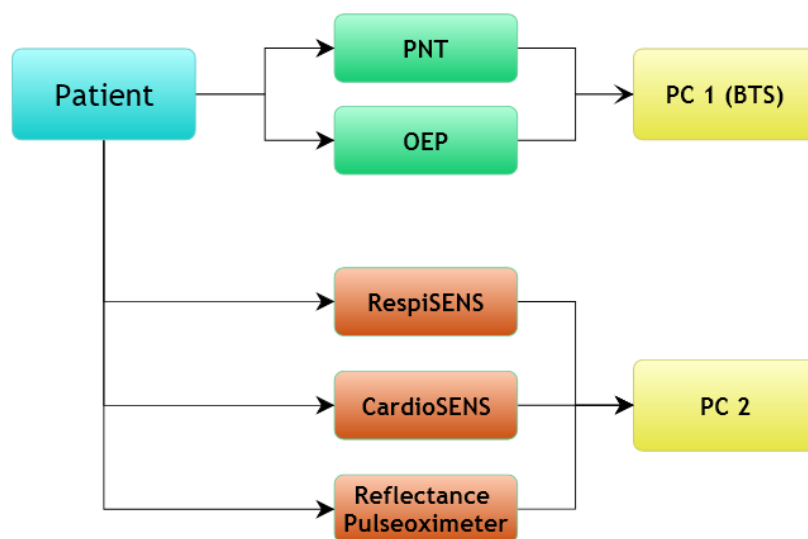


Figure 3.7: Diagram block of the experimental setup.

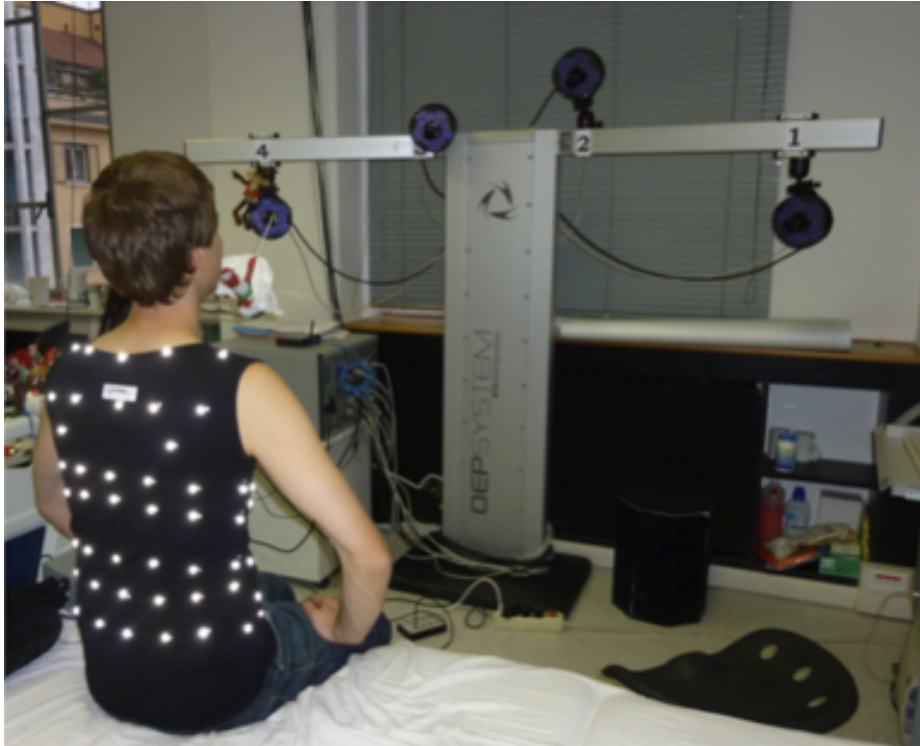


Figure 3.8: Experimental set-up for Chronious wearable validation.

3.2 Experimental protocol

As a first thing the calibration of the PNT is performed using a 3 liters precision syringe which is connected to the PNT and is pumped slowly in and out manually for 5 times. The acquired signal is consequently computed in order to gain the calibration coefficients of the PNT. The subject was asked to wear the shirt during the whole working day, without changing normal day operations, movements nor habits. The shirt was covered by the markers, as previously described. About every two hours during the day the subject underwent a measuring session. During the session the subject breathed through the PNT which signal was simultaneously acquired together with the change of the chest wall volumes by the OEP and the thoracic and abdominal volumes changes by the wearable framework. These measurements were performed in both seated and supine positions.

The subject was asked to perform the following respiratory maneuvers in sequence:

- 1) One inspiratory capacity (IC)
- 2) Four minutes of normal breathing
- 3) Increasing and decreasing breaths volume manoeuvre
- 4) Few seconds of normal breathing

The IC is used for the synchronization of the signals collected during the data analysis phase, from PNT, OEP and RespiSENS. The increasing and decreasing volumes maneuver was performed by asking the subject to breathe at increasing and then decreasing breaths volumes.

3.3 Data analysis

Five healthy subjects were studied. The respiratory parameters collected are the air flow at the mouth of the subjects measured by PNT expressed in digits, the absolute volume changes of the chest walls by OEP expressed in liters, and the abdominal and thorax volume displacement provided by the wearable system expressed in digits. The data coming from the PNT are not calibrated, for this reason we calculated the calibration coefficients m and q as follows:

$$\Delta V_T = m\Delta V_{PNT} + q \quad (1)$$

where ΔV_T is the change of volume of the 3-liter precision syringe measured by PNT and ΔV_{PNT} is the change of volume of the subject measured by PNT. This equation allowed us to determine for each subject the calibration coefficients and to express the respiratory parameters collected by PNT in liters.

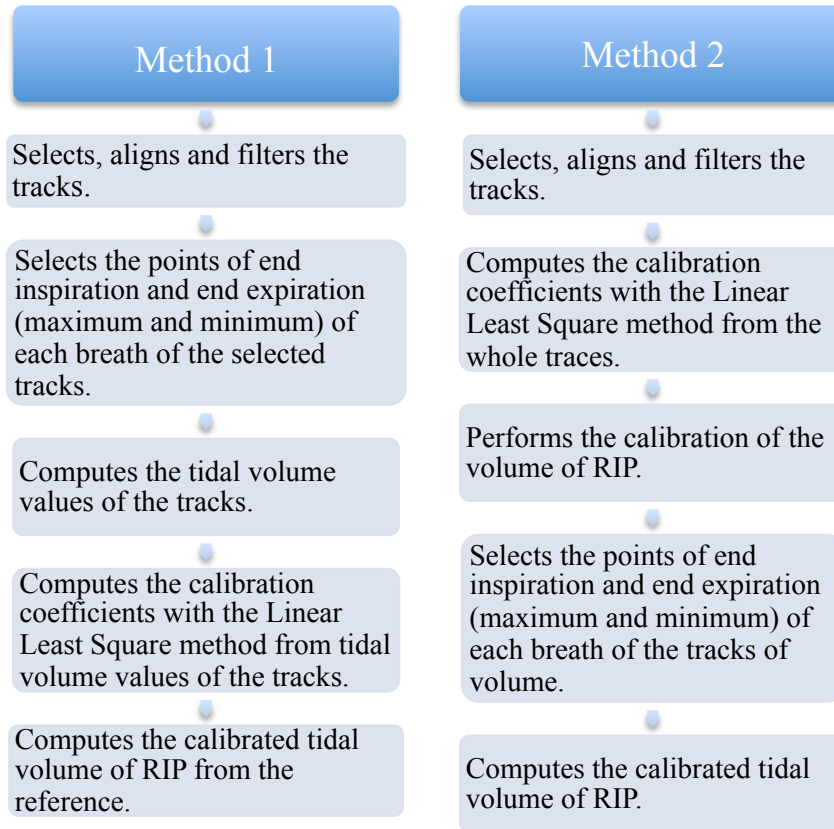
As we described in the section of the respiratory inductive plethysmography (RIP), also the RIP data are not calibrated. In order to calibrate the RIP of the Chronious wearable we adopted two different methods. Both methods are based on the two-compartment model for motion of the respiratory system:

$$\Delta V_{CW} = \Delta V_{RC} + \Delta V_{AB} \quad (2)$$

Where ΔV_{CW} is the change of volume measured by OEP or PNT, ΔV_{RC} is the change of the rib cage volume (RB) and ΔV_{AB} is the change of abdominal volume (AB) measured by a calibrated RIP.

This equation and those that follow are approximations because each compartment can potentially move with additional degrees of freedom and also show slight variation from region to region in volume-motion coefficients.

The flowcharts of the two methods are the follows:



3.3.1 Method 1

Taking into account differences in volume-motion properties of RC and AB compartments it is necessary to calibrate separately the changes of uncalibrated rib cage (ΔuV_{RC}) and changes of uncalibrated abdominal (ΔuV_{AB}) volumes approximately equals to ΔV_{CW} as follows:

$$\Delta V_{CW} \cong M[K(\Delta uV_{RC}) + \Delta uV_{AB}] \quad (3)$$

The K term in Eq. 3 establishes the electrical proportionality relationship between the uncalibrated signals from the RIP, in which the electrical gains of their amplifiers are set to be identical. K converts both ΔuV_{RC} and ΔuV_{AB} to calibrated signals because it adjusts the ratio of the two signals. The term M scales the quantity $[K(\Delta uV_{RC}) + \Delta uV_{AB}]$ to be equivalent to ΔV_{CW} as measured with OEP or PNT ^[18].

The Eq.3 allowed us to determine for each subject the two calibration coefficients with the Linear Least Square method and calculate the calibrated tidal volume of the RIP.

In order to calibrate the RIP we created three Matlab functions (see Appendix A):

- `Respisens_track_Milano_Novembre.m`
- `Respisens_Calibration_Milano_Novembre.m`
- `Respisens_Test_Milano_Novembre.m`

Respisens_track_Milano_Novembre.m is a function that selects and aligns the region of normal breathing from the tracks of RIP, OEP and PNT. This function needs as input a string (e.g. the name of the subject and position: 'ID_sitting1') and returns a .mat file and an index.txt file. The .mat file, contains the uncalibrated abdomen and thorax volume displacement of RIP, the pulmonary ribcage, abdominal ribcage and abdomen volumes of OEP, and the tidal volume of OEP and PNT. These tracks are filtered with a low pass filter (order: 5, cutoff frequency: 2Hz), the tracks of OEP and PNT are also resampled at 16 Hz and finally the SP track is integrated to obtain a track of volume. The index.txt file contains the information about the data in the .mat file, such as names of the tracks and sampling frequency. The input string is used to assign the names of the output files (e.g. ID_sitting1.mat, ID_sitting1index.txt).

Respisens_Calibration_Milano_Novembre.m is a function that calculates the calibration coefficients, with the Linear Least Square method, and the calibrated volume of RIP from OEP and PNT. This function uses the .mat file and the .mxn files created by the function *Zview.m* and need as input the same string of the previous function (e.g. the names of the .mat files to load).

Zview.m allows saving the points of end inspiration and end expiration (maximum and minimum) of each breath of the selected tracks in the .mxn files, one for each track, thus the abdominal volume of RIP, the thorax volume of RIP, the tidal volume of OEP and SP. Those points are used in the function *Respisens_Calibration_Milano_Novembre.m* to calculate the volume of each normal breath from the tracks of RIP, OEP and PNT, in Eq.2 are ΔuV_{RC} , ΔuV_{AB} , $\Delta V_{OEP_{cw}}$ and $\Delta V_{PNT_{cw}}$ respectively.

Respisens_Calibration_Milano_Novembre.m returns two matrixes, in the first there are the calibration coefficients, the mean and standard deviation tidal volumes of RIP calibrated from OEP tracks, and the mean and standard deviation ribcage and abdomen volumes of the RIP calibrated from the OEP. The RIP allows the measurement of only two compartments during respiration (ribcage and abdomen) while the OEP measures three compartments (pulmonary ribcage, abdominal ribcage and abdomen); so the volume variations measured by OEP of the pulmonary ribcage (ΔuV_{RCp}) and of the abdominal ribcage (ΔuV_{RCa}) were assigned totally to the ribcage, thus $\Delta uV_{RCp} + \Delta uV_{RCa} = \Delta uV_{RC}$. In the second matrix there are the calibration coefficients and the tidal

volume of the RIP calibrated using the PNT traces.

The *Respisens_Test_Milano_Novembre.m* function is used to apply the calibration coefficients to the uncalibrated volume traces of the next acquisitions of the same subject. This function needs the .mat file (containing the selected traces of the new acquisition), the .mxn files of the new acquisition, and in input the string, i.e. the file name, and two matrixes containing the calibration coefficients computed by the *Respisens_Calibration_Milano_Novembre.m* function. The functions returns two matrixes containing the mean and standard deviation tidal volumes calibrated from the tracks of OEP and PNT respectively.

For example, we performed two measures in the sitting position, the calibration procedure is the following:

1) `Respisens_track_Milano_Novembre('ID_sitting1');`

This function selects and aligns the region of normal breathing from the tracks of RIP, OEP and PNT of the first acquisition and returns a .mat file (ID_sitting1.mat), which contains the selected tracks and an index.txt file (ID_sitting1_index.txt), which contains the information of the .mat file.

2) `Zview('ID_sitting1.ldz');`

This function needs the .mat file created with the previous function (ID_sitting1.mat),

Returns seven .mxn files: ID_sitting1_tho.mxn, ID_sitting1_abd.mxn, ID_sitting1_res.mxn, ID_sitting1_pnt.mxn, ID_sitting1_oeo.mxn, ID_sitting1_oab.mxn and ID_sitting1_oth.mxn. These files contain the points of maximum and minimum of the uncalibrated abdomen and thorax volumes displacement of RIP, the abdomen and thorax volumes displacement of OEP, and the tidal volume of OEP and PNT.

3) `[out1,out2]=Respisens_Calibration_Milano_Novembre('ID_sitting1');`

This function needs the .mat file and the .mxn files created with the previous functions. Returns a matrix with the calibration coefficients, the mean tidal volume calibrated from RIP, the standard deviation of tidal volume calibrated from RIP, the mean and standard deviation of volume from OEP in out1 and from PNT in out2.

4) `Respisens_track_Milano_Novembre('ID_sitting2');`

This function selects and aligns the region of normal breathing from the tracks of RIP, OEP and PNT of the next acquisitions of the same subject and returns a .mat file (ID_sitting2.mat), which contains the selected tracks and an index.txt file (ID_sitting2_index.txt), which contains the information of the .mat file.

5) `Zview('ID_sitting2'.ldz');`

This function needs the .mat file created with the previous function (ID_sitting2.mat),

Returns seven .mxn files: ID_sitting2_tho.mxn, ID_sitting2_abd.mxn, ID_sitting2_res.mxn, ID_sitting2_pnt.mxn, ID_sitting2_oeo.mxn, ID_sitting2_oab.mxn and ID_sitting2_oth.mxn. These files contain the points of maximum and minimum of the uncalibrated abdomen and thorax volumes displacement of RIP, the abdomen and thorax volumes displacement of OEP, and the tidal volume of OEP and PNT.

6) `[out3,out4]=Respisens_Test_Milano_Novembre('ID_sitting2',out1,out2);`

This function needs the .mat file and the .mxn files created with the previous functions, and the calibration coefficients estimate with the calibration function, that we previously saved in [out1,out2]. These coefficients are used to calculate the RIP calibrated volume from OEP and PNT. The function returns a matrix with the calibration coefficients, the mean tidal volume calibrated from RIP, the standard deviation of tidal volume calibrated from RIP, the mean and standard deviation of volume from OEP in out3 and from PNT in out4.

The first three steps are used to compute the calibration coefficients of the RIP, the last three steps are used to verify if the RIP calibration is still consistent in the subsequent measures during the day.

Linear regression analysis was performed on the calibration results of the five healthy subjects.

3.3.2 Method 2

The second algorithm used to compute the calibration of the RIP is based on the same two-compartment model for motion of the respiratory system (see Eq. 2) of the previous method. To calibrate the rib cage (ΔV_{RC}) and abdominal (ΔV_{AB}) volumes displacement we used the following equation:

$$\Delta V_{cw} \cong M[K(\Delta V_{RC}) + \Delta V_{AB}] + Q \quad (4)$$

where M , K and Q are the coefficients used for the calibration of the RIP and are calculated with the Linear Least Square method. The difference between equation 4 and equation 3 consists in the use of the whole data of the traces of uncalibrated rib cage (ΔV_{RC}) and abdominal (ΔV_{AB}) volumes displacement, absolute volume traces of the OEP and, flow trace of the PNT instead of using only tidal volumes values.

To test this new approach we realized three Matlab functions (see Appendix A):

- *Respisens_Calibration_PDA_Mi_Novembre.m*
- *Respisens_Volume_Computation_PDA_Mi_Novembre.m*
- *Respisens_Test_PDA_Mi_Novembre.m*

Respisens_Calibration_PDA_Mi_Novembre.m is a function that allows the selection and alignment of the region of quiet breathing from the tracks of RIP, OEP and PNT, and it performs the calibration of the volume of RIP using as a reference the data acquired from the OEP and the PNT. This function needs as an input a string (e.g. the name of the subject and position: 'ID_sitting1') and the .mat file created by the function *Respisens_track_Milano_Novembre.m*. This .mat file contains the respiratory tracks from the RIP, OEP and PNT that have been previously selected, aligned and filtered by a low pass filter. Furthermore, the PNT track is integrated to obtain the track of the volume of air. The *Respisens_Calibration_PDA_Mi_Novembre.m* function returns two .mat files and an index.txt file. The first .mat file contains a matrix composed of the volumes of the calibrated RIP and the volumes of OEP and PNT. The volumes of RIP are calculated applying, to the Eq.4, the calibration coefficients, estimated with the Linear Least Square method, as described previously. The second .mat file contains a matrix of the calibration coefficients. The index.txt file contains the information about the data saved in the .mat file, such as the names of the tracks and the sampling frequency of the traces. The input string is used to assign the names to the output files (e.g. ID_sitting1_PDA.mat, ID_sitting1_PDAindex.txt).

The *Respisens_Test_PDA_Mi_Novembre.m* function is used to apply the calibration coefficients to the uncalibrated volume tracks of the other acquisitions of the same subject. This function needs the .mat file created by the function *Respisens_track_Milano_Novembre.m* which contains the tracks of the RIP, OEP and PNT in the region of normal breathing, that are filtered with a low pass filter, and the calibration coefficients estimated with the *Respisens_Calibration_PDA_Mi_Novembre.m* function. The *Respisens_track_Firenze.m* returns two .mat files and an index.txt file. The first .mat file contains a matrix with the volumes of the calibrated RIP and the volumes of OEP and PNT. The volumes of the RIP are calculated applying the calibration coefficients estimated using the tracks of the first acquisition. The second .mat file contains a matrix of the calibration coefficients. The index.txt file contains the information about the data in the .mat file, such as the names of the tracks and the sampling frequency. The input string is used to assign the names of the output files (e.g. ID_sitting2_PDA.mat, ID_sitting2_PDAindex.txt).

Respisens_Volume_Computation_PDA_MI_Novembre.m is a function that calculates the

calibrated tidal volume of the RIP. This function uses the two .mat files created with the *Respisens_Calibration_PDA_Mi_Novembre.m* and the *Respisens_Test_PDA_Mi_Novembre.m* function, the .mxn files created by the function *Zview.m* and needs as an input the same string of the previous functions (e.g. the names of the .mat files to load).

Zview.m allows saving the points of end inspiration and end expiration (maximum and minimum) of each breath of the selected tracks in eight .mxn files, one for the track of RIP tidal volume calibrated from OEP, one for the track of OEP volume, one for the track of RIP thorax tidal volume calibrated from OEP, one for the thorax track of OEP volume, one for the track of RIP abdomen tidal volume calibrated from OEP, one for the abdominal track of OEP volume, one for the track of RIP tidal volume calibrated from PNT, and one for the track of PNT volume. Those points are used in the function *Respisens_Volume_Computation_PDA_Mi_Novembre.m* to calculate the tidal volume of each normal breath from the tracks of RIP calibrated volume, OEP and SP volumes. The function returns two matrixes containing the calibration coefficients, the mean and standard deviation tidal volumes calibrated from the tracks of OEP and PNT respectively.

For example, we performed two measures in the sitting position, the calibration procedure is the following:

1) *Respisens_Calibration_PDA_Mi_Novembre.m*('ID_sitting1');

This function needs the .mat file created with the *Respisens_track_Milano_Novembre.m* which containing the tracks of the RIP, OEP and PNT in the region of normal breathing, that are filters with a low pass filter. With this function we selected the breaths that we used to estimate the calibration coefficients. These coefficients are use to calibrated the RIP volume from OEP and PNT. Returns two matrixes: *ID_sitting1_par.mat*, *ID_sitting1_PDA.mat*. The first matrix contains the calibration coefficients; the second contain the calibrated volume of the RIP from OEP and PNT, and the track of OEP and PNT.

2) *Zview*('ID_sitting1_PDA.ldz');

This function needs the .mat file that contains the calibrated volume of the RIP, the tracks of OEP and PNT. Returns eight .mxn files that contains the points of maximum and minimum for the track of:

- RIP tidal volume calibrated from OEP (*ID_sitting1_PDA_rop.mxn*),
- OEP volume (*ID_sitting1_PDA_oep.mxn*),
- OEP abdomen volume (*ID_sitting1_PDA_oab.mxn*),
- RIP abdomen tidal volume calibrated from OEP (*ID_sitting1_PDA_rab.mxn*),
- OEP thorax volume (*ID_sitting1_PDA_oth.mxn*),
- RIP thorax tidal volume calibrated from OEP (*ID_sitting1_PDA_rth.mxn*),
- RIP tidal volume calibrated from PNT (*ID_sitting1_PDA_rpn.mxn*),
- PNT volume (*ID_sitting1_PDA_pnt.mxn*).

3) [out1,out2]=Respisens_Volume_Computation_PDA_Mi_Novembre('ID_sitting1');

This function needs the two .mat files created with the *Respisens_Calibration_PDA_Mi_Novembre.m* function and the eight .mxn files. Returns two matrixes with the calibration coefficients, the mean and standard deviation tidal volumes calibrated from the tracks of OEP and PNT respectively.

4) Respisens_Test_PDA_Mi_Novembre('ID_sitting2', out1, out2);

This function needs the .mat file created with the *Respisens_track_Milano_Novembre.m* which containing the tracks of the RIP, OEP and PNT in the region of normal breathing of the second acquisition, that are filters with a low pass filter, and the calibration coefficients estimate with the calibration function, that we previously saved in [out1] and [out2]. These coefficients are used to calculate the RIP calibrated volume from OEP and PNT. Returns two matrixes: ID_sitting2_par.mat, ID_sitting2_PDA.mat. The first matrix contains the calibration coefficients; the second contain the calibrated volume of the RIP from OEP and PNT, and the track of OEP and PNT.

5) Zview('ID_sitting2_PDA.ldz');

This function needs the .mat file that contains the calibrated volume of the RIP, the tracks of OEP and PNT. Returns eight .mxn files (see point 4) that contains the points of maximum and minimum.

6) [out3,out4]=Respisens_Volume_Computation_PDA_Mi_Novembre('ID_sitting2')

This function needs the two .mat files created with the *Respisens_Test_PDA_Mi_Novembre.m* function and the eight .mxn files. Returns two matrixes with the calibration coefficients, the mean and standard deviation tidal volumes calibrated from the tracks of OEP and PNT respectively.

The first three steps are used in order to compute the calibration coefficients of the RIP of each subject from the data of OEP and PNT, in both seated and supine position. The last three steps are used to verify if the RIP calibration is still consistent in the next measures of each subject. Linear regression analysis is than performed on the calibration results of the five subjects.

3.4 Results

In this pre-testing phase, the respiratory parameters are evaluated on five healthy subjects by comparing the data collected from the acquisition system with the measurements provided by the opto-electronic plethysmography (OEP) and a pneumotachograph (PNT) as references. The respiratory parameters coming from the RIP have been calibrated with two methods, and evaluated by a linear regression analysis.

In figure 3.9 are shown the results of the tidal volume of RIP calibrated using OEP as a reference, of five subjects obtained with the first calibration method applied on the acquisitions

following the calibration acquisition. The data used to plot figure 3.9 are tidal volumes computed starting from the wearable system (RIP) versus tidal volumes computed starting from the OEP traces of the whole working day in seated and supine positions. The regression line showed poor correlation between the two sets of data: $r^2=0.41$, $m=0.672$ $q=0.096$. It is possible to see that the slope of the regression varies significantly with posture, as shown in Figures 3.10 and 3.11 in sitting and supine position, respectively.

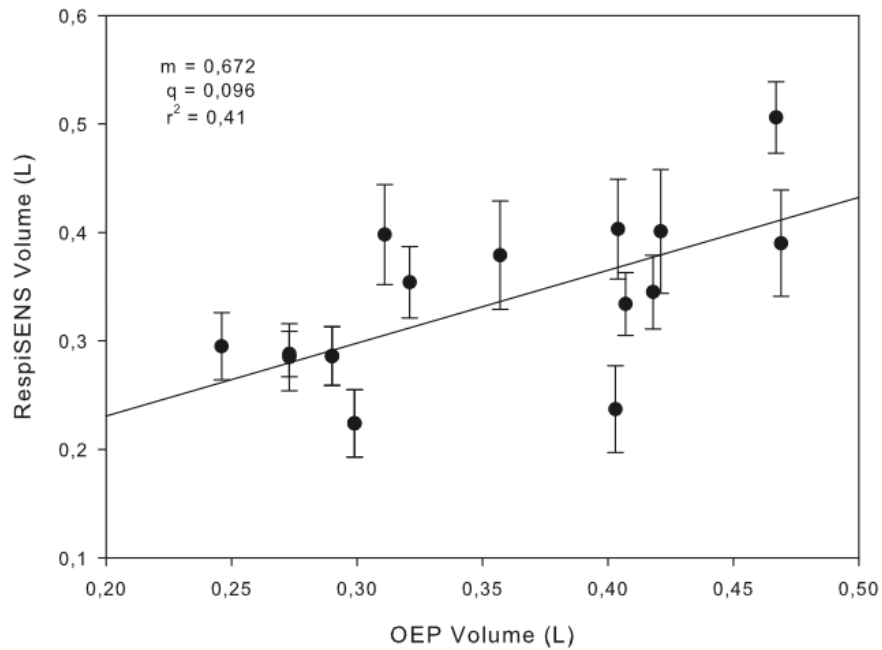


Figure 3.9: Results of calibration by OEP, with the first method.

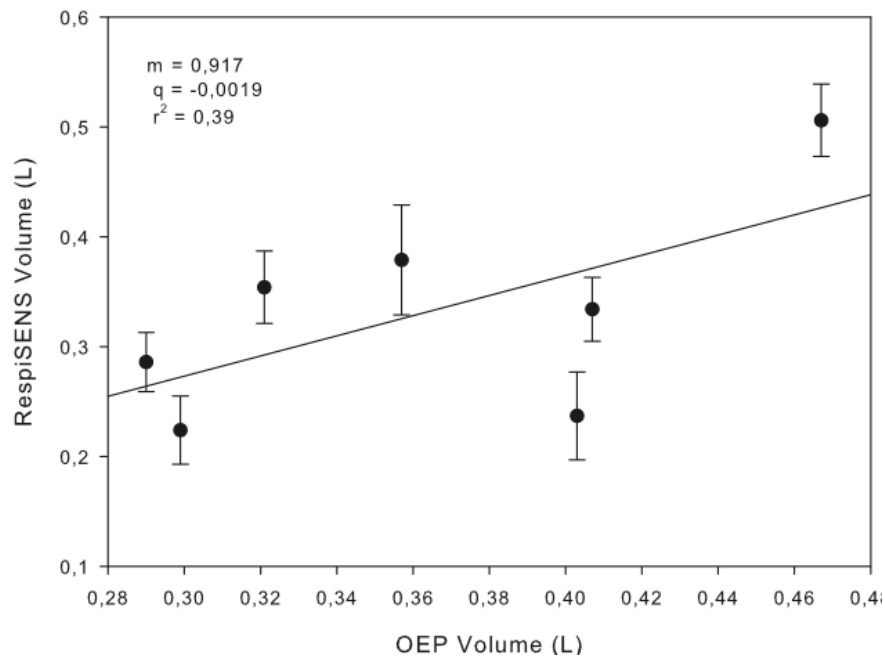


Figure 3.10: Results of calibration by OEP in sitting position, with the first method.

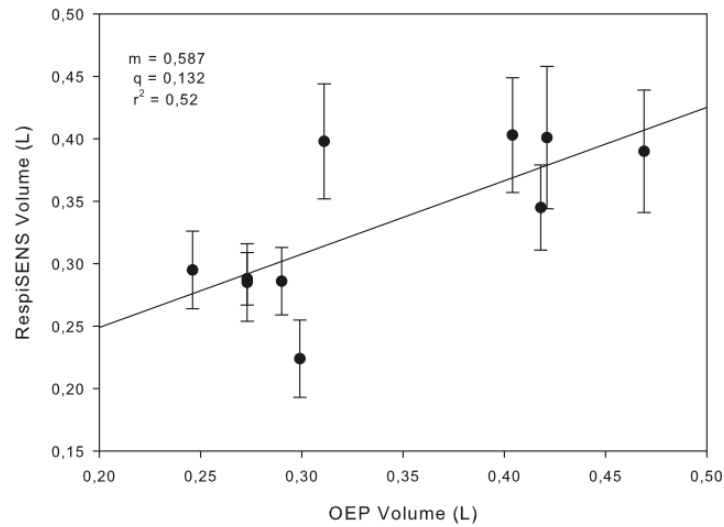


Figure 3.11: Results of calibration by OEP in supine position, with the first method.

In the supine position the volume signals produce by RespiSENS are more correlated to the volume measure by OEP than in the sitting position (sitting: $r^2=0.39$, $m=0.917$, $q=-0.0019$; supine: $r^2=0.52$, $m=0.587$, $q=0.132$).

We performed the linear regression analysis also on the tidal volume of RIP calibrated using as a reference data of the PNT. In figure 3.12 are shown the results of five subjects obtained with the first calibration method applied on the acquisitions following the calibration acquisition. The data used to plot figure 3.12 are tidal volumes computed starting from the wearable system (RIP) versus tidal volumes computed starting from the PNT traces of the whole working day in seated and supine positions. The regression line showed poor correlation between the two sets of data: $r^2=0.38$, $m=1,252$ $q=-0.113$.

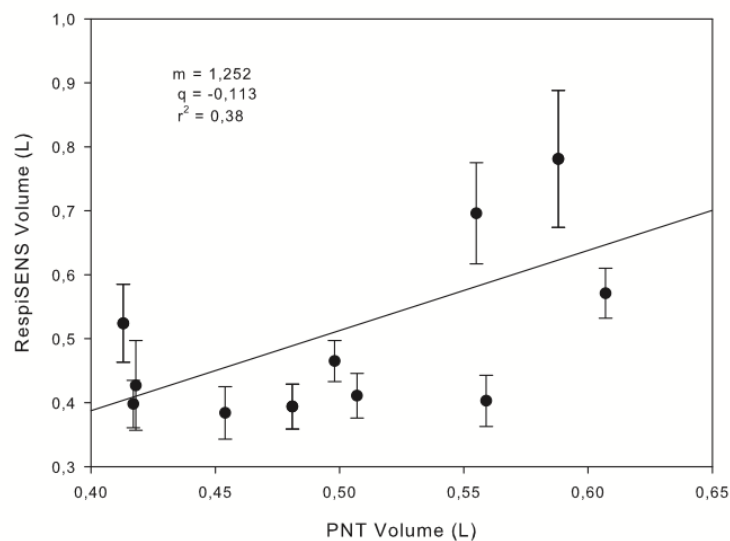


Figure 3.12: Results of calibration by PNT, with the first method.

In the next figures is possible to see that the slope of the regression varied significantly with the postures (sitting: $m=1,253$, $q=-0,095$; supine: $m=1,143$, $q=-0,078$) and that in the sitting position the volume signals produce by RespiSENS are more correlated to the volume measure by PNT than in the supine position (sitting: $r^2=0,42$; supine: $r^2=0,29$).

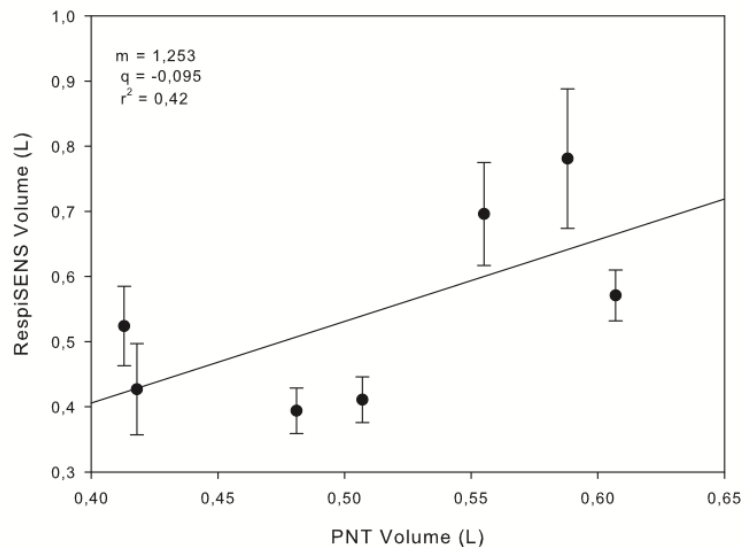


Figure 3.13: Results of calibration by PNT in sitting position, with the first method.

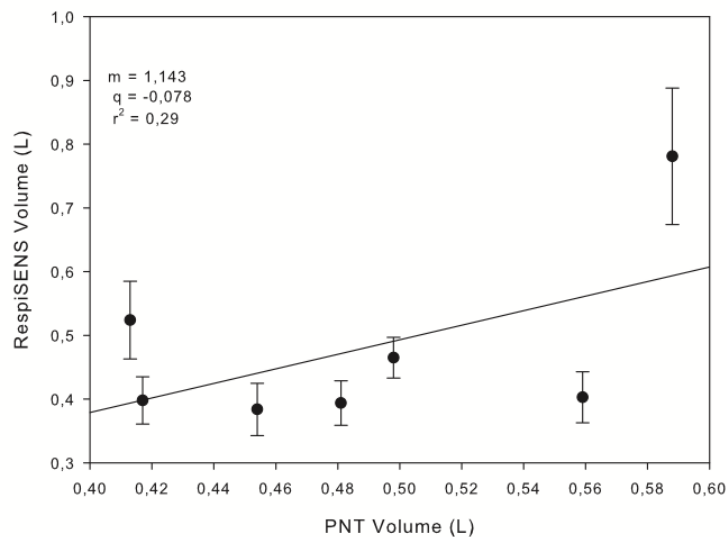


Figure 3.14: Results of calibration by PNT in supine position, with the first method.

The second method of calibration shows better correlation between the volume signals produced by RespiSENS and the volume measured by OEP and PNT. The second method uses the whole data of the traces of uncalibrated RIP, the absolute volume traces of the OEP and flow trace of the

PNT. In figure 3.15 are shown the results of the tidal volume of RIP calibrated by OEP obtained with the second calibration method.

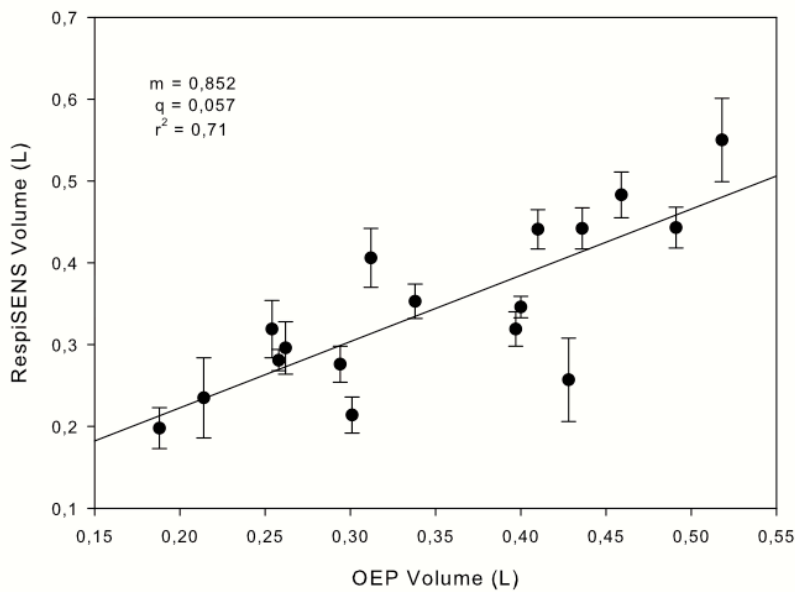


Figure 3.15 Results of calibration by OEP, with the second method.

The data used to plot figure 3.15 are tidal volumes computed starting from the wearable system (RIP) versus tidal volumes computed starting from the OEP traces of the whole working day in seated and supine positions. The regression line showed poor correlation between the two sets of data: $r^2=0.56$, $m=0.745$, $q=0.068$. In Figures 3.16 and 3.17 are shown the results in sitting and supine position, respectively.

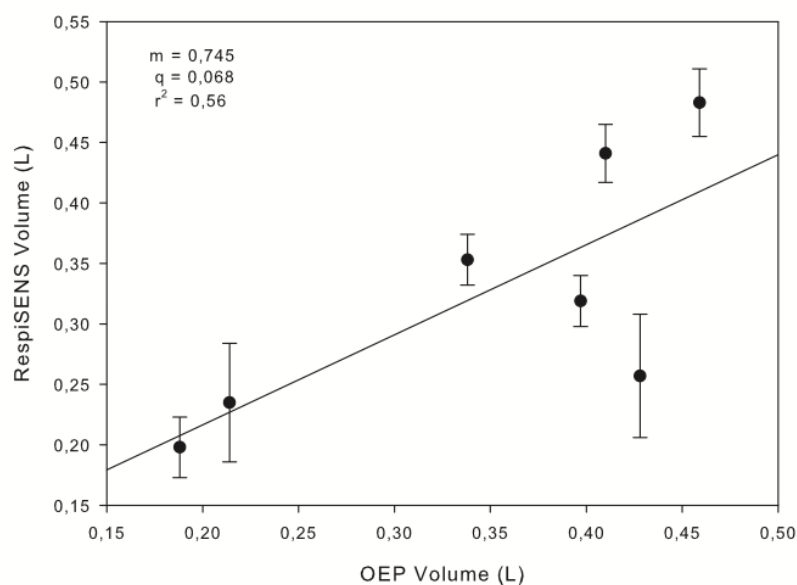


Figure 3.16: Results of calibration by OEP in sitting position, with the second method.

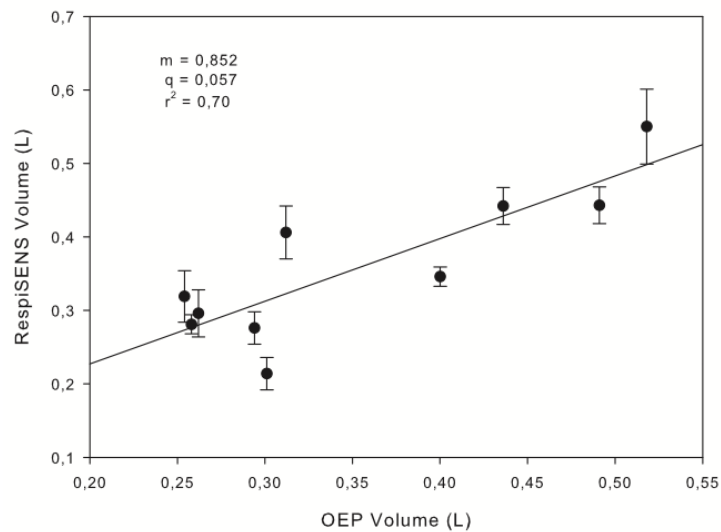


Figure 3.17: Results of calibration by OEP in supine position, with the second method.

In the supine position the volume signals produce by RespiSENS are more correlated to the volume measure by OEP than in the sitting position (sitting: $r^2=0.56$, $m=0.745$, $q=0.068$; supine: $r^2=0.70$, $m=0.852$, $q=0.0057$).

In figure 3.18 are shown the results of the tidal volume of RIP calibrated using PNT as a reference, obtained with the second calibration method applied on the acquisitions following the calibration acquisition. The data used to plot figure 3.18 are tidal volumes computed starting from RIP versus tidal volumes computed starting from the PNT traces of the whole working day in seated and supine positions. The regression line showed poor correlation between the two sets of data: $r^2=0.51$, $m=1,222$ $q=-0.116$.

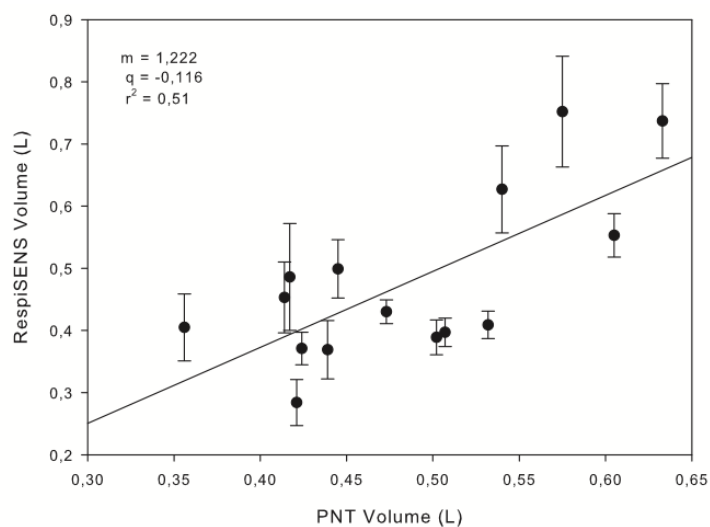


Figure 3.18: Results of calibration by PNT, with the second method.

In Figures 3.19 and 3.20 are shown the results in sitting and supine position, respectively. In the supine position the volume signals produce by RespiSENS are more correlated to the volume measure by PNT than in the sitting position (sitting: $r^2=0.36$, $m=0.945$, $q=0.047$; supine: $r^2=0.65$, $m=1.444$, $q=-0.238$).

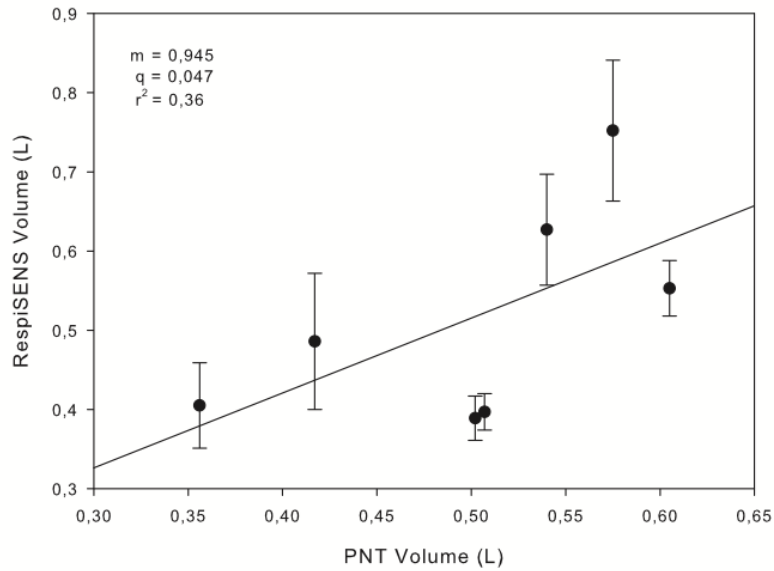


Figure 3.19: Results of calibration by PNT in sitting position, with the second method.

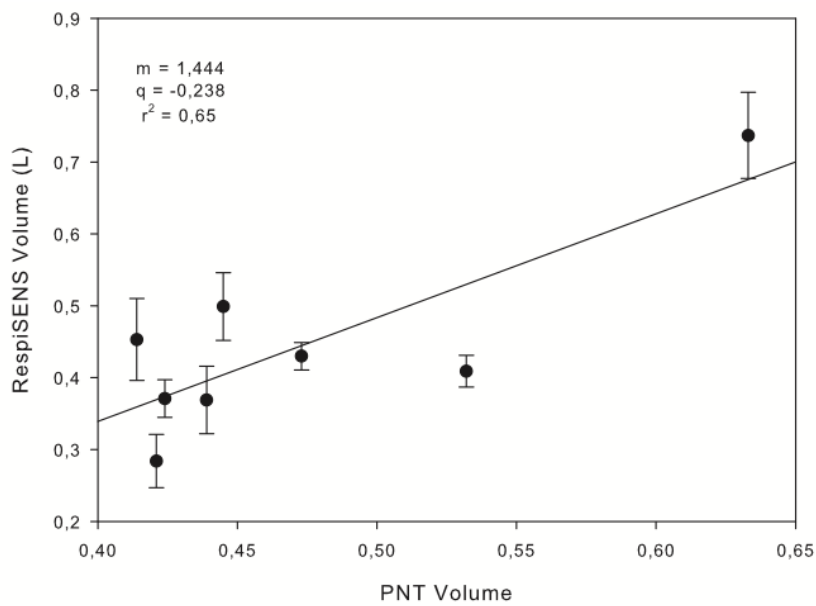


Figure 3.20: Results of calibration by PNT in supine position, with the second method.

The tables 3.1 and 3.2 show the calibration coefficient of the cases described estimated using OEP and PNT as reference.

Position	Subject	Method 1		Method 2		
		m	k	m	k	q
SITTING	1	0,017	0,994	0,020	0,594	421,821
	2	0,025	0,716	0,051	0,244	868,985
	4	0,020	0,754	0,018	0,825	407,767
	5	0,026	0,899	0,028	0,725	598,897
SUPINE	1	0,041	0,602	0,029	1,066	736,211
	2	0,028	1,269	0,048	0,701	1058,725
	3	-0,011	-3,822	0,025	1,422	702,782
	4	0,033	1,665	0,020	3,257	921,741
	5	0,038	0,952	0,046	0,734	964,460

Table 3.1: Calibration coefficients for the data measured by OEP.

Position	Subject	Method 1		Method 2		
		m	k	m	k	q
SITTING	1	0,022	0,690	0,026	0,379	466,678
	2	0,058	0,433	0,004	9,249	406,783
	3	0,036	0,689	0,042	0,506	751,967
	4	0,030	0,558	0,040	0,312	645,089
SUPINE	1	0,044	0,999	0,018	2,926	826,706
	2	0,076	0,707	-0,009	-6,847	542,501
	3	-0,014	-3,664	0,057	0,661	1117,834
	4	0,051	1,379	-0,004	-25,234	875,799

Table 3.2: Calibration coefficients for the data measured by PNT.

During the tests we registered also the electrocardiographic signals, the oxygen saturation and the heart rate. We identify PQRST waves within the three derivations in few subjects, and values of oxygen saturation and heart rate compatibles with the subjects studied.

The first test phase allowed us to develop the procedures and functions to compute the calibration of the system. Moreover, this phase of test allowed us to test the wearable system. Concerning the electronic parts we were able to use and test the acquisition boards of RIP, pulseoximeter and ECG signals from the point of view of signal quality. Concerning the wearable part of the system, the shirt, we found some issues both for RIP and for ECG electrodes. As we had the availability of only two shirt sizes we found that on thin subjects the respiratory bands were not enough tight to follow breathing movements constantly, causing the worsening of the signal's quality. We also found adherence differences between male and female subjects. We found that the signals coming from the ECG are not reliable because of the poor contact of the electrodes with subject's skin, due both

to electrodes' dimension and position. We studied some design changes of the shirt in order to improve signals' quality both of the RIP and the ECG.

Chapter 4

Validation on healthy subjects

In this chapter is presented a project phase where new improvements of the system have been applied and tested on healthy subjects in order to prepare the system for the next phase, thus the clinical validation in a hospital on COPD patients.

The accuracy of the respiratory parameters was evaluated by comparing the data collected from the wearable system with the measurements provided by a spirometer (SP) and a pneumotachograph (PNT) in both seated and supine positions.

4.1 Experimental setup

The system is based on the T-shirt with two-respiratory bands (RIP), 4 ECG electrodes and a reflectance pulseoximeter. In this phase we tested a new size S/M of the T-shirt, that is more adherent than the previous, so the parameters should be measured properly also on thin people. In the new shirt there is an elastic band on the back between the two respiratory bands, the ECG electrodes are increased in dimension and covered with a soft material on its back. These improvements allow increasing the contact between the skin and the ECG electrodes and to make the shirt more tight than the previous size S/M. Furthermore, the pocket of the microcontroller is placed on the front of the T-Shirt, instead on the back, in this way the device is more accessible.

The data coming from the sensors are collected and transmitted via wireless connection by the Data Handler to a Computer. The Data Handler is a microcontroller-based acquisition system developed by the Fraunhofer Institute for Integrated Circuits IIS. The sensing elements are directly connected to the Data Handler via a physical cable (Figure 4.1) and all the data are transmitted via bluetooth connection from the Data Handler to a computer.

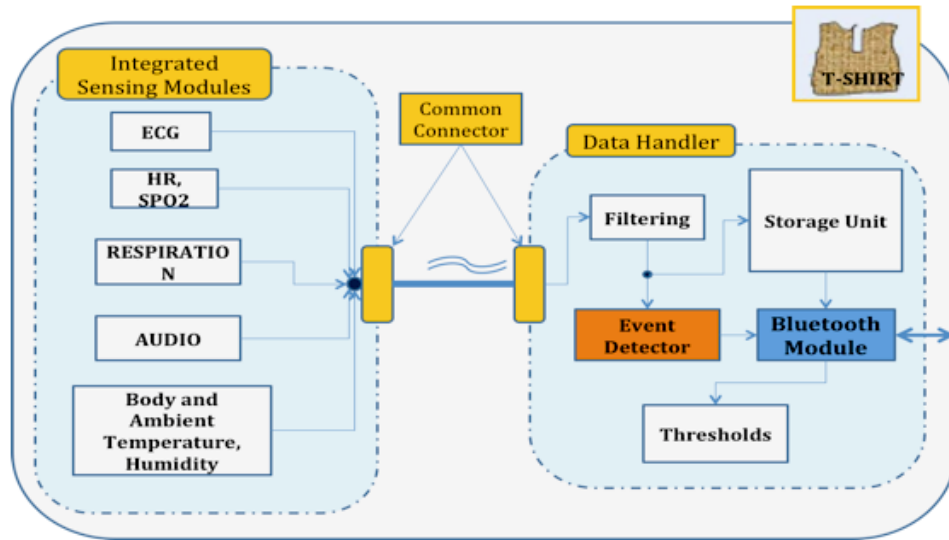


Figure 4.1: Chronious Wearable system.

In the previous figure we can see that the Data Handler (DH) is the main electronic unit of the wearable system. It undertakes the role of signal concentrator, as all signals acquired from the patient, consume a large part of its physical memory for storage purposes. Filtering procedure, event detection when a parameter value overcomes a predefined threshold, as well as, data transmission and network connections manipulation, are some of the main responsibilities of the Data Handler (Figure 4.2). The DH is used to acquire simultaneously the signals coming from the ECG, RIP, SpO2 and temperature sensors. The data are temporarily stored and sent to a computer via a bluetooth connection.

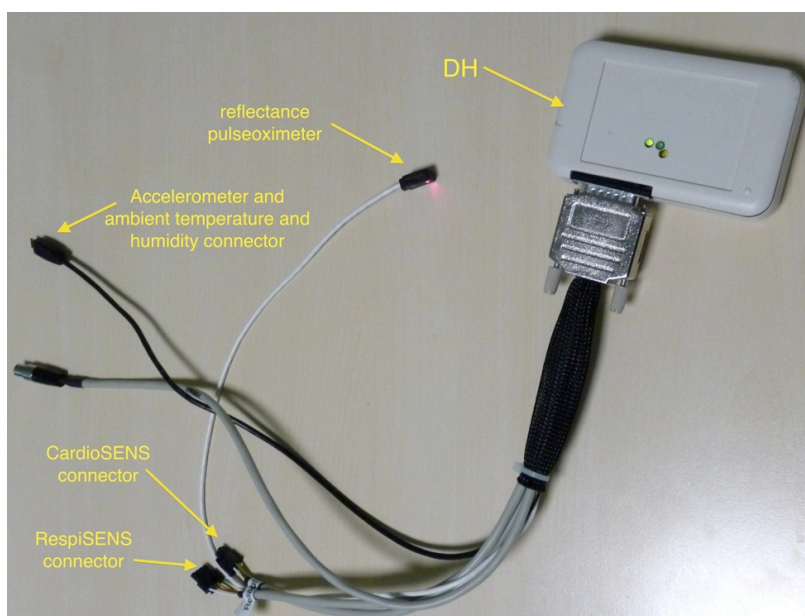


Figure 4.2: Data Handler and the cable for the connection at the shirt.

The spirometer (SP) is provided by Sibelmed (Barcelona, Spain) and is the same used as Chronious external device (see Section 2.1.3). The data coming from the SP are transmitted via bluetooth connection to a second computer. The pneumotachograph is the same used in the previous testing phase and was connected with a cable to a third computer. In this phase the SP is connected in series of a PNT (see Figure 4.3 and 4.4).

The sampling rate is set to 50 Hz for both SP and PNT, while the sampling rate for the RIP of the Chronious wearable is set to 16 Hz (as described in the previous section).

The softwares used for data acquisition from the Data Handler and from the spirometer have been realized in LabVIEW by the TBMLAB, Dipartimento di Bioingegneria, Politecnico di Milano. LabVIEW (Laboratory Virtual Instrumentation Engineering Workbench) is a platform and development environment for a visual programming language by National Instruments.

In Figure 4.3 is shown the block diagram of the experimental setup, and in figure 4.4 is shown the setup for the supine position.

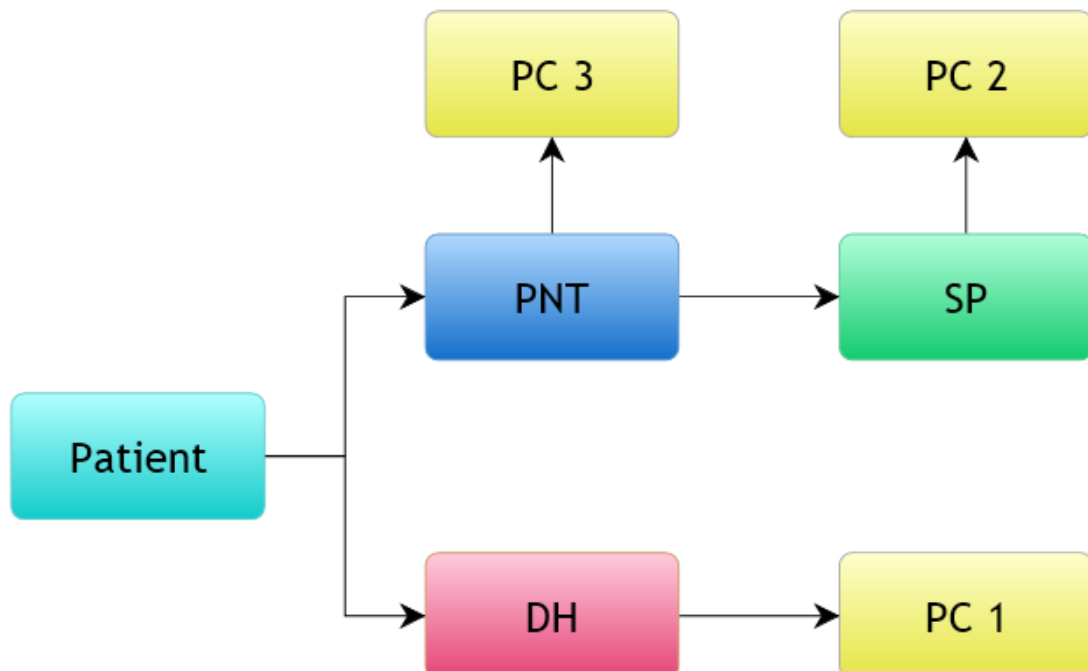


Figure 4.3: Block diagram of the experimental setup.



Figure 4.4: Experimental set-up of the supine position for the validation on healthy subjects.

4.2 Experimental protocol

As a first thing the calibration of the PNT is performed using a 3 liters precision syringe which is connected to the PNT and is pumped slowly in and out manually for 5 times. The acquiring software of PNT automatically computes the acquired signal in order to gain the calibration coefficients of the PNT. The subject was asked to wear the shirt during the whole working day, without changing normal day operations, movements nor habits. Every about two hours during the day the subject underwent a measuring session. During these sessions, we asked at the subjects to breath through a pneumotachograph and simultaneously into a spirometer in both seated and supine positions. In this way, thoracic and abdominal volume changes were measured by RIP and simultaneously was measured the flow at the mouth by SP and PNT. Before each acquisition, in order to acquire the three electrocardiographic signals we put conductive gel on the electrodes, even if those are dry electrodes because the contact between the skin and the electrodes wasn't enough to register properly electrocardiographic signals.

During all the experiments, the subject was asked to perform the following respiratory maneuvers in sequence:

- 1) One inspiratory capacity (IC)

- 2) Four minutes of normal breathing
- 3) Increasing and decreasing breaths volume manoeuvre
- 4) Few seconds of normal breathing

The IC is used for the synchronization of the signals collected during the data analysis phase, from SP, PNT and RespiSENS. The increasing and decreasing volumes maneuver was performed by asking the subject to breath at increasing and then decreasing tidal volumes.

4.3 Data analysis

Four healthy subjects were studied. In this phase we collected respiratory parameters from the Data Handler expressed in digits, from the Spirometer (SP) and the Pneumotachograph (PNT). The SP and PNT measured the air flow at the subject's mouth in liters per second.

As we described in the section of the respiratory inductive plethysmography, the RIP data are not calibrated. In order to calibrate the RIP of the Chronious wearable we adopted two different methods. Both methods are based on the two-compartments model for motion of the respiratory system as described in the previous chapter.

4.3.1 Method 1

Taking into account differences in volume-motion properties of RC and AB compartments it is necessary to calibrate separately the changes of uncalibrated rib cage (ΔuV_{RC}) and changes of uncalibrated abdominal (ΔuV_{AB}) volumes approximately equals to ΔV_{cw} as follows:

$$\Delta V_{cw} \cong M[K(\Delta uV_{RC}) + \Delta uV_{AB}] \quad (1)$$

where ΔV_{cw} is the tidal volume measured by the SP and the PNT; M and K the calibration coefficients. This equation allows us to determine for each subject the calibration coefficients with the Linear Least Square method and to compute the calibrated tidal volume of the RIP. For this purpose we realized three Matlab functions (see Appendix B):

- Respisens_track_Milano_Gennaio.m
- Respisens_Calibration_Milano_Gennaio.m

- `Respisens_Test_Milano_Gennaio.m`

Those functions are similar to the previous functions used in the pre-testing phase; the only difference is the use of the spirometer measures rather than those of OEP.

`Respisens_track_Milano_Gennaio.m` is a function that selects and aligns the region of normal breathing from the tracks of RIP, SP and PNT. This function filters the tracks with a low pass filter (order: 5, cutoff frequency: 2Hz), and integrates the SP and PNT flow tracks to compute the volume trace at the mouth of the patient.

`Respisens_Calibration_Milano_Gennaio.m` function is used to calculate the calibration coefficients of the RIP using the first acquisition data for each subject and for each position. This function computes the tidal volume for each previously selected breath. The points of end inspiration and end expiration (maximum and minimum of the volume trace) of ten to twenty normal quiet breaths are selected using the function `Zview.m` in the traces of RIP, SP and PNT. Applying Least Mean Square algorithm to the equation 1 it is possible to compute the calibration coefficients of the RIP for the first acquisition of the day. The computed K and M are then applied to calibrate the volume traces of the RIP of the next acquisition of the same subject using the `Respisens_Test_firenze.m` function.

Linear regression analysis was performed on the calibration results of the five healthy subjects, in order to demonstrate that Chronious wearable produces volume signals, which are linearly correlated to the volumes measured by spirometer and pneumotachograph.

4.3.2 Method 2

The second algorithm used to compute the calibration of the RIP is based on the same two-compartment model for motion of the respiratory system of the previous method. To calibrate the rib cage (ΔV_{RC}) and abdominal (ΔV_{AB}) volumes displacement we modify the equation 1 as following:

$$\Delta V_{cw} \cong M[K(\Delta V_{RC}) + \Delta V_{AB}] + Q \quad (2)$$

where M, K and Q are the coefficients used for the calibration of the RIP and are calculated with the Linear Least Square method. The difference between this equation and equation 1 consists in the use of the whole data of the traces of uncalibrated rib cage (ΔV_{RC}) and abdominal (ΔV_{AB}) volumes displacement, and flow traces of the SP and the PNT, instead of using only tidal volumes values.

To test this new approach we realized three Matlab functions (see Appendix B):

- *Respisens_Calibration_PDA_Mi_Gennaio.m*
- *Respisens_Volume_Computation_PDA_Mi_Gennaio.m*
- *Respisens_Test_PDA_Mi_Gennaio.m*

Those functions are similar to the previous functions used in the pre-testing phase; the only difference is the use of the spirometer measures rather than those of OEP.

Respisens_Calibration_PDA_Mi_Gennaio.m is a function that allows the selection and alignment of the region of quiet breathing from the tracks of RIP, SP and PNT, and it performs the calibration of the volume of RIP using as a reference the data acquired from the SP and the PNT. The volumes of RIP are calculated applying, to the Eq. 2 the calibration coefficients, estimated with the Linear Least Square method, as described previously.

The *Respisens_Test_PDA_Mi_Gennaio.m* function is used to apply the calibration coefficients, calculated with the previous function, to the uncalibrated volume tracks of the other acquisitions of the same subject.

The *Respisens_Volume_Computation_PDA_Mi_Gennaio.m* function is used after the *Respisens_Calibration_PDA_Mi_Gennaio.m* and *Respisens_Test_PDA_Mi_Gennaio.m* to calculate the calibrated tidal volume of the RI. This function computes the tidal volume for each previously selected breath. The points of end inspiration and end expiration (maximum and minimum of the volume trace) of ten to twenty normal quiet breaths are selected using the function *Zview.m* in the traces of RIP, SP and PNT.

For example, we performed two measures in the sitting position, the calibration procedure is the following:

7) *Respisens_Calibration_PDA_Mi_Gennaio.m*('ID_sitting1');

This function needs the .mat file created with the *Respisens_track_Milano_Gennaio.m* which containing the tracks of the RIP, SP and PNT in the region of normal breathing, that are filters with a low pass filter. With this function we selected the breaths that we used to estimate the calibration coefficients. These coefficients are use to calibrated the RIP volume from SP and PNT. Returns two matrixes: ID_sitting1_par.mat, ID_sitting1_PDA.mat. The first matrix contains the calibration coefficients; the second contain the calibrated volume of the RIP from SP and PNT, and the track of SP and PNT.

8) *Zview*('ID_sitting1_PDA.ldz');

This function needs the .mat file that contains the calibrated volume of the RIP and the tracks of SP and

PNT. Returns four .mxn files that contains the points of maximum and minimum for the track of:

- RIP tidal volume calibrated from SP (ID_sitting1_PDA_rsp.mxn),
- SP volume (ID_sitting1_PDA_spi.mxn),
- RIP tidal volume calibrated from PNT (ID_sitting1_PDA_rpn.mxn),
- PNT volume (ID_sitting1_PDA_pnt.mxn).

9) [out1,out2]=Respisens_Volume_Computation_PDA_Mi_Gennaio('ID_sitting1');

This function needs the two .mat files created with the *Respisens_Calibration_PDA_M_Gennaio.m* function and the four .mxn files. Returns two matrixes with the calibration coefficients, the mean and standard deviation tidal volumes calibrated from the tracks of SP and PNT respectively.

10) Respisens_Test_PDA_Mi_Gennaio('ID_sitting2', out1, out2);

This function needs the .mat file created with the *Respisens_track_Milano_Gennaio.m* which containing the tracks of the RIP, SP and PNT in the region of normal breathing of the second acquisition, that are filters with a low pass filter, and the calibration coefficients estimate with the calibration function, that we previously saved in [out1] and [out2]. These coefficients are used to calculate the RIP calibrated volume from SP and PNT. Returns two matrixes: ID_sitting2_par.mat, ID_sitting2_PDA.mat. The first matrix contains the calibration coefficients; the second contain the calibrated volume of the RIP from SP and PNT, and the track of SP and PNT.

11) Zview('ID_sitting2_PDA.ldz');

This function needs the .mat file that contains the calibrated volume of the RIP , the tracks of SP and PNT. Returns four .mxn files (see point 4) that contains the points of maximum and minimum.

12) [out3,out4]=Respisens_Volume_Computation_PDA_Mi_Gennaio('ID_sitting2');

This function needs the two .mat files created with the *Respisens_Test_PDA_Mi_Gennaio.m* function and the four .mxn files. Returns two matrixes with the calibration coefficients, the mean and standard deviation tidal volumes calibrated from the tracks of SP and PNT respectively.

The first three steps are used in order to compute the calibration coefficients of the RIP of each subject from the data of SP and PNT, in both seated and supine position. The last three steps are used to verify if the RIP calibration is still consistent in the other measures of each subject.

Linear regression analysis was than performed on the calibration results of the four healthy subjects.

4.4 Results

In this phase, the respiratory parameters are evaluated on four healthy subjects by comparing the data collected from the acquisition system with the measurements provided by the spirometer (SP) and the pneumotachograph (PNT) as references. The respiratory parameters coming from the RIP have been calibrated with two methods, and evaluated by a linear regression analysis.

In figure 4.5 are shown the results of the tidal volume of RIP calibrated using SP as a reference, of four subjects obtained with the first calibration method applied on the acquisitions following the calibration acquisition. The data used to plot figure 4.5 are tidal volumes computed starting from the wearable system (RIP) versus tidal volumes computed starting from the SP traces of the whole working day in seated and supine positions. The regression line showed poor correlation between the two sets of data: $r^2=0.10$, $m=0.318$ $q=0.317$. It is possible to see that the slope of the regression varies significantly with posture, as shown in Figures 4.6 and 4.7 in sitting and supine position, respectively (sitting: $m=-0.897$, $q=1.025$; supine: $r^2=0.92$, $m=0.332$, $q=0.274$).

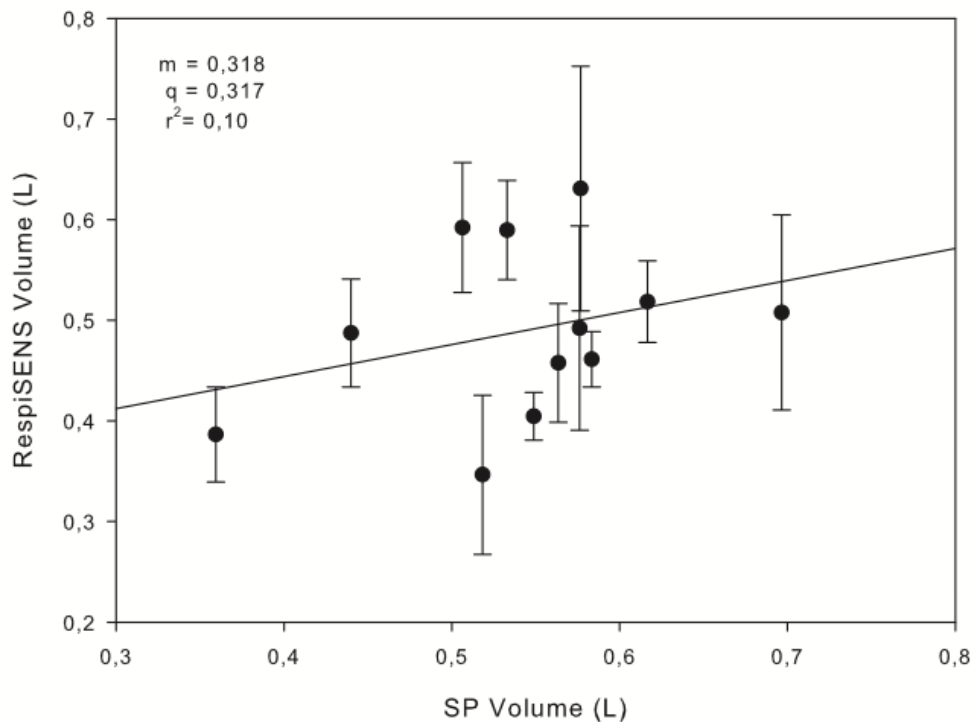


Figure 4.5: Results of calibration by SP, with the first method.

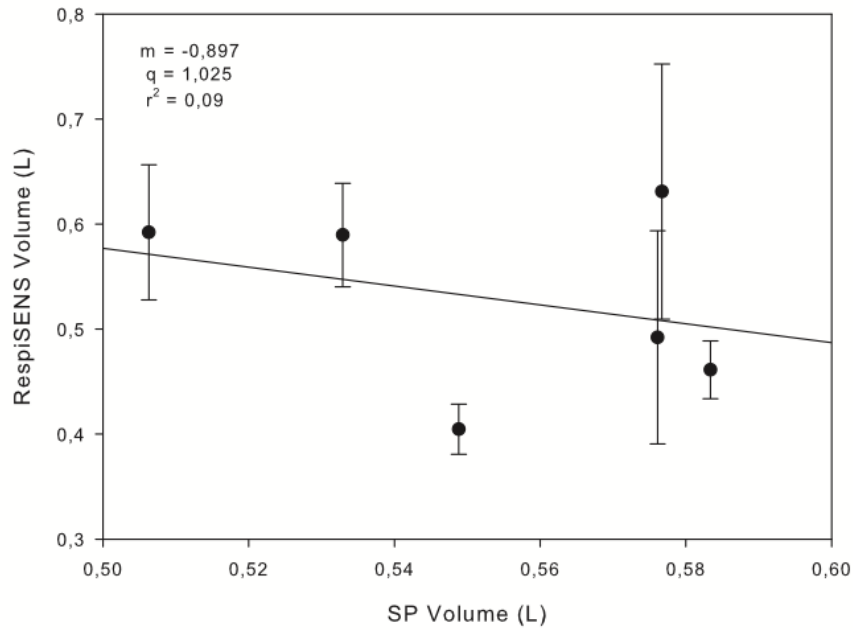


Figure 4.6: Results of calibration by SP in sitting position, with the first method.

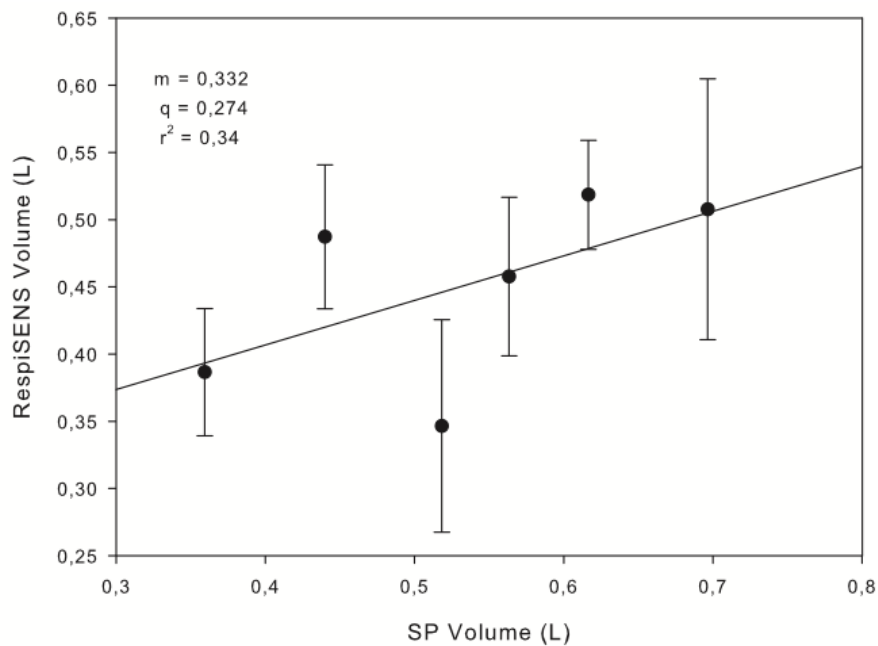


Figure 4.7: Results of calibration by SP in supine position, with the first method.

We performed the linear regression analysis also on the tidal volume of RIP calibrated using as a reference data of the PNT. In figure 4.8 are shown the results of four subjects obtained with the first calibration method applied on the acquisitions following the calibration acquisition. The data used

to plot figure 4.8 are tidal volumes computed starting from the wearable system (RIP) versus tidal volumes computed starting from the PNT traces of the whole working day in seated and supine positions. The regression line showed no correlation between the two sets of data: $r^2=0.004$, $m=0.087$, $q=0.483$.

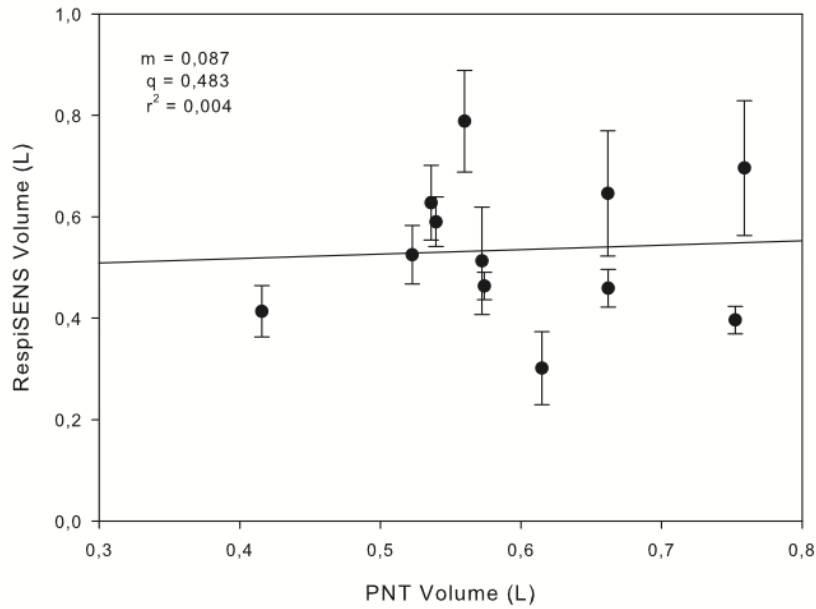


Figure 4.8: Results of calibration by PNT, with the first method.

In the next figures is possible to see that the slope of the regression varied significantly with the postures (sitting: $m=-0.589$ $q=0.896$; supine: $m=0.429$, $q=0.277$).

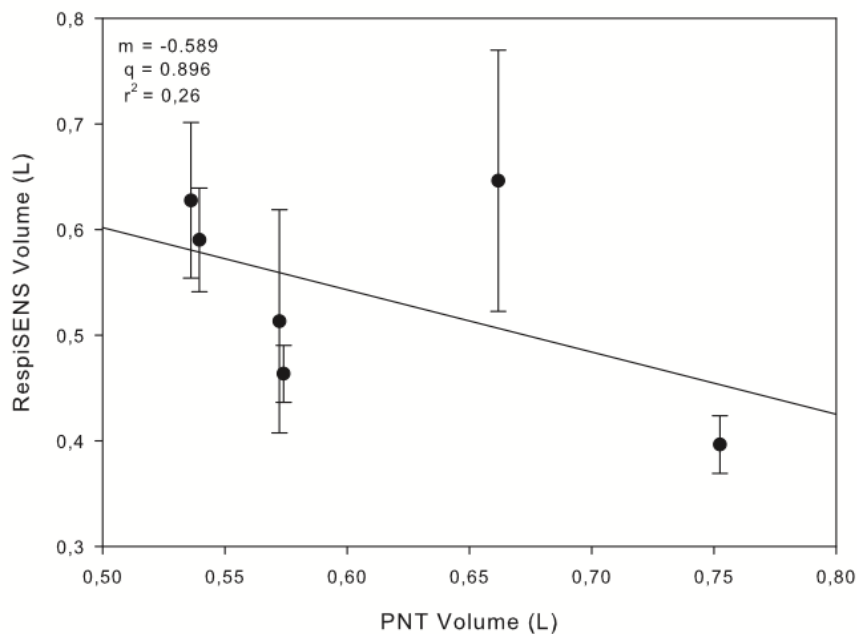


Figure 4.9: Results of calibration by PNT in sitting position, with the first method.

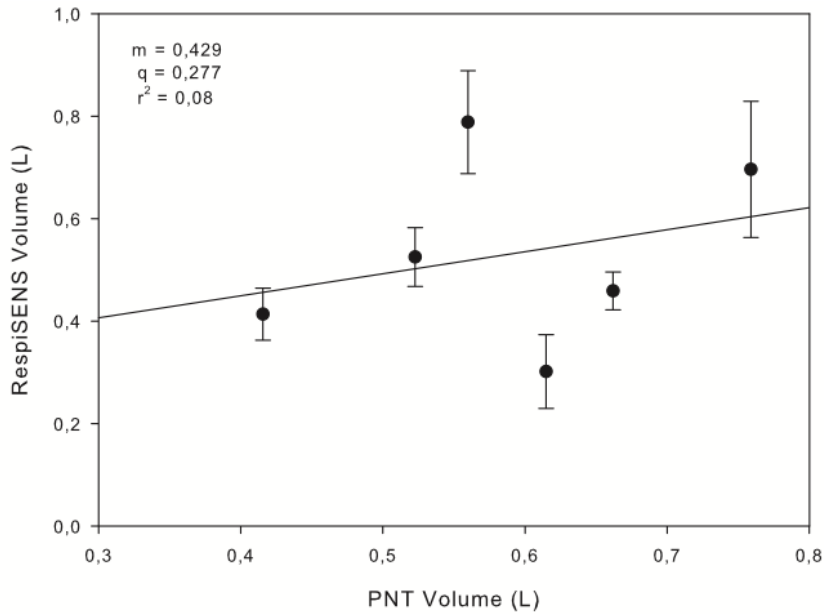


Figure 4.10: Results of calibration by PNT in supine position, with the first method.

The second method of calibration shows better correlation between the volume signals produced by RespiSENS and the volume measured by SP and PNT. The second method uses the whole data of the traces of uncalibrated RIP, the flow trace of the SP and of the PNT. In figure 4.11 are shown the results of the tidal volume of RIP calibrated by SP obtained with the second calibration method.

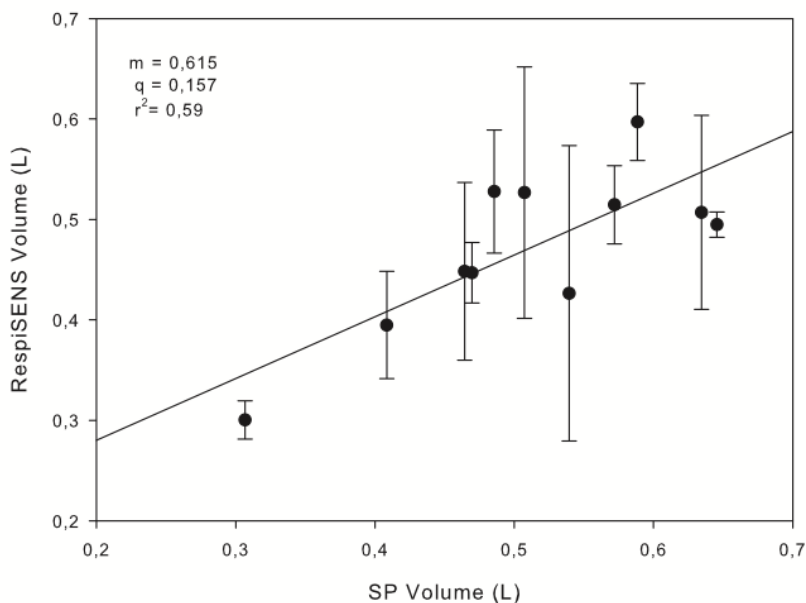


Figure 4.11: Results of calibration by SP, with the second method.

The data used to plot figure 4.11 are tidal volumes computed starting from the wearable system

(RIP) versus tidal volumes computed starting from the SP traces of the whole working day in seated and supine positions. The regression line showed poor correlation between the two sets of data: $r^2=0.59$, $m=0.615$, $q=0.157$. In Figures 4.12 and 4.13 are shown the results in sitting and supine position, respectively.

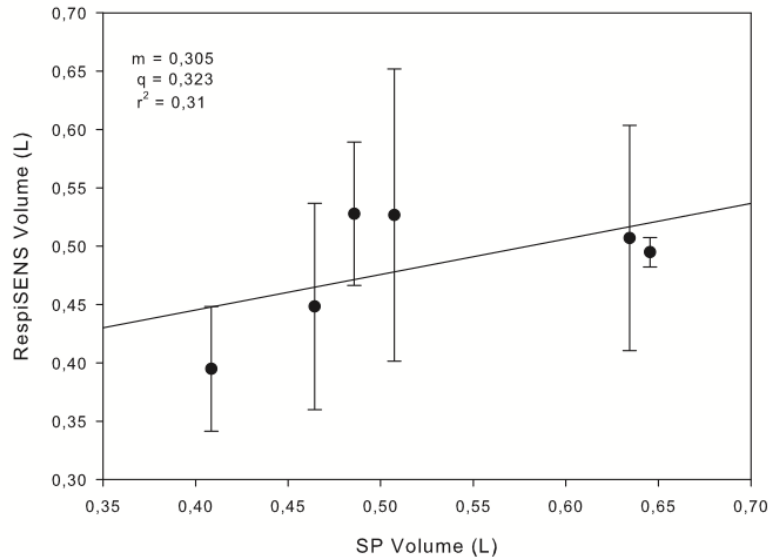


Figure 4.12: Results of calibration by SP in sitting position, with the second method.

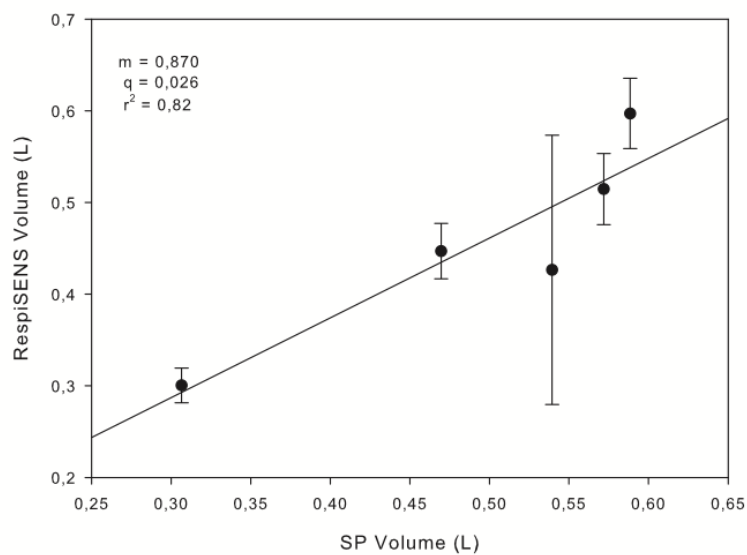


Figure 4.13: Results of calibration by SP in supine position, with the second method.

In the supine position the volume signals produce by RespIENS are much more correlated to the volume measure by SP than in the sitting position (sitting: $r^2=0.31$, $m=0.305$, $q=0.323$; supine: $r^2=0.82$, $m=0.870$, $q=0.026$).

In figure 4.15 are shown the results of the tidal volume of RIP calibrated using PNT as a reference, obtained with the second calibration method applied on the acquisitions following the

calibration acquisition. The data used to plot figure 4.15 are tidal volumes computed starting from RIP versus tidal volumes computed starting from the PNT traces of the whole working day in seated and supine positions. The regression line showed poor correlation between the two sets of data: $r^2=0.14$, $m=0,573$ $q=0,171$.

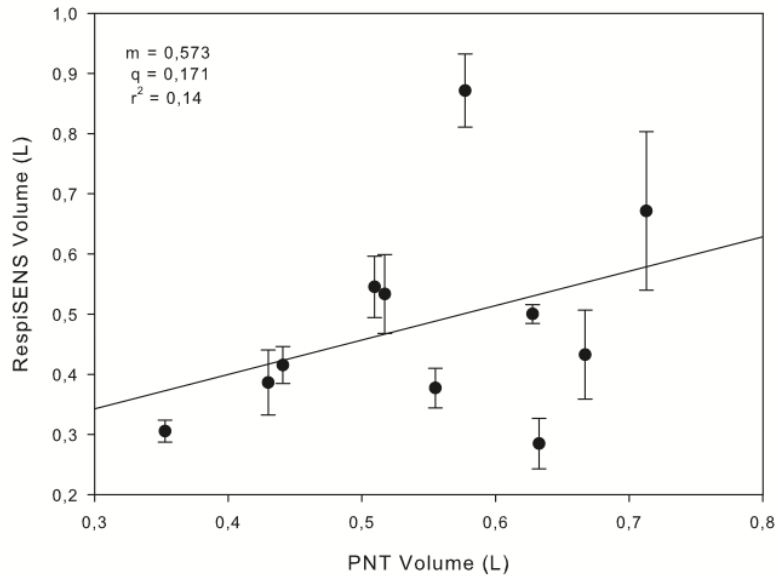


Figure 4.14: Results of calibration by PNT, with the second method.

In the figures 4.15 and 4.16 is possible to see that the slope of the regression varied significantly with the postures (sitting: $m=0.490$, $q=0.229$; supine: $m=0.586$, $q=0.151$).

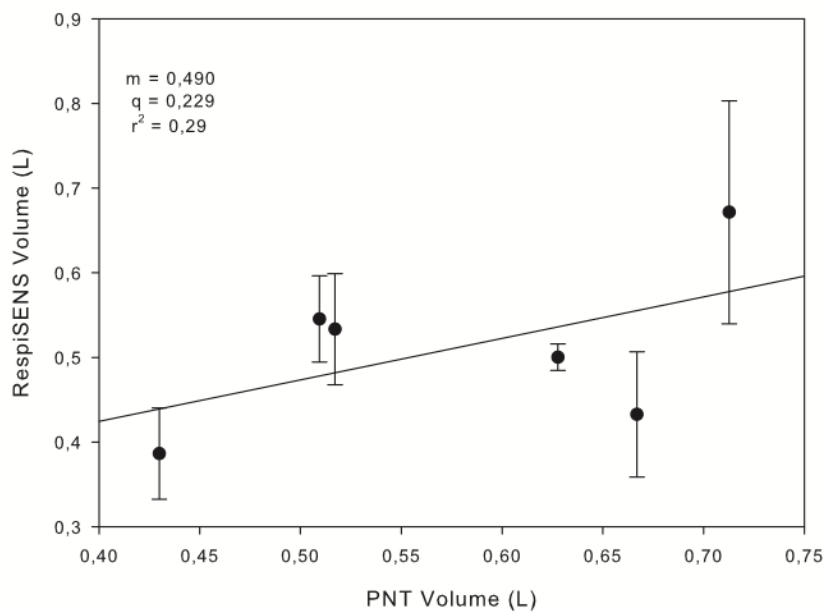


Figure 4.15: Results of calibration by PNT in sitting position, with the second method.

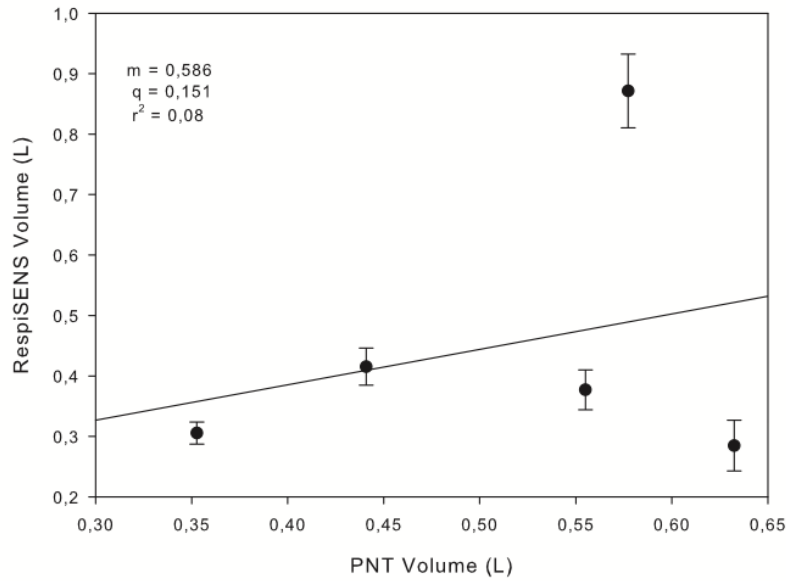


Figure 4.16: Results of calibration by PNT in supine position, with the second method.

The table 4.1 shown the parameters of the linear regression analysis:

Reference	Method 1			Method 2		
	m	q	r ²	m	q	r ²
SP	0,318	0,317	0,10	0,615	0,157	0,59
sitting	-0,897	1,025	0,09	0,305	0,323	0,31
supine	0,332	0,274	0,34	0,870	0,026	0,82
PNT	0,087	0,483	0,004	0,573	0,171	0,14
sitting	-0,589	0,896	0,26	0,490	0,229	0,29
supine	0,429	0,277	0,08	0,586	0,151	0,08

Table 4.1: Parameters of the linear regression analysis.

The tables 4.2 and 4.3 show the calibration coefficient of the cases described estimated using SP and PNT as reference.

Position	Subject	Method 1		Method 2		
		m	k	m	k	q
SITTING	1	0,008	2,899	0,046	-1,072	164,509
	2	0,027	0,029	0,021	-1,026	81,822
	3	0,008	2,052	0,027	0,176	327,831
	4	0,030	1,390	0,020	1,477	405,983
SUPINE	1	0,013	0,859	0,013	1,794	304,431
	2	0,019	0,340	0,017	-0,016	169,931
	3	0,008	3,165	0,006	6,098	317,902
	4	0,052	0,190			

Table 4.2: Calibration coefficients for the data measured by SP.

Position	Subject	Method 1		Method 2		
		m	k	m	k	q
SITTING	1	0,010	2,277	0,021	0,039	250,705
	2	0,028	-0,036	0,021	-1,181	59,938
	3	0,006	2,710	0,022	0,369	292,266
	4	0,032	1,297	0,021	1,975	472,497
SUPINE	1	0,019	1,612	0,017	3,261	583,415
	2	0,020	0,393	0,016	-0,975	63,731
	3	0,007	3,719	0,008	0,735	131,870
	4	0,055	0,530			

Table 4.3: Calibration coefficients for the data measured by PNT.

During the tests we registered also the electrocardiographic signals, the oxygen saturation and the heart rate. We identified PQRST waves within the three derivations in all subjects, and values of oxygen saturation and heart rate compatibles with the subjects studied.

This test phase allowed us to develop the procedures and functions to compute the calibration of the system by the spirometer. Moreover, this phase of test allowed us to assess the set up for the clinical validation on COPD patients and to test the wearable system. In fact, we observed that the on the females the shirt wasn't tight enough, even if we used the new shirt designed to be more adherent on the thin people, and the signals of the two respiratory bands weren't satisfactory. Consequently, we decided a lower bound of the BMI for the selection of the COPD patients for the clinical validation. Instead, we found an increase of the contact of the ECG electrodes with subject's skin. This new shirt allowed us to register on thin subjects signals coming from the RIP and ECG that are more reliable than those measured with the previous S/M size.

Chapter 5

Validation on COPD patients

In this chapter is presented the phase of the project in which the Chronious Wearable framework has been tested on COPD patients in a fully-controlled environment, in the University Hospital of Careggi – Firenze, Thoracic Physiopathology Ward, under the direct and permanent supervision of the medical staff. The institutional ethics committee approved the study, and written informed consent was obtained by each subject.

In this experimental activity the accuracy of the wearable system was tested including the respiratory parameters, the pulseoximeter and the ambient temperature and humidity sensors.

5.1 Experimental setup

The system is based on the shirt with two-respiratory bands (RIP), 4 ECG electrodes, a reflectance pulseoximeter, a sensor for the skin temperature and a sensor for the ambient temperature and humidity, and the Data Handler (DH) for data collection. The sensing elements are directly connected to the Data Handler via a physical cable (Figure 5.1) and all the data are transmitted via bluetooth connection from the Data Handler to a computer.

In this phase were available three sizes of the shirt: S/M, L/XL and the new S/M. The new size S/M has been introduced because the old one was not very adherent on thin subjects and in the previous tests we had some difficulties to measure properly electrocardiographic and respiratory parameters. In this new shirt is inserted an elastic band on its back that makes the shirt more tight on the chest, furthermore the ECG electrodes are bigger and covered with a soft material on its back. These improvements are necessary for increasing the contact between the skin and the ECG electrode, and the contact between the skin and the two respiratory bands. The pocket of the Data Handler has been moved on the front of the T-Shirt, so in this way the device is more accessible also for old and obese people.

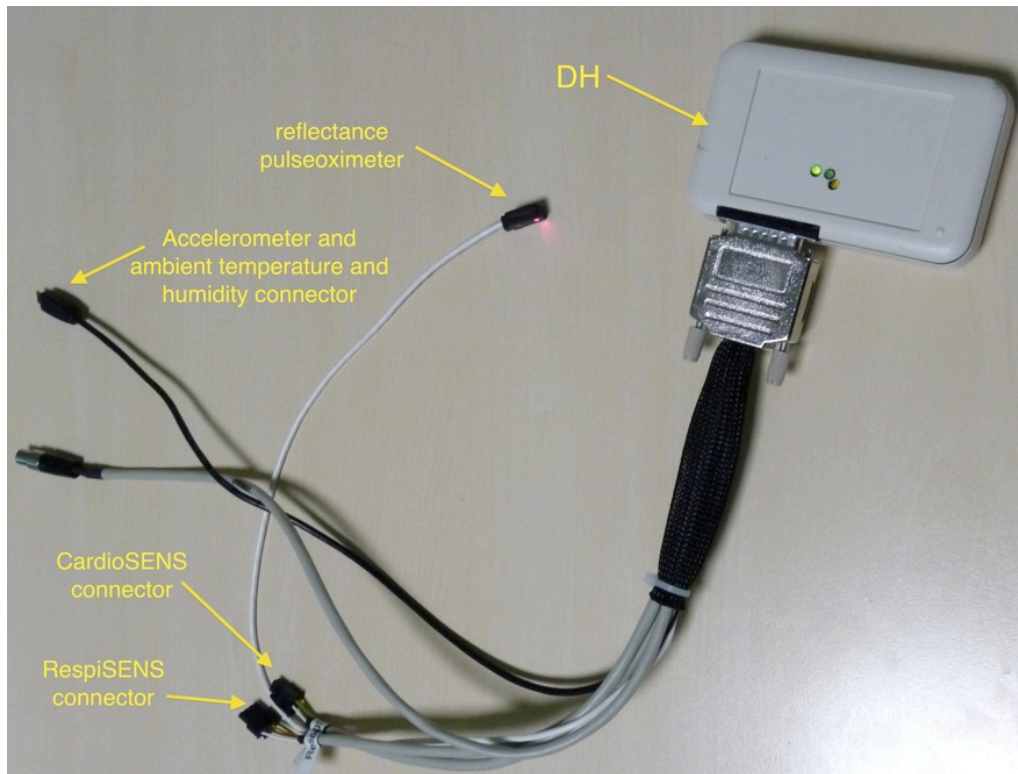


Figure 5.1: Data Handler connected with a cable, in which are included the connectors of the sensing elements of the shirt.

The performance of the system is evaluated by comparison of the measures of the Chronious Wearable system with the measures provided by a spirometer, a finger clip pulseoximeter and two external temperature and humidity sensors. The spirometer is a Sibelmed (the same used in the previous phase on healthy subjects) and its collected data are transmitted via bluetooth connection to a second computer at which is also connected via usb cable a finger clip pulseoximeter (NONIN, Plymouth, Minnesota, USA). Nonin provided the acquiring software of this device.

The softwares used for data acquisition from the Data Handler and from the spirometer have been realized in LabVIEW by the TBMLAB, Dipartimento di Bioingegneria, Politecnico di Milano. LabVIEW (Laboratory Virtual Instrumentation Engineering Workbench) is a platform and development environment for a visual programming language by National Instruments.

The sampling rate of the two respiratory bands is set to 16 Hz, while the sampling rate of the spirometer is set to 50 Hz. The sampling rate of the ECG signals is set to 128 Hz and that of the skin, ambient temperature and humidity sensors is < 1 Hz ($\approx 0,65$ Hz).

In the following figure is shown the block diagram of the experimental set-up and in figure 5.3-5.4 is shown an example of sitting and supine positions acquisition.

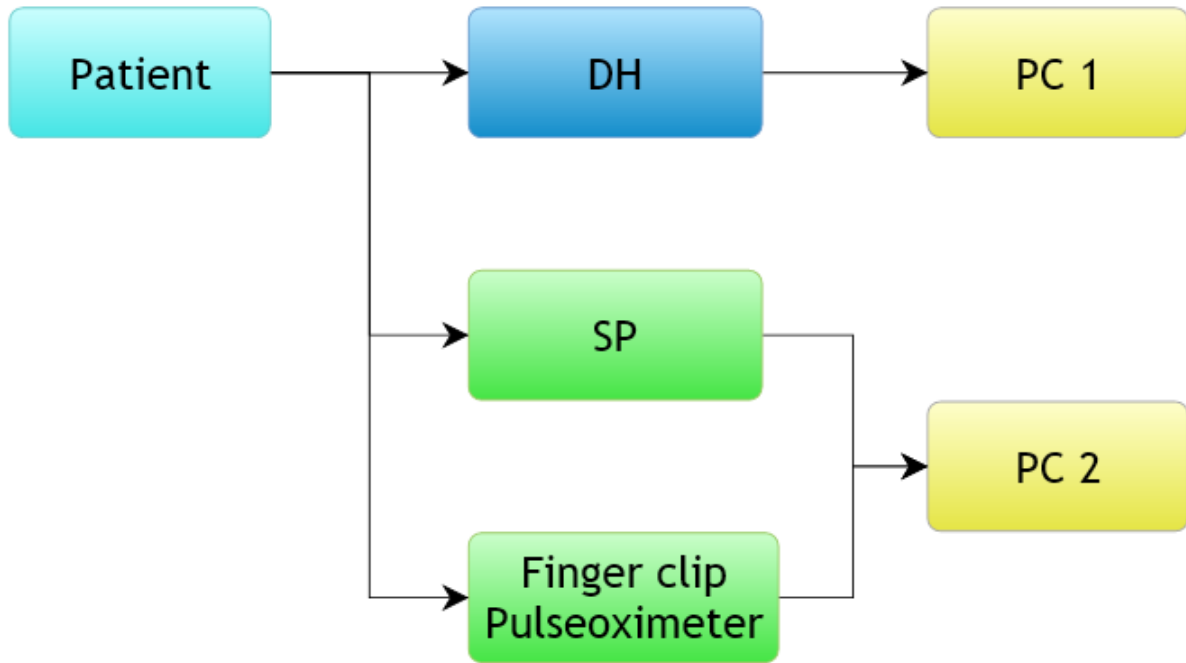


Figure 5.2: Block diagram of the experimental set-up.

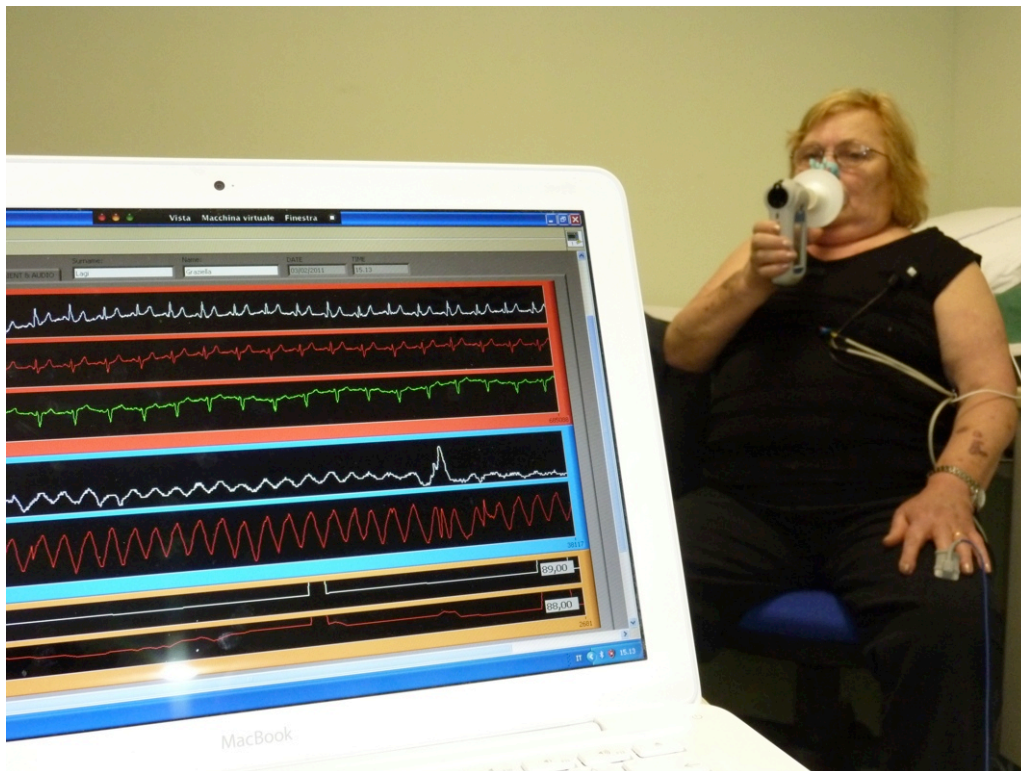


Figure 5.3: Experimental set-up for sitting position acquisition.

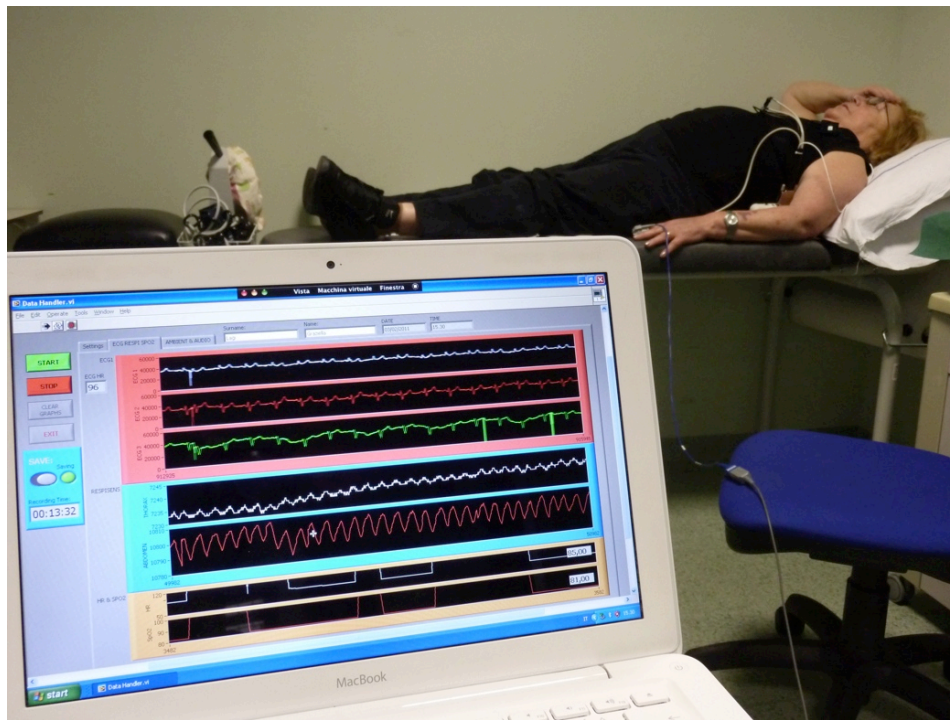


Figure 5.4: Experimental set-up for supine position acquisition.

5.2 Experimental protocol

The patients were asked to wear the shirt and to breathe spontaneously for one hour in both seated and supine positions. Before each acquisition, in order to acquire the three electrocardiographic signals we put conductive gel on the electrodes, even if those are dry electrodes because the contact between the skin and the electrodes wasn't enough to register properly electrocardiographic signals.

At the beginning and at the end of each hour flow at the mouth was also measured by a spirometer, heart rate (HR) and oxygen saturation (SpO_2) by a finger clip pulseoximeter for 10 minutes, to get reference values for comparison. At the end, the 6 minutes walking test (6MWT) was performed.

The 6 minutes walking test is used as an outcome measure in clinical trials of lung disease. This test is widely used because it involves a familiar daily activity and involves the use of minimal technical resources [22]. It measures the distance that a patient can quickly walk on a flat, hard surface in a period of 6 minutes. The 6MWT was performed indoors, along a long, flat, straight, enclosed corridor with a hard surface that is seldom traveled. The walking course was 32m long.

Before the start of the test, a medical staff member measured pulse frequency and blood pressures of the patient, and an index of the dyspnea's level was evaluated using the Borg scale ^[6]. The medical staff member walked behind the participant and measured the heart rate and oxygen saturation by a finger clip pulseoximeter. At each minute during the walk, the staff member told the participant how much time had elapsed, the remaining time and asked how was the level of dyspnea. At the end of the 6 minutes, the participant was told to stop, and the distance walked was recorded. The test was also stopped if oxygen saturation was too low, or if the heart rate was too high, or if the dyspnea was intolerable or if the patient couldn't walk anymore.

5.3 Data analysis

In this phase we collected data from the Data Handler, the Spirometer and the finger clip pulseoximeter. The reference measurements are provided by the SP which measured the air flow at the patient's mouth in liters per second and by the pulseoximeter which provided the heart rate (HR) (Beat Per Minute) and oxygen saturation (SpO_2) (%).

The parameters collected by the DH are the abdominal and thorax volume displacement signals provided by the two respiratory bands (RIP) in digits; the heart rate (HR) and oxygen saturation (S_pO_2) provided by the reflectance pulseoximeter; the three electrocardiographic signals provided by the ECG electrodes and the skin and ambient temperature and humidity provided by the respective sensors. The heart rate, the oxygen saturation, the skin and ambient temperatures and the humidity acquired with the Chronious wearable framework are compared to the references values. Linear regression analysis is computed for these data in order to evaluate the accuracy and usability of Chronious wearable framework.

Furthermore, as explained in the section of the respiratory inductive plethysmography the data coming from the RIP are not calibrated, so in order to calibrate the RIP of the Chronious wearable we adopted two different methods. Both methods are based on the two-compartment model for motion of the respiratory system as described in Chapter 3.

5.3.1 Method 1

Taking into account differences in volume-motion properties of RC and AB compartments it is necessary to calibrate separately the changes of uncalibrated rib cage (ΔuV_{RC}) and changes of uncalibrated abdominal (ΔuV_{AB}) volumes approximately equals to ΔV_{CW} as follows:

$$\Delta V_{cw} \cong M[K(\Delta uV_{RC}) + \Delta uV_{AB}] \quad (1)$$

where ΔV_{cw} is the tidal volume measured by the SP; M and K the calibration coefficients. This equation allows us to determine for each subject the calibration coefficients with the Linear Least Square method and to compute the calibrated tidal volume of the RIP. For this purpose we realized three Matlab functions (see Appendix C):

- *Respisens_track_Firenze.m*
- *Respisens_Calibration_Firenze.m*
- *Respisens_Test_Firenze.m*

These functions are similar to the ones described in the previous chapter. The *Respisens_track_Firenze.m* function is used to select and align the volume tracks of the two respiratory bands to the spirometer data. This function filters the tracks with a low pass filter (order: 5, cutoff frequency: 2Hz), and integrates the SP flow track to compute the volume trace at the mouth of the patient.

The *Respisens_Calibration_Firenze.m* function is used to calculate the calibration coefficients of the RIP using the first acquisition data for each subject and for each position. This function computes the tidal volume for each previously selected breath. The points of end inspiration and end expiration (maximum and minimum of the volume trace) of ten to twenty normal quiet breaths are selected using the function *Zview.m* in the traces of RIP and SP. Applying Least Mean Square algorithm to the equation 1 it is possible to compute the calibration coefficients of the RIP for the first acquisition of the day.

The computed K and M are then applied to calibrate the volume traces of the RIP of the next acquisition of the same subject using the *Respisens_Test_firenze.m* function.

Linear regression analysis is then performed on the calibration results of the nine patients.

5.3.2 Method 2

The second algorithm used to compute the calibration of the RIP is based on the same two-compartment model for motion of the respiratory system of the previous method. To calibrate the rib cage (ΔV_{RC}) and abdominal (ΔV_{AB}) volumes displacement we modify the equation 1 as following:

$$\Delta V_{cw} \cong M[K(\Delta V_{RC}) + \Delta V_{AB}] + Q \quad (2)$$

where M, K and Q are the coefficients used for the calibration of the RIP and are calculated with the Linear Least Square method. The difference between this equation and equation 1 consists in the use of the whole data of the traces of uncalibrated rib cage (ΔV_{RC}) and abdominal (ΔV_{AB}) volumes displacement and flow trace of the SP instead of using only tidal volumes values.

To test this new approach we realized three Matlab functions (see Appendix C):

- *Respisens_Calibration_PDA.m*
- *Respisens_Volume_Computation_PDA.m*
- *Respisens_Test_PDA.m*

These functions are similar to the ones described in the previous chapter.

Respisens_Calibration_PDA.m is a function that allows the selection and alignment of the region of quiet breathing from the tracks of RIP and SP, and it performs the calibration of the volume of RIP using as a reference the data acquired from the SP. This function needs as an input a string (e.g. the name of the subject and position: 'ID_sitting1') and the .mat file created by the function *Respisens_track_Firenze.m*. This .mat file contains the respiratory tracks from the RIP and SP that have been previously selected, aligned and filtered by a low pass filter. Furthermore, the SP track is integrated to obtain the track of the volume of air. The *Respisens_Calibration_PDA.m* function returns two .mat files and an index.txt file. The first .mat file contains a matrix composed of the volumes of the calibrated RIP and the volumes of SP. The volumes of RIP are calculated applying, to the Eq.2, the calibration coefficients, estimated with the Linear Least Square method, as described previously. The second .mat file contains a matrix of the calibration coefficients. The index.txt file contains the information about the data saved in the .mat file, such as the names of the tracks and the sampling frequency of the traces. The input string is used to assign the names to the output files (e.g. ID_sitting1_PDA.mat, ID_sitting1_PDAindex.txt).

The *Respisens_Test_PDA.m* function is used to apply the calibration coefficients to the uncalibrated volume tracks of the other acquisitions of the same subject. This function needs the .mat file created by the function *Respisens_track_Firenze.m* which contains the tracks of the RIP and SP in the region of normal breathing, that are filtered with a low pass filter, and the calibration coefficients estimated with the *Respisens_Calibration_PDA.m* function. The *Respisens_track_Firenze.m* returns two .mat files and an index.txt file. The first .mat file contains a matrix with the volumes of the calibrated RIP and the volumes of SP. The volumes of the RIP are

calculates applying the calibration coefficients estimated using the tracks of the first acquisition. The second .mat file contains a matrix of the calibration coefficients. The index.txt file contains the information about the data in the .mat file, such as the names of the tracks and the sampling frequency. The input string is used to assign the names of the output files (e.g. ID_sitting2_PDA.mat, ID_sitting2_PDAindex.txt).

Respisens_Volume_Computation_PDA.m is a function that calculates the calibrated tidal volume of the RIP. This function uses the two .mat files created with the *Respisens_Calibration_PDA.m* and the *Respisens_Test_PDA.m* function, the .mxn files created by the function *Zview.m* and needs as an input the same string of the previous functions (e.g. the names of the .mat files to load).

Zview.m allows saving the points of end inspiration and end expiration (maximum and minimum) of each breath of the selected tracks in two .mxn files, one for the track of RIP calibrated tidal volume and one for the track of SP volume. Those points are used in the function *Respisens_Volume_Computation_PDA.m* to calculate the tidal volume of each normal breath from the tracks of RIP calibrated volume and SP volume. The function returns a matrix containing the calibration coefficients, the mean tidal volume calibrated from the tracks of SP, the standard deviation of tidal volume calibrated from RIP, the mean and standard deviation of volume from SP.

For example, we performed two measures in the sitting position, the calibration procedure is the following:

13) *Respisens_Calibration_PDA.m*('ID_sitting1');

This function needs the .mat file created with the *Respisens_track_Firenze.m* which containing the tracks of the RIP and SP in the region of normal breathing, that are filters with a low pass filter. With this function we selected the breaths that we used to estimate the calibration coefficients. This coefficients are use to calibrated the RIP volume from SP. Returns two matrixes: ID_sitting1_par.mat, ID_sitting1_PDA.mat. The first matrix contains the calibration coefficients; the second contain the calibrated volume of the RIP and the track of SP.

14) *Zview*('ID_sitting1_PDA.ldz');

This function needs the .mat file that contains the calibrated volume of the RIP and the tracks of SP. Returns two .mxn files: ID_sitting1_PDA_res.mxn, ID_sitting1_PDA_spi.mxn. This files contains the points of maximum and minimum.

15) [out]=*Respisens_Volume_Computation_PDA*('ID_sitting1');

This function needs the two .mat files created with the *Respisens_Calibration_PDA.m* function and the two

.mxn files. Returns a matrix with the calibration coefficients, the mean tidal volume calibrated from RIP, the standard deviation of tidal volume calibrated from RIP, the mean and standard deviation of volume from SP.

16) `Respisens_Test_PDA('ID_sitting2', out);`

This function needs the .mat file created with the `Respisens_track_Firenze.m` which containing the tracks of the RIP and SP in the region of normal breathing of the second acquisition, that are filters with a low pass filter, and the calibration coefficients estimate with the calibration function, that we previously saved in [out]. These coefficients are used to calculate the RIP calibrated volume from SP. Returns two matrixes: `ID_sitting2_par.mat`, `ID_sitting2_PDA.mat`. The first matrix contains the calibration coefficients; the second contain the calibrated volume of the RIP and the track of SP.

17) `Zview('ID_sitting2_PDA.ldz');`

This function needs the .mat file that contains the calibrated volume of the RIP and the tracks of SP.

Returns two .mxn files: `ID_sitting2_PDA_res.mxn`, `ID_sitting2_PDA_spi.mxn`. This files contains the points of maximum and minimum.

18) `[out2]=Respisens_Volume_Computation_PDA('ID_sitting2')`

This function needs the two .mat files created with the `Respisens_Test_PDA.m` function and the two .mxn files. Returns a matrix with the calibration coefficients, the mean tidal volume calibrated from RIP, the standard deviation of tidal volume calibrated from RIP, the mean and standard deviation of volume from SP.

The first three steps are used in order to compute the calibration coefficients of the RIP of each subject in both seated and supine position. The last three steps are used to verify if the RIP calibration is still consistent in the second measure of each subject.

Linear regression analysis is than performed on the calibration results of the nine patients.

5.4 Results

Nine COPD patients were studied, whose characteristics and lung functions are shown in Table 5.1.

In this phase, the respiratory parameters are evaluated by comparing the data collected from the Chronious wearable framework with the measurements provided by the spirometer (SP). The respiratory parameters have been calibrated with two methods and evaluated by a linear regression analysis. In the following figure are shown the results of the tidal volume of RIP calibrated using SP as a reference, of nine patients obtained with the first calibration method applied on the acquisitions following the calibration acquisition. The data used to plot figure 5.5 are tidal volumes

Subjects	Age	Ht. (cm)	Wt. (Kg)	BMI (Kg/m ²)	TLC		RV		FEV1		FEV1/VC		VC		IC	COPD - risk level
					L	% pred	L	% pred	L	% pred	%	pred (%)	L	% pred		
n																
COPD																
mean	70,78	168,11	84,56	29,50	5,90	95,13	2,95	123,00	1,21	45,11	45,56	81,67	2,73	78,11	1,85	2,33
sd	6,55	9,55	20,01	4,57	0,67	17,06	0,53	28,77	0,32	8,95	8,32	0,50	0,80	19,24	0,55	0,71

Table 5.1: Physical characteristics and Spirometric data of

computed starting from the wearable system (RIP) versus tidal volumes computed starting from the SP traces of the whole working day in seated and supine positions. The regression line showed linearly correlation between the two sets of data: $r^2=0.86$, $m=1.109$ $q=-0.063$. It is possible to see that the slope of the regression varies significantly with posture, as shown in Figures 5.6 and 5.7 in sitting and supine position, respectively.

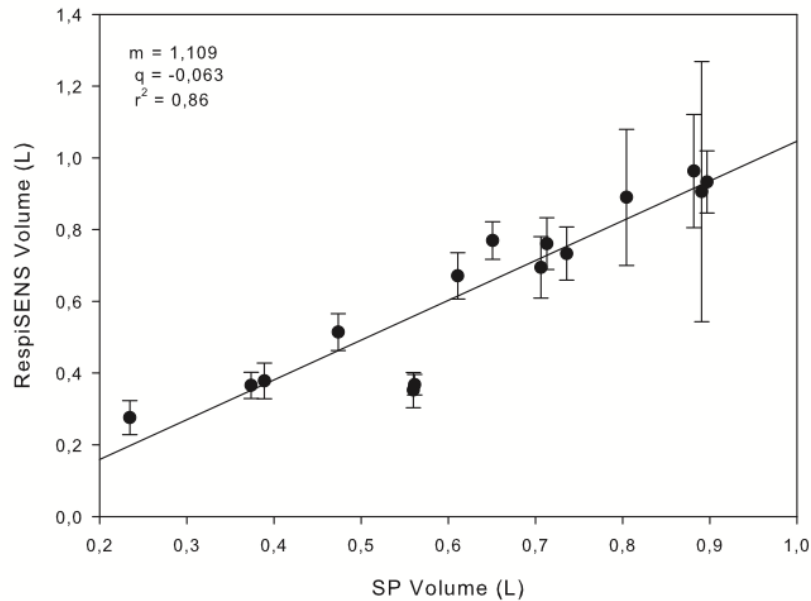


Figure 5.5: Results of RIP calibration by SP, with the first method.

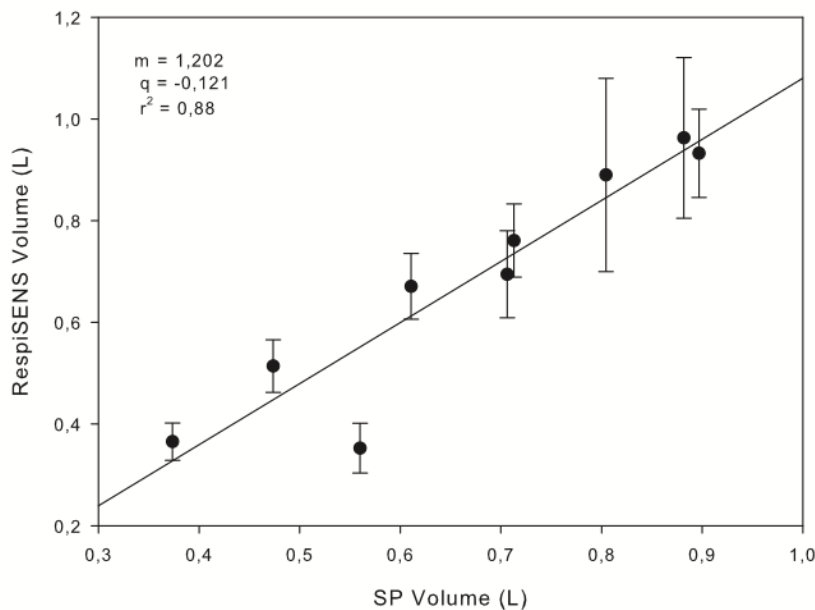


Figure 5.6: Results of RIP calibration by SP in sitting position, with the first method.

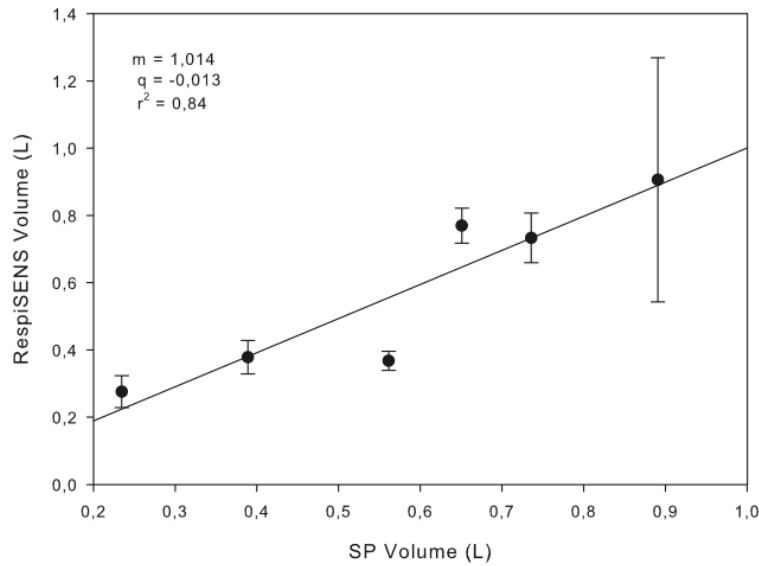


Figure 5.7: Results of RIP calibration by SP in supine position, with the first method.

In these figures the regression line showed correlation between the two sets of data. Furthermore, in the sitting position the volume signals produce by RespiSENS are more correlated to the volume measure by SP than in the supine position (sitting: $r^2=0.88$, $m=1.202$, $q=-0.121$; supine: $r^2=0.84$, $m=1.014$, $q=-0.013$).

The second method of calibration shows lower correlation between the volume signals produced by RespiSENS and the volume measured by SP. The second method uses the whole data of the traces of uncalibrated RIP and the flow trace of the SP. In figure 5.8 are shown the results of the tidal volume of RIP calibrated by SP obtained with the second calibration method.

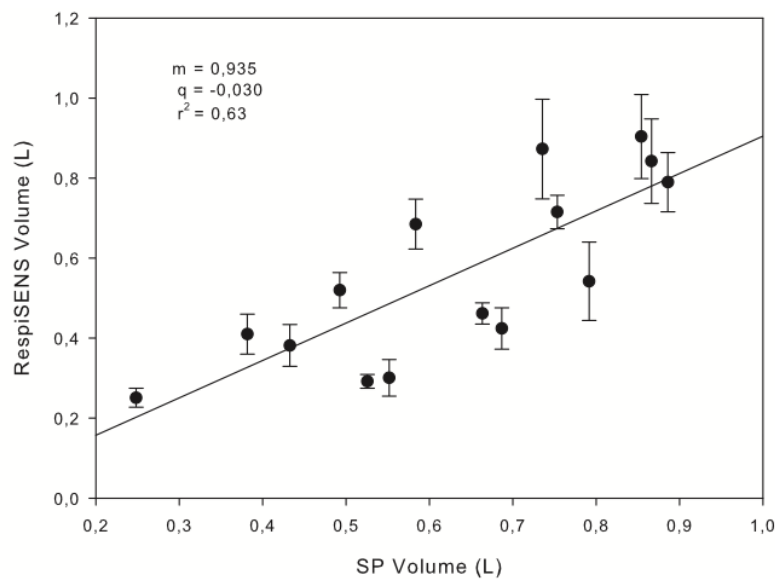


Figure 5.8: Results of RIP calibration by SP, with the second method.

The data used to plot figure 5.8 are tidal volumes computed starting from the wearable system (RIP) versus tidal volumes computed starting from the SP traces of the whole working day in seated and supine positions. The regression line showed poor correlation between the two sets of data: $r^2=0.63$, $m=0.935$, $q=-0.030$. In Figures 5.9 and 5.10 are shown the results in sitting and supine position, respectively.

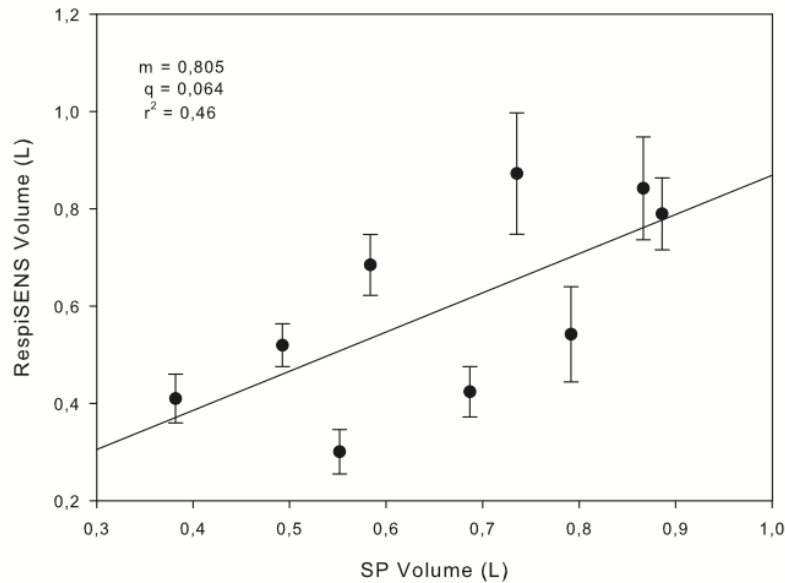


Figure 5.9: Results of RIP calibration by SP in sitting position, with the second method.

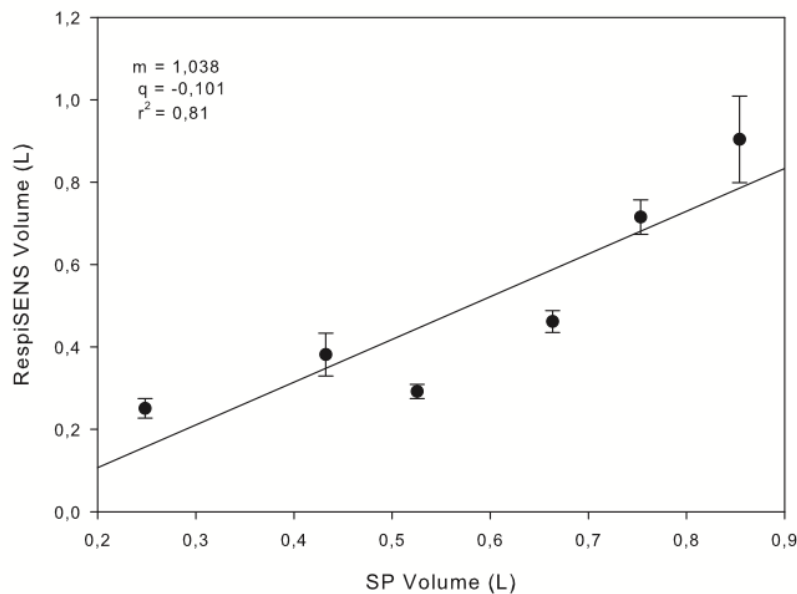


Figure 5.10: Results of RIP calibration by SP in supine position, with the second method.

In the supine position the volume signals produce by RespiSENS are much more correlated to the

volume measure by SP than in the sitting position (sitting: $r^2=0.46$, $m=0.805$, $q=0.064$; supine: $r^2=0.81$, $m=1.038$, $q=-0.101$).

The table 5.2 shown the parameters of the linear regression analysis:

Reference	Method 1			Method 2		
	m	q	r^2	m	q	r^2
SP	1,109	-0,063	0,86	0,935	-0,030	0,63
sitting	1,202	-0,121	0,88	0,805	0,064	0,46
supine	1,014	-0,013	0,84	1,038	-0,101	0,81

Table 5.2: Parameters of the linear regression analysis.

The table 5.3 shows the calibration coefficient of the cases described estimated using SP as reference.

Position	Subject	Method 1		Method 2		
		m	k	m	k	q
SITTING	1	0,013	1,709	0,010	2,367	333,934
	2	0,014	1,101	0,007	2,443	225,432
	3	0,019	1,177	0,021	0,784	319,625
	4	0,016	1,923	0,031	0,723	474,240
	5	0,028	-0,057	0,012	0,933	199,867
	6	0,010	1,089	0,009	1,431	181,940
	7	0,013	1,402	0,011	3,675	410,283
	8	0,010	1,312	0,013	0,227	168,078
	9	0,021	-0,191	0,021	-0,116	204,350
SUPINE	1	0,024	0,524	0,026	0,490	332,427
	2	0,016	0,697	0,008	1,289	180,538
	3	0,018	0,735	0,012	1,177	234,517
	4	0,046	1,315	0,042	0,982	769,445
	5	0,022	0,587	0,023	0,830	360,754
	6	0,012	0,980	0,011	1,399	219,969
	7	0,017	-1,473	0,015	-1,735	-26,230
	8	0,015	-4,112	0,009	2,017	217,218
	9	0,019	0,382	0,018	-0,398	150,523

Table 5.3: Calibration coefficients for the data measured by SP.

The oxygen saturation and the heart rate acquired by the Chronious wearable framework are compared with the measures provided by a finger clip pulseoximeter and evaluated by a linear regression analysis. In the next figure are shown the results of the linear regression analysis for the oxygen saturation:

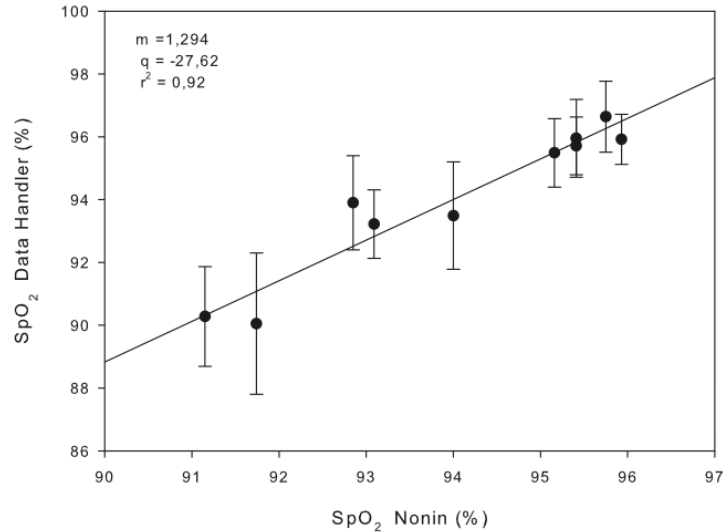


Figure 5.11: Oxygen saturation.

The data used to plot figure 5.11 are oxygen saturation values measured from the wearable system versus oxygen saturation values measured from a finger clip pulseoximeter in the whole testing session in seated and supine positions. The regression line showed high correlation between the two sets of data: $r^2=0.92$, $m=1.294$, $q=-27.62$.

In figure 5.12 are shown the results of the linear regression analysis for the heart rate. The data used to plot figure 5.12 are heart rate values measured from the wearable system versus heart rate values measured from a finger clip pulseoximeter in the whole testing session in seated and supine positions. The regression line showed high correlation between the two sets of data: $r^2=0.99$, $m=1.002$, $q=-0.321$.

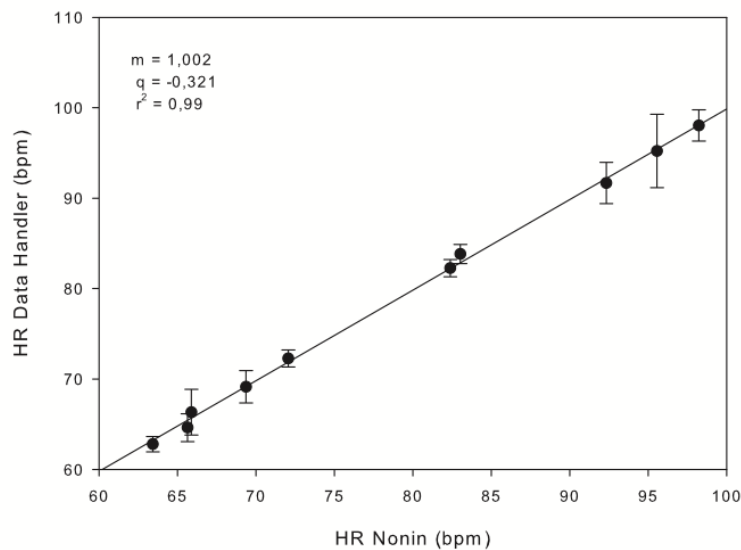


Figure 5.12: Heart rate.

Concerning the electrocardiographic signals, during the tests we identified PQRST complex waves within the 3 derivations, in every patient, and evaluated them from a qualitative point of view (see Figure 5.13).

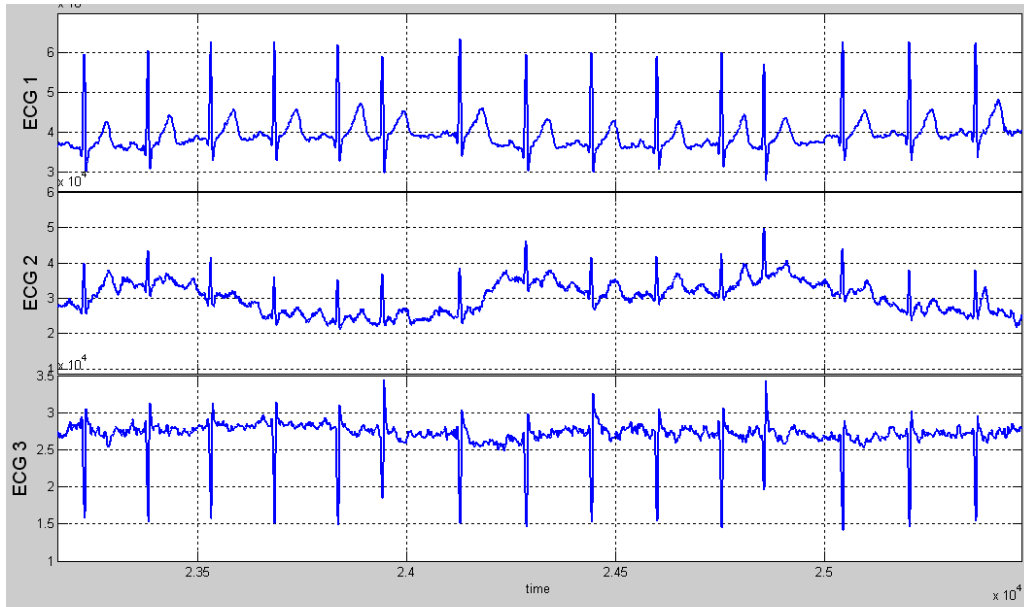


Figure 5.13: Example of the ECG signals acquired on one patient.

Concerning the skin and ambient temperatures and the humidity acquired with the Chronious wearable framework we observed that the measures are not consistent to the reference. In the next table are represented the mean values of skin and ambient temperatures and the humidity acquired with the Chronious wearable (DH) and with the reference (Ref.):

	N° Subjects	Humidity Ref. (%)	Humidity DH (%)	Error (%)	Ambient Temperature e Ref. (°C)	Ambient Temperature DH (°C)	Error (%)
COPD mean	9	26,444	22,518	-15,059	23,944	30,347	26,824

Table 5.3: Ambient temperature and humidity sensors.

The error for the mean values of humidity is computed with the following equation:

$$\text{Error} = \frac{\text{Humidity DH} - \text{Humidity Ref}}{\text{Humidity Ref}} \cdot 100$$

The same equation is used for the mean values of the ambient temperature. In this table is possible

to see that the error between the values acquired by the DH and the external humidity and temperature sensors is very high, so the linear regression analysis is not performed.

The oxygen saturation and the heart rate acquired during the six minute walking test (6MWT) by the Chronious wearable framework are compared with the measures provided by a finger clip pulseoximeter. This analysis involves only six patients, the ones from which we could gain good quality signals. The results shown that the measures are not very consistent to the reference, in table 5.4 are represented the mean values of oxygen saturation and heart rate acquired with the Chronious wearable (DH) and with the finger clip pulseoximeter (Ref.).

	N° Subjects	HR Ref. (bpm)	HR DH (bpm)	Error (%)	SpO2 Ref. (%)	SpO2 DH (%)	Error (%)
COPD mean	6	103,613	96,452	-6,912	92,774	85,774	-7,545

Table 5.4: Oxygen saturation and heart rate during 6MWT.

The error is computed with the same equation used for the humidity and temperature sensors. The linear regression analysis shows that there is no correlation between the values of oxygen saturation and heart rate acquired during the 6MWT by the DH and the finger clip pulseoximeter. However, in the following figure is possible to see that in some subjects the values acquired by the wearable system during the 6MWT are consistent to the reference, both values and trends.

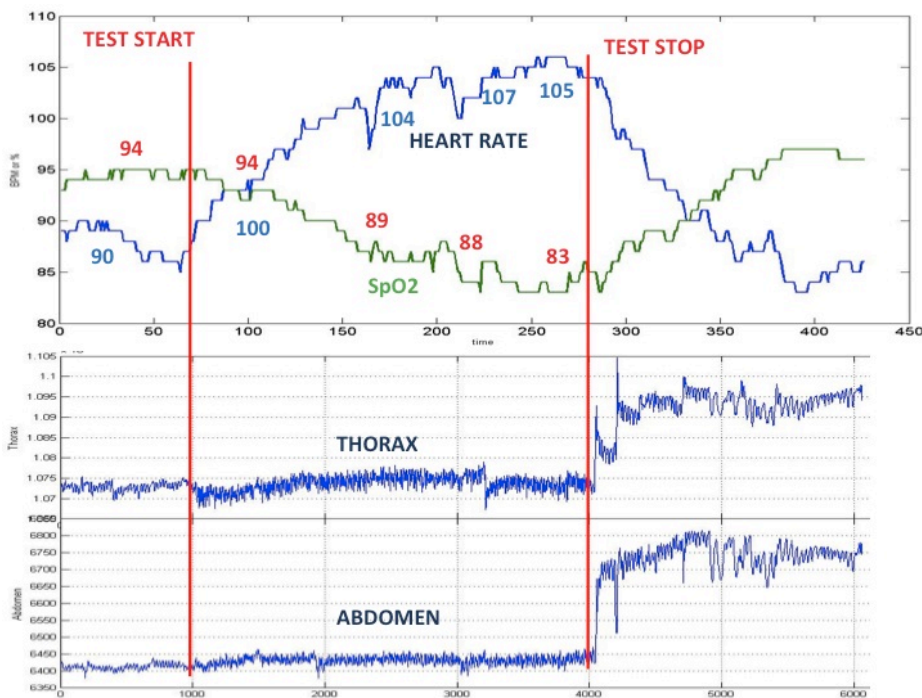


Figure 5.14: Example of the signals acquired by the wearable during the 6MWT. The values of SpO₂ (in red) and heart rate (in blue) are measured by the finger clip pulseoximeter.

Instead, in figure 5.15 is possible to see that the values of oxygen saturation and heart rate measured by the wearable system are not consistent to the reference; but the trend are similar.

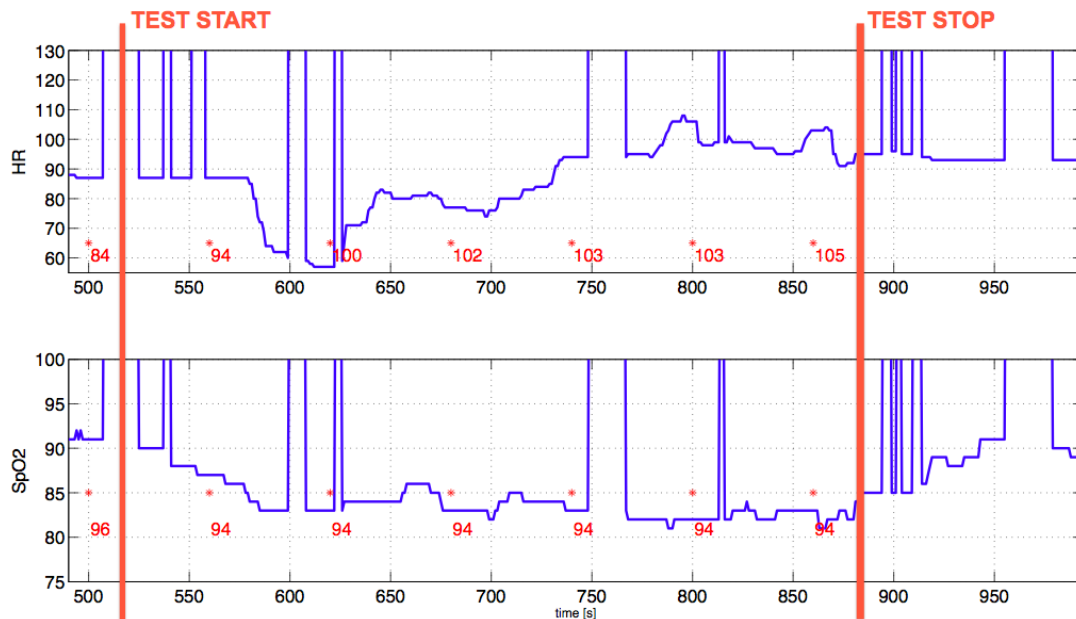


Figure 5.15: Example of the SpO₂ and heart rate acquired by the wearable during the 6MWT. The values in red are measured by the finger clip pulseoximeter.

This test phase allowed us to test the wearable system in nine COPD patients. Concerning the wearable part of the system, the shirt, we had the availability of three shirt sizes (S/M, L/XL and new S/M). We found that some modifications on the design of the wearable are necessary in order to improve the patient comfort and the system usability. In particular, it was noted that several patients had difficulties in wearing the t-shirt without the help of a second person. The problem was evident because they were not able to completely close the lateral zip. In the original version the zip is located in the lateral position and we decided to move it to a more central position. Concerning the skin and ambient temperatures and the humidity acquired with the wearable system we found that the signals are not reliable and some changes on the sensors or in its position are necessary in order to improve signals' quality. As concerns the reflectance pulseoximeter we found some issues to place it in the correct location; the wrong location causes an underestimation of the oxygen saturation and heart rate. This underestimation is more evident during the 6MWT, because the walk causes the movement of the sensor. During the 6MWT we had also some issues to acquire the ECG signals because in some case the conductive gel dried and consequently there was poor contact between the electrodes and the subject's skin.

Conclusion and future developments

The work of this thesis is focused on the validation of the wearable sensing framework of the Chronious platform. In particular, it is focused on the assessment of the respiratory system and on the assessment of the devices used to collect respiratory parameters. In order to achieve these objectives we performed preliminary tests (useful to identify flaws and problems and to design new specifications to improve the system) and a final evaluation on COPD patients.

In the pre-testing phase of the project a first prototype of the wearable device has been assembled and evaluated on five healthy subjects. The respiratory parameters accuracy was determined by comparing the data collected from the wearable system with the measurements provided by opto-electronic plethysmography (OEP) and pneumotachography (PNT). This phase allowed us to develop the procedures and functions to compute the calibration of the RIP and to test the wearable system. We suggested some improvements on the RespiSENS module and we studied some design changes of the shirt in order to improve signals' quality both of the RIP and the ECG. These improvements have been introduced and a new prototype of the wearable system has been produced. This prototype has been tested and evaluated on four healthy subjects: two males, with a normal body mass index (BMI) and two females, with a low BMI. In this experimental activity, the accuracy of the respiratory parameters has been evaluated by comparing the data collected from the wearable system with the measurements provided by a spirometer (SP) and a PNT. During these sessions of test we observed that on some subjects (low BMI females) the shirt wasn't tight enough, even if we used the new shirt designed to be more adherent on thin people, and the signal acquired weren't satisfactory. Consequently, a lower bound of the BMI has been decided and the nine COPD patients were selected for the clinical validation of the wearable system with a BMI greater than XX. In the clinical validation study, the accuracy of the whole wearable system including the respiratory parameters, the pulseoximeter and the ambient temperature and humidity sensors has been tested on nine COPD patients. The performance of the system has been evaluated by comparing the measures provided by the Chronious Wearable system with the ones provided by a spirometer, a finger clip pulseoximeter and two external temperature and humidity sensors. Concerning the wearable part of the system, the shirt, we had the availability of three shirt sizes (S/M, L/XL and new S/M) and we found that some modifications on the design of the wearable are

still necessities in order to improve the patient comfort and the system usability. In particular, it was noted that several patients had difficulties in wearing the t-shirt without the help of a second person. The problem was evident because they were not able to completely close the lateral zip. In the original version the zip is located in the lateral position and we decided to move it to a more central position. Concerning the electrocardiographic signals, we identified P, QRS and T waves within the 3 derivations, in every patient. The ECG signals are reliable, but was necessary to put conductive gel on the electrodes, even if those were suppose to be dry electrodes, because of a poor contact between the skin and the electrodes. For a more user-friendly system it would be necessary to change the ECG electrodes with others that allow acquiring the ECG signals without the use of the conductive gel. As regard to the measurement of the oxygen saturation and the heart rate, we found that the data measured by the wearable system are reliable and consistent with the measures of the finger clip pulseoximeter. The linear regression analysis for the oxygen saturation showed high correlation between the data acquired by the Chronious wearable framework and by a finger clip pulseoximeter: $r^2=0.92$, $m=1.294$, $q=-27.62$. Also the linear regression of the heart rate showed high correlation between the two sets of data: $r^2=0.99$, $m=1.002$, $q=-0.321$. However, we observed that the pulseoximeter is very sensible to its location, if is not collocated on the shoulder in the correct position either the values are lower than the actual ones or the device indicated an error in the acquisition. Concerning the skin and ambient temperatures and humidity we observed that the wearable system underestimates the measures. Future works are necessary to improve these sensors. The temperatures measured on the body with the wearable system have to be correct considering the effects of the external temperature in order to estimate appropriately the temperature of the core of the body from the temperature measured on the skin. Furthermore also the positions of these sensors need to be studied in order to understand if choosing other locations the data can be more consistent with reference values.

Regarding the calibration of the RIP, two different methods have been developed in order to define a calibration procedure suitable to be implemented on smart assistance device (PDA). The first method uses the tidal volume values of the uncalibrated rib cage (RB) and abdominal (AB) provided by RIP and the tidal volume values simultaneously measured by a gold reference device (e.g. OEP, PNT, SP) to compute the calibration coefficients. The second method uses the whole data of these traces. This second method has been developed because in the first one the alignment of the traces and the selection of the tidal volumes are performed manually and Chronious system requires only completely automatic procedures. The experimental data shows that the first method is more accurate than the second one. In fact, we found that the second method has some issues if

the traces of RIP are not perfectly aligned with the trace of the reference system and consequently the computation of the calibration coefficients is less accurate and reliable. The clinical validation study on COPD patients shows that the respiratory parameters of RIP calibrated with the first method using the SP as reference are reliable. The linear regression showed linear correlation between the two sets of data: $r^2=0.86$, $m=1.109$ $q=-0.063$. We also observed that the slope of the regression varies significantly with posture (sitting: $r^2=0.88$, $m=1.202$, $q=-0.121$; supine: $r^2=0.84$, $m=1.014$, $q=-0.013$). For these reason, future works will focus on the implementation of the first method of calibration in the smart assistant device and on the patient's calibration procedure. This step is necessary to perform the second clinical validation of the Chronious project in which the system will be tested on patient's house.

The thesis describes a series of experimental activities in which the Chronious system has been developed, improved and validated on COPD patients. The final results suggest that the Chronious wearable system could to be a promising platform for the management of COPD patients at home.

Appendix A

1) Functions for the first method of calibration used in the pre-testing phase:

```
function []=Respisens_track_Milano_Novembre(string)

% ----- LOAD DATA -----
% RespiSENS:
[filename,pathname]=uigetfile('*..*', 'Select file from RespiSENS ABDOMEN
(_Abdomen.asc)');
Abdomen = load([pathname filename]);

[filename,pathname]=uigetfile('*..*', 'Select file from RespiSENS THORAX
(_Thorax.asc)');
Thorax = load([pathname filename]);

% OEP
[filename,pathname]=uigetfile('*..*', 'Select file from OEP (.dat)');
dataOEP = load([pathname filename]);

Ribcage_30Hz = dataOEP(:,2);
AbdRibcage_30Hz = dataOEP(:,3);
AbdominalVolume_30Hz = dataOEP(:,4);
VtOEP_30Hz=dataOEP(:,5);
FlowOEP_30Hz=dataOEP(:,6);

%Resample OEP signals at 16Hz
Ribcage = resample(Ribcage_30Hz,16,30);
AbdRibcage = resample(AbdRibcage_30Hz,16,30);
AbdominalVolume = resample(AbdominalVolume_30Hz,16,30);
VtOEP = resample(VtOEP_30Hz,16,30);
FlowOEP = resample(FlowOEP_30Hz,16,30);

figure()
ax(1)=subplot(4,1,1);
plot(Thorax);
ylabel('thorax');
ax(2)=subplot(4,1,2);
plot(Abdomen);
ylabel('abdomen');
ax(3)=subplot(4,1,3);
plot(VtOEP);
ylabel('Vt OEP');
ax(4)=subplot(4,1,4);
plot(FlowOEP);
ylabel('Flow Pneumotac');
%linkaxes(ax,'x');

% ----- FILTER DATA -----

%FIR, 6th order, 2 Hz cutoff, 16 Hz sample freq
% Wn=fcutoff/(fsamp/2)
%n1 = fir1(6, 0.25, 'low');
n1 = fir1(5, 0.5, 'low');
```

```

d1 = 1;

AbdomenFilt = -filtfilt(n1,d1,Abdomen);
ThoraxFilt = -filtfilt(n1,d1,Thorax);

Ribcage = filtfilt(n1,d1,Ribcage);
AbdRibcage = filtfilt(n1,d1,AbdRibcage);
AbdominalVolume = filtfilt(n1,d1,AbdominalVolume);
VtOEP = filtfilt(n1,d1,VtOEP);
FlowOEP = filtfilt(n1,d1,FlowOEP);
PntVol = detrend((1/16)*cumsum(FlowOEP));
% ----- SELECT DATA -----

figure();
title('Select initial and final points for spirometer test');
ax(1)=subplot(4,1,1);
grid on;
hold on;
plot(ThoraxFilt);
ylabel('thorax');
ax(2)=subplot(4,1,2);
grid on;
hold on;
plot(AbdomenFilt);
ylabel('abdomen');
subplot(4,1,3);
plot(VtOEP);
hold on;
grid on;
title('Vt OEP');
subplot(4,1,4);
plot(PntVol);
hold on;
grid on;
title('Pneumotac');

linkaxes(ax,'x');

H3=uicontrol('Style','togglebutton','String','Seleziona','Position',[450 7 60
20],'callback','uiresume');
zoom on;
uiwait;

% select breaths for RESPISENS
x_respi=[];
for i=1:2
    [x,y]=ginput(1);
    x_respi=[x_respi; round(x)];
    subplot(4,1,1);
    plot(x_respi,ThoraxFilt(x_respi),'Or');
    subplot(4,1,2);
    plot(x_respi,AbdomenFilt(x_respi),'Or');
end

% select breaths for OEP
subplot(4,1,3);
x_oeep=[];
for i=1:2
    [x,y]=ginput(1);
    x_oeep=[x_oeep; round(x)];
    plot(x_oeep,VtOEP(x_oeep),'Or');
end

```

```

% select breaths for PNEUMOTAC
subplot(4,1,4);
x_pnt=[];
for i=1:2
    [x,y]=ginput(1);
    x_pnt=[x_pnt; round(x)];
    plot(x_pnt,PntVol(x_pnt),'Or');
end

thorax_vol=ThoraxFilt(x_respi(1):x_respi(2));
abdomen_vol=AbdomenFilt(x_respi(1):x_respi(2));
respi_vol=thorax_vol+abdomen_vol;
oep_vol=VtOEP(x_oep(1):x_oep(2));
pnt_vol = PntVol(x_pnt(1):x_pnt(2));

%OEP compartments
oep_rb = Ribcage(x_oep(1):x_oep(2));
oep_abdRb = AbdRibcage(x_oep(1):x_oep(2));
oep_abd =AbdominalVolume(x_oep(1):x_oep(2));

close all
figure ();
ax(1)=subplot(3,1,1);
plot(respi_vol);
title('RESPISENS');
ax(2)=subplot(3,1,2);
plot(oep_vol);
title('OEP');
ax(3)=subplot(3,1,3);
plot(pnt_vol);
title('PNEUMOTAC');

figure ();
ax(1)=subplot(4,1,1);
plot(oep_vol);
title('OEP - Vt');
ax(2)=subplot(4,1,2);
plot(oep_rb);
title('OEP - Ribcage Volume');
ax(3)=subplot(4,1,3);
plot(oep_abdRb);
title('OEP - Abdominal Ribcage Volume');
ax(3)=subplot(4,1,4);
plot(oep_abd);
title('OEP - Abdominal Volume');

oep_tho=oep_rb + oep_abdRb; %OEP Thorax = Ribcage + Ribcage abdominal
H3=uicontrol('Style','togglebutton','String','Continue','Position',[450 7 60
20],'callback','uiresume');
uiwait;

if((length(respi_vol)>length(oep_vol)) && (length(respi_vol)>=length(pnt_vol)))
    pnt_vol=[pnt_vol; pnt_vol(length(pnt_vol))*ones(length(respi_vol)-
length(pnt_vol),1)];
    oep_vol=[oep_vol; oep_vol(length(oep_vol))*ones(length(respi_vol)-
length(oep_vol),1)];
end

if((length(respi_vol)>length(oep_vol)) && (length(respi_vol)<=length(pnt_vol)))
    thorax_vol=[thorax_vol; thorax_vol(length(thorax_vol))*ones(length(pnt_vol)-
length(thorax_vol),1)];
    abdomen_vol=[abdomen_vol;
abdomen_vol(length(abdomen_vol))*ones(length(pnt_vol)-length(abdomen_vol),1)];

```

```

    respi_vol=[respi_vol; respi_vol(length(respi_vol))*ones(length(pnt_vol)-
length(respi_vol),1)];
    oep_vol=[oep_vol; oep_vol(length(oep_vol))*ones(length(pnt_vol)-
length(oep_vol),1)];
end

if((length(respi_vol)>length(pnt_vol)) && (length(respi_vol)<length(oep_vol)))
    thorax_vol=[thorax_vol; thorax_vol(length(thorax_vol))*ones(length(oep_vol)-
length(thorax_vol),1)];
    abdomen_vol=[abdomen_vol;
abdomen_vol(length(abdomen_vol))*ones(length(oep_vol)-length(abdomen_vol),1)];
    respi_vol=[respi_vol; respi_vol(length(respi_vol))*ones(length(oep_vol)-
length(respi_vol),1)];
    pnt_vol=[pnt_vol; pnt_vol(length(pnt_vol))*ones(length(oep_vol)-
length(pnt_vol),1)];
end

if((length(pnt_vol)>length(oep_vol)) && (length(pnt_vol)>length(respi_vol)))
    thorax_vol=[thorax_vol; thorax_vol(length(thorax_vol))*ones(length(pnt_vol)-
length(thorax_vol),1)];
    abdomen_vol=[abdomen_vol;
abdomen_vol(length(abdomen_vol))*ones(length(pnt_vol)-length(abdomen_vol),1)];
    respi_vol=[respi_vol; respi_vol(length(respi_vol))*ones(length(pnt_vol)-
length(respi_vol),1)];
    oep_vol=[oep_vol; oep_vol(length(oep_vol))*ones(length(pnt_vol)-
length(oep_vol),1)];
end

if((length(oep_vol)>length(pnt_vol)) && (length(oep_vol)>length(respi_vol)))
    thorax_vol=[thorax_vol; thorax_vol(length(thorax_vol))*ones(length(oep_vol)-
length(thorax_vol),1)];
    abdomen_vol=[abdomen_vol;
abdomen_vol(length(abdomen_vol))*ones(length(oep_vol)-length(abdomen_vol),1)];
    respi_vol=[respi_vol; respi_vol(length(respi_vol))*ones(length(oep_vol)-
length(respi_vol),1)];
    pnt_vol=[pnt_vol; pnt_vol(length(pnt_vol))*ones(length(oep_vol)-
length(pnt_vol),1)];
end

if(length(oep_vol)>length(oep_tho))
    oep_tho = [oep_tho; oep_tho(length(oep_tho))*ones(length(oep_vol)-
length(oep_tho),1)];
    oep_abd = [oep_abd; oep_abd(length(oep_abd))*ones(length(oep_vol)-
length(oep_abd),1)];
end

dati=[thorax_vol abdomen_vol respi_vol oep_vol pnt_vol oep_tho oep_abd];
matldz=dati;
stringa=[string '.mat'];
eval(['save ',stringa,' matldz;']);

nomefile=[string 'index.txt'];
fp=fopen(nomefile,'w');
fprintf(fp,'variabile          colonna\n');
fprintf(fp,'THORAX              1\nABDOMEN              2\nRESPISENS
3\nOEP                      4\nPNEUMOTAC              5\nOEP_THORAX
6\nOEP_ABDOMEN              7\n');
fprintf(fp,'\n PARAMETRI USATI:\n\n Fc= 16.000 Hz for RespiSENS, Fc= 16.000 Hz
for OEP and Pneumotacograph');
fclose(fp);
close all
end

```

```

function [out1, out2]=Respisens_Calibration_Milano_Novembre(string)

% ----- LOAD FILES -----

thorax_mxn=load([string '_tho.mxn']);
abdomen_mxn=load([string '_abd.mxn']);
respi_mxn=load([string '_res.mxn']);
oep_mxn=load([string '_oep.mxn']);
oepTho_mxn=load([string '_oth.mxn']);
oepAbd_mxn=load([string '_oab.mxn']);
pnt_mxn=load([string '_pnt.mxn']);

data=load([string '.mat']);
data=data.matldz;
thorax_vol=data(:,1);
abdomen_vol=data(:,2);
respi_vol=data(:,3);
oep_vol=data(:,4);
pnt_vol=data(:,5);
oep_tho_vol=data(:,6);
oep_abd_vol=data(:,7);

% ----- VOLUMES COMPUTING -----

% Volume amplitude computing of Vinsp and exp of every trace, using as mxn
% for respisens only the respi.mxn, not taking into account any eventual
% paradoxycal movements, nor asynchronies.

Vinsp_thorax=[];
Vexp_thorax=[];
Vinsp_abdomen=[];
Vexp_abdomen=[];
Vinsp_respi=[];
Vexp_respi=[];
Vinsp_oep=[];
Vexp_oep=[];
Vinsp_pnt=[];
Vexp_pnt=[];
Vthorax=[];
Vabdomen=[];
Vrespi=[];
Voep=[];
Vpnt=[];
Voep_tho=[];
Voep_abd=[];

j=2;
for i=1:length(find(thorax_mxn(:,1)==1))

    if (thorax_mxn(j,1)==-1)
        j=j+1;
    end

    % creating separated vectors for inspiratory volumes and expiratory
    % volumes. Considering mxn file starting with a minimum and finishing with
    % a minimum, even in interruptions.

    Vinsp_thorax=[Vinsp_thorax; thorax_vol(thorax_mxn(j,2))-
thorax_vol(thorax_mxn(j-1,2))];
    Vexp_thorax=[Vexp_thorax; thorax_vol(thorax_mxn(j,2))-
thorax_vol(thorax_mxn(j+1,2))];

```

```

        Vinsp_abdomen=[Vinsp_abdomen; abdomen_vol(abdomen_mxn(j,2))-
abdomen_vol(abdomen_mxn(j-1,2))];
        Vexp_abdomen=[Vexp_abdomen; abdomen_vol(abdomen_mxn(j,2))-
abdomen_vol(abdomen_mxn(j+1,2))];

        %Vinsp_respi=[Vinsp_respi; respi_vol(respi_mxn(j,2))-respi_vol(respi_mxn(j-
1,2))];
        %Vexp_respi=[Vexp_respi; respi_vol(respi_mxn(j,2))-
respi_vol(respi_mxn(j+1,2))];

        Vinsp_oeop=[Vinsp_oeop; oeop_vol(oeop_mxn(j,2))-oeop_vol(oeop_mxn(j-1,2))];
        Vexp_oeop=[Vexp_oeop; oeop_vol(oeop_mxn(j,2))-oeop_vol(oeop_mxn(j+1,2))];

        Vinsp_pnt=[Vinsp_pnt; pnt_vol(pnt_mxn(j,2))-pnt_vol(pnt_mxn(j-1,2))];
        Vexp_pnt=[Vexp_pnt; pnt_vol(pnt_mxn(j,2))-pnt_vol(pnt_mxn(j+1,2))];

        % creating one vector that contains insp and exp volumes respect
        % mininum and max of total volume
        Vthorax=[Vthorax; thorax_vol(respi_mxn(j,2))-thorax_vol(respi_mxn(j-1,2))];
        Vthorax=[Vthorax; thorax_vol(respi_mxn(j,2))-thorax_vol(respi_mxn(j+1,2))];

        Vabdomen=[Vabdomen; abdomen_vol(respi_mxn(j,2))-abdomen_vol(respi_mxn(j-
1,2))];
        Vabdomen=[Vabdomen; abdomen_vol(respi_mxn(j,2))-
abdomen_vol(respi_mxn(j+1,2))];

        %Vrespi=[Vrespi; respi_vol(respi_mxn(j,2))-respi_vol(respi_mxn(j-1,2))];
        %Vrespi=[Vrespi; respi_vol(respi_mxn(j,2))-respi_vol(respi_mxn(j+1,2))];

        Voep=[Voep; oeop_vol(oeop_mxn(j,2))-oeop_vol(oeop_mxn(j-1,2))];
        Voep=[Voep; oeop_vol(oeop_mxn(j,2))-oeop_vol(oeop_mxn(j+1,2))];

        %OEP compartments
        Voep_tho=[Voep_tho; oeop_tho_vol(oeopTho_mxn(j,2))-oeop_tho_vol(oeopTho_mxn(j-
1,2))];
        Voep_tho=[Voep_tho; oeop_tho_vol(oeopTho_mxn(j,2))-
oeop_tho_vol(oeopTho_mxn(j+1,2))];

        Voep_abd=[Voep_abd; oeop_abd_vol(oeopAbd_mxn(j,2))-oeop_abd_vol(oeopAbd_mxn(j-
1,2))];
        Voep_abd=[Voep_abd; oeop_abd_vol(oeopAbd_mxn(j,2))-
oeop_abd_vol(oeopAbd_mxn(j+1,2))];

        Vpnt=[Vpnt; pnt_vol(pnt_mxn(j,2))-pnt_vol(pnt_mxn(j-1,2))];
        Vpnt=[Vpnt; pnt_vol(pnt_mxn(j,2))-pnt_vol(pnt_mxn(j+1,2))];

        j=j+2;

end

% ----- CALIBRATION -----
%CALIBRATION with OEP
% m and k computing
[m_insp_oeop,k_insp_oeop] = LinearLeastSquare(Vinsp_oeop, Vinsp_thorax,
Vinsp_abdomen);
[m_exp_oeop,k_exp_oeop] = LinearLeastSquare(Vexp_oeop, Vexp_thorax, Vexp_abdomen);
[m_oeop,k_oeop] = LinearLeastSquare(Voep, Vthorax, Vabdomen);

% calibration of volume traces
respi_vol_inspcal_oeop = m_insp_oeop*(k_insp_oeop*(thorax_vol) + abdomen_vol);
respi_vol_expcal_oeop = m_exp_oeop*(k_exp_oeop*(thorax_vol) + abdomen_vol);
respi_vol_cal_oeop = m_oeop*(k_oeop*(thorax_vol) + abdomen_vol);
% Tidal volume values calibration

```

```

Vrespi_inspcal_oep = m_insp_oep*(k_insp_oep*(Vthorax) + Vabdomen);
Vrespi_expcal_oep = m_exp_oep*(k_exp_oep*(Vthorax) + Vabdomen);
Vrespi_cal_oep = m_oep*(k_oep*(Vthorax) + Vabdomen);

% mean and standard deviation computings
Vrespi_inspcal_oep_mean = mean(Vrespi_inspcal_oep);
Vrespi_inspcal_oep_sd = std(Vrespi_inspcal_oep);
Vrespi_expcal_oep_mean = mean(Vrespi_expcal_oep);
Vrespi_expcal_oep_sd = std(Vrespi_expcal_oep);
Vrespi_cal_oep_mean = mean(Vrespi_cal_oep);
Vrespi_cal_oep_sd = std(Vrespi_cal_oep);
Voep_mean = mean(Voep);
Voep_sd = std (Voep);

%compare with oep compartments
Vrespi_abd= m_oep*Vabdomen;
Vrespi_tho = m_oep*k_oep*Vthorax;

Vrespi_abd_mean=mean(Vrespi_abd);
Vrespi_abd_sd=std(Vrespi_abd);
Vrespi_tho_mean=mean(Vrespi_tho);
Vrespi_tho_sd=std(Vrespi_tho);

Voep_abd_mean = mean(Voep_abd);
Voep_abd_sd = std(Voep_abd);
Voep_tho_mean = mean(Voep_tho);
Voep_tho_sd = std(Voep_tho);

%CALIBRATION with PNEUMOTAC
% m and k computing
[m_insp_pnt,k_insp_pnt] = LinearLeastSquare(Vinsp_pnt, Vinsp_thorax,
Vinsp_abdomen);
[m_exp_pnt,k_exp_pnt] = LinearLeastSquare(Vexp_pnt, Vexp_thorax, Vexp_abdomen);
[m_pnt,k_pnt] = LinearLeastSquare(Vpnt, Vthorax, Vabdomen);

% calibration of volume traces
respiivol_inspcal_pnt = m_insp_pnt*(k_insp_pnt*(thorax_vol) + abdomen_vol);
respiivol_expcal_pnt = m_exp_pnt*(k_exp_pnt*(thorax_vol) + abdomen_vol);
respiivol_cal_pnt = m_pnt*(k_pnt*(thorax_vol) + abdomen_vol);

% Tidal volume values calibration
Vrespi_inspcal_pnt = m_insp_pnt*(k_insp_pnt*(Vthorax) + Vabdomen);
Vrespi_expcal_pnt = m_exp_pnt*(k_exp_pnt*(Vthorax) + Vabdomen);
Vrespi_cal_pnt = m_pnt*(k_pnt*(Vthorax) + Vabdomen);

% mean and standard deviation computings
Vrespi_inspcal_pnt_mean = mean(Vrespi_inspcal_pnt);
Vrespi_inspcal_pnt_sd = std(Vrespi_inspcal_pnt);
Vrespi_expcal_pnt_mean = mean(Vrespi_expcal_pnt);
Vrespi_expcal_pnt_sd = std(Vrespi_expcal_pnt);
Vrespi_cal_pnt_mean = mean(Vrespi_cal_pnt);
Vrespi_cal_pnt_sd = std(Vrespi_cal_pnt);
Vpnt_mean = mean(Vpnt);
Vpnt_sd = std (Vpnt);

% data saving

out1=[m_oep k_oep Voep_mean Voep_sd Vrespi_cal_oep_mean Vrespi_cal_oep_sd
Voep_tho_mean Voep_tho_sd Vrespi_tho_mean Vrespi_tho_sd Voep_abd_mean
Voep_abd_sd Vrespi_abd_mean Vrespi_abd_sd];

out2=[m_pnt k_pnt Vpnt_mean Vpnt_sd Vrespi_cal_pnt_mean Vrespi_cal_pnt_sd];

```

```

% ----- PLOTTING -----

figure();
ax(1)=subplot(4,1,1);
grid on;
hold on;
plot(respivol_inspcal_oep);
title('OEP')
ylabel('inspcal');
ax(2)=subplot(4,1,2);
grid on;
hold on;
plot(respivol_expcal_oep);
ylabel('expcal');
ax(3)=subplot(4,1,3);
grid on;
hold on;
plot(respivol_cal_oep);
ylabel('cal');
ax(4)=subplot(4,1,4);
grid on;
hold on;
plot(oep_vol);
ylabel('oep');
linkaxes (ax,'x');

figure();
ax(1)=subplot(4,1,1);
grid on;
hold on;
plot(respivol_inspcal_pnt);
title('PNEUMOTAC')
ylabel('inspcal');
ax(2)=subplot(4,1,2);
grid on;
hold on;
plot(respivol_expcal_pnt);
ylabel('expcal');
ax(3)=subplot(4,1,3);
grid on;
hold on;
plot(respivol_cal_pnt);
ylabel('cal');
ax(4)=subplot(4,1,4);
grid on;
hold on;
plot(pnt_vol);
ylabel('pnt');
linkaxes (ax,'x');

function [out1,out2]=Respisens_Test_Milano_Novembre(string,cal1,cal2)

m_oep=cal1(1);
k_oep=cal1(2);
m_pnt=cal2(1);
k_pnt=cal2(2);

thorax_mxn=load([string '_tho.mxn']);
abdomen_mxn=load([string '_abd.mxn']);
respi_mxn=load([string '_res.mxn']);
oep_mxn=load([string '_oep.mxn']);

```

```

oepTho_mxn=load([string '_oth.mxn']);
oepAbd_mxn=load([string '_oab.mxn']);
pnt_mxn=load([string '_pnt.mxn']);

data=load([string '.mat']);
data=data.matldz;
thorax_vol=data(:,1);
abdomen_vol=data(:,2);
respi_vol=data(:,3);
oep_vol=data(:,4);
pnt_vol=data(:,5);
oep_tho_vol=data(:,6);
oep_abd_vol=data(:,7);

% ----- VOLUMES COMPUTING -----

% Volume amplitude computing of Vinsp and exp of every trace, using as mxn
% for respisens only the respi.mxn, not taking into account any eventual
% paradoxyal movements, nor asynchories.

Vinsp_thorax=[];
Vexp_thorax=[];
Vinsp_abdomen=[];
Vexp_abdomen=[];
Vinsp_respi=[];
Vexp_respi=[];
Vinsp_oep=[];
Vexp_oep=[];
Vinsp_pnt=[];
Vexp_pnt=[];
Vthorax=[];
Vabdomen=[];
Vrespi=[];
Voep=[];
Vpnt=[];
Voep_tho=[];
Voep_abd=[];

j=2;
for i=1:length(find(thorax_mxn(:,1)==1))

    if (thorax_mxn(j,1)==-1)
        j=j+1;
    end

    % creating separated vectors for inspiratory volumes and expiratory
    % volumes. Considering mxn file starting with a minimum and finishing with
    % a minimum, even in interruptions.
    Vinsp_thorax=[Vinsp_thorax; thorax_vol(thorax_mxn(j,2))-
thorax_vol(thorax_mxn(j-1,2))];
    Vexp_thorax=[Vexp_thorax; thorax_vol(thorax_mxn(j,2))-
thorax_vol(thorax_mxn(j+1,2))];

    Vinsp_abdomen=[Vinsp_abdomen; abdomen_vol(abdomen_mxn(j,2))-
abdomen_vol(abdomen_mxn(j-1,2))];
    Vexp_abdomen=[Vexp_abdomen; abdomen_vol(abdomen_mxn(j,2))-
abdomen_vol(abdomen_mxn(j+1,2))];

    %Vinsp_respi=[Vinsp_respi; respi_vol(respi_mxn(j,2))-respi_vol(respi_mxn(j-
1,2))];
    %Vexp_respi=[Vexp_respi; respi_vol(respi_mxn(j,2))-
respi_vol(respi_mxn(j+1,2))];

```

```

Vinsp_oeop=[Vinsp_oeop; oep_vol(oep_mxn(j,2))-oep_vol(oep_mxn(j-1,2))];
Vexp_oeop=[Vexp_oeop; oep_vol(oep_mxn(j,2))-oep_vol(oep_mxn(j+1,2))];

Vinsp_pnt=[Vinsp_pnt; pnt_vol(pnt_mxn(j,2))-pnt_vol(pnt_mxn(j-1,2))];
Vexp_pnt=[Vexp_pnt; pnt_vol(pnt_mxn(j,2))-pnt_vol(pnt_mxn(j+1,2))];

% creating one vector that contains insp and exp volumes respect
% mininum and max of total volume
Vthorax=[Vthorax; thorax_vol(respi_mxn(j,2))-thorax_vol(respi_mxn(j-1,2))];
Vthorax=[Vthorax; thorax_vol(respi_mxn(j,2))-thorax_vol(respi_mxn(j+1,2))];

Vabdomen=[Vabdomen; abdomen_vol(respi_mxn(j,2))-abdomen_vol(respi_mxn(j-
1,2))];
Vabdomen=[Vabdomen; abdomen_vol(respi_mxn(j,2))-
abdomen_vol(respi_mxn(j+1,2))];

%Vrespi=[Vrespi; respi_vol(respi_mxn(j,2))-respi_vol(respi_mxn(j-1,2))];
%Vrespi=[Vrespi; respi_vol(respi_mxn(j,2))-respi_vol(respi_mxn(j+1,2))];

Voep=[Voep; oep_vol(oep_mxn(j,2))-oep_vol(oep_mxn(j-1,2))];
Voep=[Voep; oep_vol(oep_mxn(j,2))-oep_vol(oep_mxn(j+1,2))];

%OEP compartments
Voep_tho=[Voep_tho; oep_tho_vol(oepTho_mxn(j,2))-oep_tho_vol(oepTho_mxn(j-
1,2))];
Voep_tho=[Voep_tho; oep_tho_vol(oepTho_mxn(j,2))-
oep_tho_vol(oepTho_mxn(j+1,2))];

Voep_abd=[Voep_abd; oep_abd_vol(oepAbd_mxn(j,2))-oep_abd_vol(oepAbd_mxn(j-
1,2))];
Voep_abd=[Voep_abd; oep_abd_vol(oepAbd_mxn(j,2))-
oep_abd_vol(oepAbd_mxn(j+1,2))];

Vpnt=[Vpnt; pnt_vol(pnt_mxn(j,2))-pnt_vol(pnt_mxn(j-1,2))];
Vpnt=[Vpnt; pnt_vol(pnt_mxn(j,2))-pnt_vol(pnt_mxn(j+1,2))];

j=j+2;

end

% ----- CALIBRATION -----

%OEP
respi_vol_cal_oeop = m_oeop*(k_oeop*(thorax_vol) + abdomen_vol);

% Tidal volume values calibration
Vrespi_cal_oeop = m_oeop*(k_oeop*(Vthorax) + Vabdomen);

% mean and standard deviation computings
Vrespi_cal_oeop_mean = mean(Vrespi_cal_oeop);
Vrespi_cal_oeop_sd = std(Vrespi_cal_oeop);
Voep_mean = mean(Voep);
Voep_sd = std (Voep);

Vrespi_abd= m_oeop*Vabdomen;
Vrespi_tho = m_oeop*k_oeop*Vthorax;

Vrespi_abd_mean=mean(Vrespi_abd);
Vrespi_abd_sd=std(Vrespi_abd);
Vrespi_tho_mean=mean(Vrespi_tho);
Vrespi_tho_sd=std(Vrespi_tho);

Voep_abd_mean = mean(Voep_abd);

```

```

Voep_abd_sd = std(Voep_abd);
Voep_tho_mean = mean(Voep_tho);
Voep_tho_sd = std(Voep_tho);

% data saving
out1=[m_oep k_oep Voep_mean Voep_sd Vrespi_cal_oep_mean Vrespi_cal_oep_sd
Voep_tho_mean Voep_tho_sd Vrespi_tho_mean Vrespi_tho_sd Voep_abd_mean
Voep_abd_sd Vrespi_abd_mean Vrespi_abd_sd];

%PNEUMOTAC
respi_vol_cal_pnt = m_pnt*(k_pnt*(thorax_vol) + abdomen_vol);

% Tidal volume values calibration
Vrespi_cal_pnt = m_pnt*(k_pnt*(Vthorax) + Vabdomen);

% mean and standard deviation computings
Vrespi_cal_pnt_mean = mean(Vrespi_cal_pnt);
Vrespi_cal_pnt_sd = std(Vrespi_cal_pnt);
Vpnt_mean = mean(Vpnt);
Vpnt_sd = std (Vpnt);

% data saving
out2=[m_pnt k_pnt Vpnt_mean Vpnt_sd Vrespi_cal_pnt_mean Vrespi_cal_pnt_sd];

end

```

2) Functions for the second method of calibration used in the pre-testing phase:

```

function []=Respisens_Calibration_PDA_Mi_Novembre(string)

data=load([string '.mat']);
data=data.matldz;
thorax_vol=data(:,1);
abdomen_vol=data(:,2);
respi_vol=data(:,3);
oep_vol=data(:,4);
pnt_vol=data(:,5);
oep_tho_vol=data(:,6);
oep_abd_vol=data(:,7);

figure();
title('Select initial and final points for spirometer test');
subplot(3,1,1);
grid on;
hold on;
plot(respi_vol);
title('RESPISENS');
subplot(3,1,2);
plot(oep_vol);
hold on;
grid on;
title ('OEP');
subplot(3,1,3);
plot(pnt_vol);
hold on;

```

```

grid on;
title ('PNEUMOTAC');

H3=icontrol('Style','togglebutton','String','Seleziona','Position',[450 7
60 20],'callback','uiresume');
zoom on;
uiwait;

% select breaths for RESPISENS
x_respi=[];
for i=1:2
    [x,y]=ginput(1);
    x_respi=[x_respi; round(x)];
    subplot(3,1,1);
    plot(x_respi, respi_vol(x_respi), 'Or');
end

% select breaths for OEP
subplot(3,1,2);
x_oepl=[];
for i=1:2
    [x,y]=ginput(1);
    x_oepl=[x_oepl; round(x)];
    plot(x_oepl, oep_vol(x_oepl), 'Or');
end

% select breaths for PNEUMOTAC
subplot(3,1,3);
x_pnt=[];
for i=1:2
    [x,y]=ginput(1);
    x_pnt=[x_pnt; round(x)];
    plot(x_pnt, pnt_vol(x_pnt), 'Or');
end

tho_track=thorax_vol(x_respi(1):x_respi(2));
abd_track=abdomen_vol(x_respi(1):x_respi(2));
res_track=respi_vol(x_respi(1):x_respi(2));
oep_tho_track=oep_tho_vol(x_oepl(1):x_oepl(2));
oep_abd_track=oep_abd_vol(x_oepl(1):x_oepl(2));
oep_track=oep_vol(x_oepl(1):x_oepl(2));
pnt_track=pnt_vol(x_pnt(1):x_pnt(2));

figure();
subplot(3,1,1);
grid on;
plot(res_track);
title('respisens');
subplot(3,1,2);
plot(oep_track);
grid on;
title ('OEP');
subplot(3,1,3);
plot(pnt_track);
grid on;
title ('PNEUMOTAC');

oep_interp=interpft(oep_track, length(res_track));

```

```
oep_tho_interp=interpft(oep_tho_track, length(res_track));
oep_abd_interp=interpft(oep_abd_track, length(res_track));
pnt_interp=interpft(pnt_track, length(res_track));

figure();
subplot(3,1,1);
plot(res_track);
grid on;
title('respisens');
subplot(3,1,2);
plot(oep_interp);
grid on;
title ('OEP');
subplot(3,1,3);
plot(pnt_interp);
grid on;
title ('PNEUMOTAC');

figure();
subplot(3,1,1);
plot(oep_interp);
grid on;
title('OEP');
subplot(3,1,2);
plot(oep_tho_interp);
grid on;
title ('OEP thorax');
subplot(3,1,3);
plot(oep_abd_interp);
grid on;
title ('OEP abdomen');

close all

%%% CALIBRATION BY OEP
[m_oe,k_oe,q_oe]=LinearLeastSquare_PDA(oep_interp,tho_track,abd_track);

Vrespi_cal_oe = m_oe*(k_oe*(tho_track) + abd_track) + q_oe;

figure();
subplot(2,1,1);
plot(Vrespi_cal_oe);
grid on;
title('respisens Calibrato');
subplot(2,1,2);
plot(oep_interp);
grid on;
title ('OEP');

%compare with oep compartments
Vrespi_abd= m_oe*abd_track;
Vrespi_tho = m_oe*k_oe*tho_track;

%%% CALIBRATION BY PNEUMOTAC
[m_pnt,k_pnt,q_pnt]=LinearLeastSquare_PDA(pnt_interp,tho_track,abd_track);

Vrespi_cal_pnt = m_pnt*(k_pnt*(tho_track) + abd_track) + q_pnt;

figure();
```

```

subplot(2,1,1);
plot(Vrespi_cal_pnt);
grid on;
title('respisens Calibrato');
subplot(2,1,2);
plot(pnt_interp);
grid on;
title ('PNEUMOTAC');

%%% SAVE DATA
data=[Vrespi_cal_oeo oep_interp oep_tho_interp Vrespi_tho oep_abd_interp
Vrespi_abd Vrespi_cal_pnt pnt_interp ];
matldz=data;

stringa=[string '_PDA.mat'];
eval(['save ',stringa,' matldz;']);

nomefile=[string '_PDAindex.txt'];
fp=fopen(nomefile,'w');
fprintf(fp,'variabile          colonna\n');
fprintf(fp,'RESPISENS-OEP          1\nOEP
2\nOEP-THORAX          3\nRESPI-THORAX
4\nOEP-ABDOMEN          5\nRESPI-ABDOMEN
6\nRESPISENS-PNT          7\nPNUEMOTAC          8\n');
fprintf(fp,'\n PARAMETRI USATI:\n\n Fc= 16.000 Hz ');
fclose(fp);

[out]= [m_oeo k_oeo q_oeo m_pnt k_pnt q_pnt];
par=out;
stringa2=[string '_par.mat'];
eval(['save ',stringa2,' par;']);

end

function []=Respisens_Test_PDA_Mi_Novembre(string,out1,out2)

data=load([string '.mat']);
data=data.matldz;
thorax_vol=data(:,1);
abdomen_vol=data(:,2);
respi_vol=data(:,3);
oeo_vol=data(:,4);
pnt_vol=data(:,5);
oeo_tho_vol=data(:,6);
oeo_abd_vol=data(:,7);

m_oeo=out1(1);
k_oeo=out1(2);
q_oeo=out1(3);

m_pnt=out2(1);
k_pnt=out2(2);
q_pnt=out2(3);

figure();
title('Select initial and final points for spirometer test');
subplot(3,1,1);

```

```

grid on;
hold on;
plot(respi_vol);
title('RESPISENS');
subplot(3,1,2);
plot(oep_vol);
hold on;
grid on;
title ('OEP');
subplot(3,1,3);
plot(pnt_vol);
hold on;
grid on;
title ('PNEUMOTAC');

H3=uicontrol('Style','togglebutton','String','Seleziona','Position',[450 7
60 20],'callback','uiresume');
zoom on;
uiwait;

% select breaths for RESPISENS
x_respi=[];
for i=1:2
    [x,y]=ginput(1);
    x_respi=[x_respi; round(x)];
    subplot(3,1,1);
    plot(x_respi,respi_vol(x_respi),'Or');
end

% select breaths for OEP
subplot(3,1,2);
x_oep=[];
for i=1:2
    [x,y]=ginput(1);
    x_oep=[x_oep; round(x)];
    plot(x_oep,oep_vol(x_oep),'Or');
end

% select breaths for PNEUMOTAC
subplot(3,1,3);
x_pnt=[];
for i=1:2
    [x,y]=ginput(1);
    x_pnt=[x_pnt; round(x)];
    plot(x_pnt,pnt_vol(x_pnt),'Or');
end

tho_track=thorax_vol(x_respi(1):x_respi(2));
abd_track=abdomen_vol(x_respi(1):x_respi(2));
res_track=respi_vol(x_respi(1):x_respi(2));
oep_tho_track=oep_tho_vol(x_oep(1):x_oep(2));
oep_abd_track=oep_abd_vol(x_oep(1):x_oep(2));
oep_track=oep_vol(x_oep(1):x_oep(2));
pnt_track=pnt_vol(x_pnt(1):x_pnt(2));

figure();
subplot(3,1,1);
grid on;
plot(res_track);

```

```

title('respisens');
subplot(3,1,2);
plot(oep_track);
grid on;
title ('OEP');
subplot(3,1,3);
plot(pnt_track);
grid on;
title ('PNEUMOTAC');

oep_interp=interpft(oep_track, length(res_track));
oep_tho_interp=interpft(oep_tho_track, length(res_track));
oep_abd_interp=interpft(oep_abd_track, length(res_track));
pnt_interp=interpft(pnt_track, length(res_track));

figure();
subplot(3,1,1);
plot(res_track);
grid on;
title('respisens');
subplot(3,1,2);
plot(oep_interp);
grid on;
title ('OEP');
subplot(3,1,3);
plot(pnt_interp);
grid on;
title ('PNEUMOTAC');

figure();
subplot(3,1,1);
plot(oep_interp);
grid on;
title('OEP');
subplot(3,1,2);
plot(oep_tho_interp);
grid on;
title ('OEP thorax');
subplot(3,1,3);
plot(oep_abd_interp);
grid on;
title ('OEP abdomen');

close all

%%% CALIBRATION BY OEP
Vrespi_cal_oep = m_oep*(k_oep*(tho_track) + abd_track) + q_oep;

figure();
subplot(2,1,1);
plot(Vrespi_cal_oep);
grid on;
title('respisens Calibrato');
subplot(2,1,2);
plot(oep_interp);
grid on;
title ('OEP');

%compare with oep compartments

```

```

Vrespi_abd= m_oe*p*abd_track;
Vrespi_tho = m_oe*p*k_oe*p*tho_track;
%%% CALIBRATION BY PNEUMOTAC
Vrespi_cal_pnt = m_pnt*(k_pnt*(tho_track) + abd_track) + q_pnt;

figure();
subplot(2,1,1);
plot(Vrespi_cal_pnt);
grid on;
title('respisens Calibrato');
subplot(2,1,2);
plot(pnt_interp);
grid on;
title ('PNEUMOTAC');

%%% SAVE DATA
data=[Vrespi_cal_oe p_oe_interp oep_tho_interp Vrespi_tho oep_abd_interp
Vrespi_abd Vrespi_cal_pnt pnt_interp ];
matldz=data;

stringa=[string '_PDA.mat'];
eval(['save ',stringa,' matldz;']);

nomefile=[string '_PDAindex.txt'];
fp=fopen(nomefile,'w');
fprintf(fp,'variabile          colonna\n');
fprintf(fp,'RESPISENS-OEP          1\nOEP
2\nOEP-THORAX          3\nRESPI-THORAX
4\nOEP-ABDOMEN          5\nRESPI-ABDOMEN
6\nRESPISENS-PNT          7\nPNEUMOTAC          8\n');
fprintf(fp,'\n PARAMETRI USATI:\n\n Fc= 16.000 Hz ');
fclose(fp);

[out]= [m_oe k_oe q_oe m_pnt k_pnt q_pnt];
par=out;
stringa2=[string '_par.mat'];
eval(['save ',stringa2,' par;']);

end

function [out1,out2]=Respisens_Volume_Computation_PDA_Mi_Novembre(string)

data=load([string '_PDA.mat']);
data=data.matldz;

p = load([string '_par.mat']);
p = p.par;
m_oe=p(1);
k_oe=p(2);
q_oe=p(3);
m_pnt=p(4);
k_pnt=p(5);
q_pnt=p(6);

respi_oe_mxn=load([string '_PDA_rop.mxn']);
oe_mxn=load([string '_PDA_oe.mxn']);
res_tho_mxn=load([string '_PDA_rth.mxn']);

```

```

oep_tho_mxn=load([string '_PDA_oth.mxn']);
res_abd_mxn=load([string '_PDA_rab.mxn']);
oep_abd_mxn=load([string '_PDA_oab.mxn']);
respi_pnt_mxn=load([string '_PDA_rpn.mxn']);
pnt_mxn=load([string '_PDA_pnt.mxn']);

respi_oep_vol= data(:,1);
oep_vol=data(:,2);
oep_tho_vol=data(:,3);
res_tho_vol=data(:,4);
oep_abd_vol=data(:,5);
res_abd_vol=data(:,6);
respi_pnt_vol=data(:,7);
pnt_vol=data(:,8);

Vrespi_oep=[];
Voep=[];
Vres_tho=[];
Voep_tho=[];
Vres_abd=[];
Voep_abd=[];
Vrespi_pnt=[];
Vpnt=[];

j=2;
for i=1:length(find(respi_oep_mxn(:,1)==1))

    if (respi_oep_mxn(j,1)==-1)
        j=j+1;
    end

    Vrespi_oep=[Vrespi_oep; respi_oep_vol(respi_oep_mxn(j,2))-
respi_oep_vol(respi_oep_mxn(j-1,2))];
    Vrespi_oep=[Vrespi_oep; respi_oep_vol(respi_oep_mxn(j,2))-
respi_oep_vol(respi_oep_mxn(j+1,2))];

    Voep=[Voep; oep_vol(oep_mxn(j,2))-oep_vol(oep_mxn(j-1,2))];
    Voep=[Voep; oep_vol(oep_mxn(j,2))-oep_vol(oep_mxn(j+1,2))];

    Vres_tho=[Vres_tho; res_tho_vol(res_tho_mxn(j,2))-
res_tho_vol(res_tho_mxn(j-1,2))];
    Vres_tho=[Vres_tho; res_tho_vol(res_tho_mxn(j,2))-
res_tho_vol(res_tho_mxn(j+1,2))];

    Voep_tho=[Voep_tho; oep_tho_vol(oep_tho_mxn(j,2))-
oep_tho_vol(oep_tho_mxn(j-1,2))];
    Voep_tho=[Voep_tho; oep_tho_vol(oep_tho_mxn(j,2))-
oep_tho_vol(oep_tho_mxn(j+1,2))];

    Vres_abd=[Vres_abd; res_abd_vol(res_abd_mxn(j,2))-
res_abd_vol(res_abd_mxn(j-1,2))];
    Vres_abd=[Vres_abd; res_abd_vol(res_abd_mxn(j,2))-
res_abd_vol(res_abd_mxn(j+1,2))];

    Voep_abd=[Voep_abd; oep_abd_vol(oep_abd_mxn(j,2))-
oep_abd_vol(oep_abd_mxn(j-1,2))];
    Voep_abd=[Voep_abd; oep_abd_vol(oep_abd_mxn(j,2))-
oep_abd_vol(oep_abd_mxn(j+1,2))];

    Vrespi_pnt=[Vrespi_pnt; respi_pnt_vol(respi_pnt_mxn(j,2))-

```

```

respi_pnt_vol(respi_pnt_mxn(j-1,2));
Vrespi_pnt=[Vrespi_pnt; respi_pnt_vol(respi_pnt_mxn(j,2))-
respi_pnt_vol(respi_pnt_mxn(j+1,2))];

Vpnt=[Vpnt; pnt_vol(pnt_mxn(j,2))-pnt_vol(pnt_mxn(j-1,2))];
Vpnt=[Vpnt; pnt_vol(pnt_mxn(j,2))-pnt_vol(pnt_mxn(j+1,2))];

j=j+2;

end

%%% OEP
Vrespi_oep_mean = mean(Vrespi_oep);
Vrespi_oep_sd = std(Vrespi_oep);
Voep_mean = mean(Voep);
Voep_sd = std(Voep);

Vrespi_abd_mean=mean(Vres_abd);
Vrespi_abd_sd=std(Vres_abd);
Vrespi_tho_mean=mean(Vres_tho);
Vrespi_tho_sd=std(Vres_tho);

Voep_abd_mean = mean(Voep_abd);
Voep_abd_sd = std(Voep_abd);
Voep_tho_mean = mean(Voep_tho);
Voep_tho_sd = std(Voep_tho);

err = ((Vrespi_oep_mean - Voep_mean)/Voep_mean)*100;

out1 = [m_oep k_oep q_oep Voep_mean Voep_sd Vrespi_oep_mean Vrespi_oep_sd
err Voep_tho_mean Voep_tho_sd Vrespi_tho_mean Vrespi_tho_sd Voep_abd_mean
Voep_abd_sd Vrespi_abd_mean Vrespi_abd_sd];

%%% PNEUMOTAC
Vrespi_pnt_mean = mean(Vrespi_pnt);
Vrespi_pnt_sd = std(Vrespi_pnt);
Vpnt_mean = mean(Vpnt);
Vpnt_sd = std (Vpnt);

err = ((Vrespi_pnt_mean - Vpnt_mean)/Vpnt_mean)*100;

out2 = [m_pnt k_pnt q_pnt Vpnt_mean Vpnt_sd Vrespi_pnt_mean Vrespi_pnt_sd
err];

end

```

Appendix B

1) Functions for the first method of calibration used in the second testing phase:

```
function []=Respisens_track_Milano_Gennaio(string)

% ----- LOAD DATA -----
% RespiSENS:
[filename,pathname]=uigetfile('*.*', 'Select file from RespiSENS
(_RESPISENS.txt)');
dataRespiS = load([pathname filename]);

Abdomen = dataRespiS(:,1);
Thorax = dataRespiS(:,2);

%SPIROMETER
[filename,pathname]=uigetfile('*.*', 'Select file from SPIROMETER
(_SPIROMETER.txt)');
dataSpir = load([pathname filename]);

%PNEUMOTAC
[filename,pathname]=uigetfile('*.*', 'Select file from PNEUMOTAC (_.lab)');
dataPnt= load([pathname filename]);

Spir_50Hz = dataSpir(:,2);
Pnt_50Hz = dataPnt(:,1);
Spir_15Hz= resample(Spir_50Hz,15,50);
Pnt_15Hz = resample(Pnt_50Hz,15,50);

%Spir_15Hz = resample(Spir_50Hz,16,50);

figure()
ax(1)=subplot(4,1,1);
plot(Thorax);
ylabel('thorax');
ax(2)=subplot(4,1,2);
plot(Abdomen);
ylabel('abdomen');
ax(3)=subplot(4,1,3);
plot(Spir_15Hz);
ylabel('Spirometer');
ax(4)=subplot(4,1,4);
plot(Pnt_15Hz);
ylabel('Pneumotac');
%linkaxes(ax,'x');

% ----- FILTER DATA -----

%FIR, 6th order, 2 Hz cutoff, 16 Hz sample freq
% Wn=fcutoff/(fsamp/2)
%n1 = fir1(6, 0.25, 'low');
n1 = fir1(5, 0.5, 'low');
```

```

d1 = 1;

AbdomenFilt = -filtfilt(n1,d1,Abdomen);
ThoraxFilt = -filtfilt(n1,d1,Thorax);
SpirFilt= filtfilt(n1,d1,Spir_15Hz);
SpirVol=detrend((1/15)*cumsum(SpirFilt));
PntFilt= filtfilt(n1,d1,Pnt_15Hz);
PntVol=detrend((1/15)*cumsum(PntFilt));

% ----- SELECT DATA -----

figure();
title('Select initial and final points for spirometer test');
ax(1)=subplot(4,1,1);
grid on;
hold on;
plot(ThoraxFilt);
ylabel('thorax');
ax(2)=subplot(4,1,2);
grid on;
hold on;
plot(AbdomenFilt);
ylabel('abdomen');
subplot(4,1,3);
plot(SpirVol);
hold on;
grid on;
title ('SPIROMETER');
subplot(4,1,4);
plot(PntVol);
hold on;
grid on;
title ('PNEUMOTAC');

linkaxes(ax,'x');

H3=uicontrol('Style','togglebutton','String','Seleziona','Position',[450 7
60 20],'callback','uiresume');
zoom on;
uiwait;

% select breaths for RESPISENS
x_respi=[];
for i=1:2
    [x,y]=ginput(1);
    x_respi=[x_respi; round(x)];
    subplot(4,1,1);
    plot(x_respi,ThoraxFilt(x_respi),'Or');
    subplot(4,1,2);
    plot(x_respi,AbdomenFilt(x_respi),'Or');
end

% select breaths for SPIROMETER
subplot(4,1,3);
x_spiro=[];
for i=1:2
    [x,y]=ginput(1);
    x_spiro=[x_spiro; round(x)];
    plot(x_spiro,SpirVol(x_spiro),'Or');
end

```

```

% select breaths for PNEUMOTAC
subplot(4,1,4);
x_pnt=[];
for i=1:2
    [x,y]=ginput(1);
    x_pnt=[x_pnt; round(x)];
    plot(x_pnt,PntVol(x_pnt),'Or');
end

thorax_vol=ThoraxFilt(x_respi(1):x_respi(2));
abdomen_vol=AbdomenFilt(x_respi(1):x_respi(2));
respi_vol=thorax_vol+abdomen_vol;
spiro_vol=SpirVol(x_spiro(1):x_spiro(2));
pnt_vol = PntVol(x_pnt(1):x_pnt(2));

close all
figure ();
ax(1)=subplot(3,1,1);
plot(respi_vol);
title('RESPISENS');
ax(2)=subplot(3,1,2);
plot(spiro_vol);
title('SPIROMETER');
ax(2)=subplot(3,1,3);
plot(pnt_vol);
title('PNEUMOTAC');

H3=uicontrol('Style','togglebutton','String','Continue','Position',[450 7 60
20],'callback','uiresume');
uiwait;

% pareggio la lunghezza dei tre vettori

% if length(respi_vol)<length(spiro_vol)
%     thorax_vol=[thorax_vol;
thorax_vol(length(thorax_vol))*ones(length(spiro_vol)-
length(thorax_vol),1)];
%     abdomen_vol=[abdomen_vol;
abdomen_vol(length(abdomen_vol))*ones(length(spiro_vol)-
length(abdomen_vol),1)];
%     respi_vol=[respi_vol;
respi_vol(length(respi_vol))*ones(length(spiro_vol)-length(respi_vol),1)];
% else
%     spiro_vol=[spiro_vol;
spiro_vol(length(spiro_vol))*ones(length(respi_vol)-length(spiro_vol),1)];
% end

if((length(respi_vol)>length(spiro_vol)) &&
(length(respi_vol)>length(pnt_vol)))
    pnt_vol=[pnt_vol; pnt_vol(length(pnt_vol))*ones(length(respi_vol)-
length(pnt_vol),1)];
    spiro_vol=[spiro_vol;
spiro_vol(length(spiro_vol))*ones(length(respi_vol)-length(spiro_vol),1)];
end

if((length(respi_vol)>length(spiro_vol)) &&
(length(respi_vol)<length(pnt_vol)))
    thorax_vol=[thorax_vol;
thorax_vol(length(thorax_vol))*ones(length(pnt_vol)-length(thorax_vol),1)];
    abdomen_vol=[abdomen_vol;

```

```

abdomen_vol(length(abdomen_vol))*ones(length(pnt_vol)-
length(abdomen_vol),1)];
    respi_vol=[respi_vol; respi_vol(length(respi_vol))*ones(length(pnt_vol)-
length(respi_vol),1)];
    spiro_vol=[spiro_vol; spiro_vol(length(spiro_vol))*ones(length(pnt_vol)-
length(spiro_vol),1)];
end

if((length(respi_vol)>length(pnt_vol)) &&
(length(respi_vol)<length(spiro_vol)))
    thorax_vol=[thorax_vol;
thorax_vol(length(thorax_vol))*ones(length(spiro_vol)-
length(thorax_vol),1)];
    abdomen_vol=[abdomen_vol;
abdomen_vol(length(abdomen_vol))*ones(length(spiro_vol)-
length(abdomen_vol),1)];
    respi_vol=[respi_vol;
respi_vol(length(respi_vol))*ones(length(spiro_vol)-length(respi_vol),1)];
    pnt_vol=[pnt_vol; pnt_vol(length(pnt_vol))*ones(length(spiro_vol)-
length(pnt_vol),1)];
end

if((length(pnt_vol)>length(spiro_vol)) &&
(length(pnt_vol)>length(respi_vol)))
    thorax_vol=[thorax_vol;
thorax_vol(length(thorax_vol))*ones(length(pnt_vol)-length(thorax_vol),1)];
    abdomen_vol=[abdomen_vol;
abdomen_vol(length(abdomen_vol))*ones(length(pnt_vol)-
length(abdomen_vol),1)];
    respi_vol=[respi_vol; respi_vol(length(respi_vol))*ones(length(pnt_vol)-
length(respi_vol),1)];
    spiro_vol=[spiro_vol; spiro_vol(length(spiro_vol))*ones(length(pnt_vol)-
length(spiro_vol),1)];
end

if((length(spiro_vol)>length(pnt_vol)) &&
(length(spiro_vol)>length(respi_vol)))
    thorax_vol=[thorax_vol;
thorax_vol(length(thorax_vol))*ones(length(spiro_vol)-
length(thorax_vol),1)];
    abdomen_vol=[abdomen_vol;
abdomen_vol(length(abdomen_vol))*ones(length(spiro_vol)-
length(abdomen_vol),1)];
    respi_vol=[respi_vol;
respi_vol(length(respi_vol))*ones(length(spiro_vol)-length(respi_vol),1)];
    pnt_vol=[pnt_vol; pnt_vol(length(pnt_vol))*ones(length(spiro_vol)-
length(pnt_vol),1)];
end

dati=[thorax_vol abdomen_vol respi_vol spiro_vol pnt_vol];
matldz=dati;
stringa=[string '.mat'];
eval(['save ',stringa,' matldz;']);

nomefile=[string 'index.txt'];
fp=fopen(nomefile,'w');
fprintf(fp,'variabile          colonna\n');
fprintf(fp,'THORAX          1\nABDOMEN          2\nRESPISENS
3\nSPIROMETER          4\nPNEUMOTAC          5\n');
fprintf(fp,'\n PARAMETRI USATI:\n\n Fc= 16.000 Hz for RespiSENS, Fc= 15.000

```

```

Hz for Spirometer and Pneumotacograph');
fclose(fp);
close all;
end

```

```

function [out1, out2]=Respisens_Calibration_Milano_Gennaio(string)

```

```

% ----- LOAD FILES -----

thorax_mxn=load([string '_tho.mxn']);
abdomen_mxn=load([string '_abd.mxn']);
respi_mxn=load([string '_res.mxn']);
spiro_mxn=load([string '_spi.mxn']);
pnt_mxn=load([string '_pnt.mxn']);
data=load([string '.mat']);
data=data.matldz;
thorax_vol=data(:,1);
abdomen_vol=data(:,2);
respi_vol=data(:,3);
spiro_vol=data(:,4);
pnt_vol=data(:,5);

% ----- VOLUMES COMPUTING -----

% Volume amplitude computing of Vinsp and exp of every trace, using as mxn
% for respisens only the respi.mxn, not taking into account any eventual
% paradoxycal movements, nor asynchronies.

Vinsp_thorax=[];
Vexp_thorax=[];
Vinsp_abdomen=[];
Vexp_abdomen=[];
Vinsp_respi=[];
Vexp_respi=[];
Vinsp_spiro=[];
Vexp_spiro=[];
Vinsp_pnt=[];
Vexp_pnt=[];
Vthorax=[];
Vabdomen=[];
Vrespi=[];
Vspiro=[];
Vpnt=[];

j=2;
for i=1:length(find(thorax_mxn(:,1)==1))

    if (thorax_mxn(j,1)==-1)
        j=j+1;
    end

    % creating separated vectors for inspiratory volumes and expiratory
    % volumes. Considering mxn file starting with a minimum and finishing
with
    % a minimum, even in interruptions.
    Vinsp_thorax=[Vinsp_thorax; thorax_vol(thorax_mxn(j,2))-
thorax_vol(thorax_mxn(j-1,2))];
    Vexp_thorax=[Vexp_thorax; thorax_vol(thorax_mxn(j,2))-

```

```

thorax_vol(thorax_mxn(j+1,2));

Vinsp_abdomen=[Vinsp_abdomen; abdomen_vol(abdomen_mxn(j,2))-
abdomen_vol(abdomen_mxn(j-1,2))];
Vexp_abdomen=[Vexp_abdomen; abdomen_vol(abdomen_mxn(j,2))-
abdomen_vol(abdomen_mxn(j+1,2))];

%Vinsp_respi=[Vinsp_respi; respi_vol(respi_mxn(j,2))-
respi_vol(respi_mxn(j-1,2))];
%Vexp_respi=[Vexp_respi; respi_vol(respi_mxn(j,2))-
respi_vol(respi_mxn(j+1,2))];

Vinsp_spiro=[Vinsp_spiro; spiro_vol(spiro_mxn(j,2))-
spiro_vol(spiro_mxn(j-1,2))];
Vexp_spiro=[Vexp_spiro; spiro_vol(spiro_mxn(j,2))-
spiro_vol(spiro_mxn(j+1,2))];

Vinsp_pnt=[Vinsp_pnt; pnt_vol(pnt_mxn(j,2))-pnt_vol(pnt_mxn(j-1,2))];
Vexp_pnt=[Vexp_pnt; pnt_vol(pnt_mxn(j,2))-pnt_vol(pnt_mxn(j+1,2))];

% creating one vector that contains insp and exp volumes respect
% mininum and max of total volume
Vthorax=[Vthorax; thorax_vol(respi_mxn(j,2))-thorax_vol(respi_mxn(j-
1,2))];
Vthorax=[Vthorax; thorax_vol(respi_mxn(j,2))-
thorax_vol(respi_mxn(j+1,2))];

Vabdomen=[Vabdomen; abdomen_vol(respi_mxn(j,2))-abdomen_vol(respi_mxn(j-
1,2))];
Vabdomen=[Vabdomen; abdomen_vol(respi_mxn(j,2))-
abdomen_vol(respi_mxn(j+1,2))];

%Vrespi=[Vrespi; respi_vol(respi_mxn(j,2))-respi_vol(respi_mxn(j-1,2))];
%Vrespi=[Vrespi; respi_vol(respi_mxn(j,2))-respi_vol(respi_mxn(j+1,2))];

Vspiro=[Vspiro; spiro_vol(spiro_mxn(j,2))-spiro_vol(spiro_mxn(j-1,2))];
Vspiro=[Vspiro; spiro_vol(spiro_mxn(j,2))-spiro_vol(spiro_mxn(j+1,2))];

Vpnt=[Vpnt; pnt_vol(pnt_mxn(j,2))-pnt_vol(pnt_mxn(j-1,2))];
Vpnt=[Vpnt; pnt_vol(pnt_mxn(j,2))-pnt_vol(pnt_mxn(j+1,2))];

j=j+2;

end

% ----- CALIBRATION -----

% per i dati fino a Fi015 seduto1!!!!!!!!!!!!!!
% % TEMPORANEO!! HO SCAMBIATO THORAX CON ABDOMINAL!!!
% % m and k computing
% [m_insp,k_insp] = LinearLeastSquare(Vinsp_spiro, Vinsp_abdomen,
Vinsp_thorax);
% [m_exp,k_exp] = LinearLeastSquare(Vexp_spiro, Vexp_abdomen, Vexp_thorax);
% [m,k] = LinearLeastSquare(Vspiro, Vabdomen, Vthorax);
%
% % calibration of volume traces
% respivol_inspcal = m_insp*(k_insp*(abdomen_vol) + thorax_vol);
% respivol_expcal = m_exp*(k_exp*(abdomen_vol) + thorax_vol);
% respivol_cal = m*(k*(abdomen_vol) + thorax_vol);
%

```

```

% % Tidal volume values calibration
% Vrespi_inspcal = m_insp*(k_insp*(Vabdomen) + Vthorax);
% Vrespi_expcal = m_exp*(k_exp*(Vabdomen) + Vthorax);
% Vrespi_cal = m*(k*(Vabdomen) + Vthorax);

%CALIBRATION with SPIROMETER
% m and k computing
[m_insp_spiro,k_insp_spiro] = LinearLeastSquare(Vinsp_spiro, Vinsp_thorax,
Vinsp_abdomen);
[m_exp_spiro,k_exp_spiro] = LinearLeastSquare(Vexp_spiro, Vexp_thorax,
Vexp_abdomen);
[m_spiro,k_spiro] = LinearLeastSquare(Vspiro, Vthorax, Vabdomen);

% calibration of volume traces
respivol_inspcal_spiro = m_insp_spiro*(k_insp_spiro*(thorax_vol) +
abdomen_vol);
respivol_expcal_spiro = m_exp_spiro*(k_exp_spiro*(thorax_vol) +
abdomen_vol);
respivol_cal_spiro = m_spiro*(k_spiro*(thorax_vol) + abdomen_vol);

% Tidal volume values calibration
Vrespi_inspcal_spiro = m_insp_spiro*(k_insp_spiro*(Vthorax) + Vabdomen);
Vrespi_expcal_spiro = m_exp_spiro*(k_exp_spiro*(Vthorax) + Vabdomen);
Vrespi_cal_spiro = m_spiro*(k_spiro*(Vthorax) + Vabdomen);

% mean and standard deviation computings
Vrespi_inspcal_spiro_mean = mean(Vrespi_inspcal_spiro);
Vrespi_inspcal_spiro_sd = std(Vrespi_inspcal_spiro);
Vrespi_expcal_spiro_mean = mean(Vrespi_expcal_spiro);
Vrespi_expcal_spiro_sd = std(Vrespi_expcal_spiro);
Vrespi_cal_spiro_mean = mean(Vrespi_cal_spiro);
Vrespi_cal_spiro_sd = std(Vrespi_cal_spiro);
Vspiro_mean = mean(Vspiro);
Vspiro_sd = std (Vspiro);

%CALIBRATION with PNEUMOTAC
% m and k computing
[m_insp_pnt,k_insp_pnt] = LinearLeastSquare(Vinsp_pnt, Vinsp_thorax,
Vinsp_abdomen);
[m_exp_pnt,k_exp_pnt] = LinearLeastSquare(Vexp_pnt, Vexp_thorax,
Vexp_abdomen);
[m_pnt,k_pnt] = LinearLeastSquare(Vpnt, Vthorax, Vabdomen);

% calibration of volume traces
respivol_inspcal_pnt = m_insp_pnt*(k_insp_pnt*(thorax_vol) + abdomen_vol);
respivol_expcal_pnt = m_exp_pnt*(k_exp_pnt*(thorax_vol) + abdomen_vol);
respivol_cal_pnt = m_pnt*(k_pnt*(thorax_vol) + abdomen_vol);

% Tidal volume values calibration
Vrespi_inspcal_pnt = m_insp_pnt*(k_insp_pnt*(Vthorax) + Vabdomen);
Vrespi_expcal_pnt = m_exp_pnt*(k_exp_pnt*(Vthorax) + Vabdomen);
Vrespi_cal_pnt = m_pnt*(k_pnt*(Vthorax) + Vabdomen);

% mean and standard deviation computings
Vrespi_inspcal_pnt_mean = mean(Vrespi_inspcal_pnt);
Vrespi_inspcal_pnt_sd = std(Vrespi_inspcal_pnt);
Vrespi_expcal_pnt_mean = mean(Vrespi_expcal_pnt);
Vrespi_expcal_pnt_sd = std(Vrespi_expcal_pnt);
Vrespi_cal_pnt_mean = mean(Vrespi_cal_pnt);
Vrespi_cal_pnt_sd = std(Vrespi_cal_pnt);

```

```
Vpnt_mean = mean(Vpnt);
Vpnt_sd = std (Vpnt);

% data saving
out1=[m_spiro k_spiro Vspiro_mean Vspiro_sd Vrespi_cal_spiro_mean
Vrespi_cal_spiro_sd];
out2=[m_pnt k_pnt Vpnt_mean Vpnt_sd Vrespi_cal_pnt_mean Vrespi_cal_pnt_sd];

% ----- PLOTTING -----

figure();

ax(1)=subplot(4,1,1);
grid on;
hold on;
plot(respivol_inspcal_spiro);
title('SPIROMETER')
ylabel('inspcal');

ax(2)=subplot(4,1,2);
grid on;
hold on;
plot(respivol_expcal_spiro);
ylabel('expcal');

ax(3)=subplot(4,1,3);
grid on;
hold on;
plot(respivol_cal_spiro);
ylabel('cal');

ax(4)=subplot(4,1,4);
grid on;
hold on;
plot(spiro_vol);
ylabel('spiro');

linkaxes (ax,'x');

figure();

ax(1)=subplot(4,1,1);
grid on;
hold on;
plot(respivol_inspcal_pnt);
title('PNEUMOTAC')
ylabel('inspcal');

ax(2)=subplot(4,1,2);
grid on;
hold on;
plot(respivol_expcal_pnt);
ylabel('expcal');

ax(3)=subplot(4,1,3);
grid on;
hold on;
plot(respivol_cal_pnt);
ylabel('cal');
```

```

ax(4)=subplot(4,1,4);
grid on;
hold on;
plot(pnt_vol);
ylabel('pnt');

linkaxes (ax,'x');

function [out1,out2]=Respisens_Test_Milano_Gennaio(string,call,cal2)

m_spiro=call(1);
k_spiro=call(2);
m_pnt=cal2(1);
k_pnt=cal2(2);

% thorax_mxn=load([string '_tho.mxn']);
% abdomen_mxn=load([string '_abd.mxn']);
respi_mxn=load([string '_res.mxn']);
spiro_mxn=load([string '_spi.mxn']);
pnt_mxn=load([string '_pnt.mxn']);
data=load([string '.mat']);
data=data.matldz;
thorax_vol=data(:,1);
abdomen_vol=data(:,2);
respi_vol=data(:,3);
spiro_vol=data(:,4);
pnt_vol=data(:,5);
% ----- VOLUMES COMPUTING -----

% Volume amplitude computing of Vinsp and exp of every trace, using as mxn
% for respisens only the respi.mxn, not taking into account any eventual
% paradoxycal movements, nor asynchories.

Vinsp_thorax=[];
Vexp_thorax=[];
Vinsp_abdomen=[];
Vexp_abdomen=[];
Vinsp_respi=[];
Vexp_respi=[];
Vinsp_spiro=[];
Vexp_spiro=[];
Vinsp_pnt=[];
Vexp_pnt=[];
Vthorax=[];
Vabdomen=[];
Vrespi=[];
Vspiro=[];
Vpnt=[];

j=2;
for i=1:length(find(respi_mxn(:,1)==1))

    if (respi_mxn(j,1)==-1)
        j=j+1;
    end

    % creating separated vectors for inspiratory volumes and expiratory
    % volumes. Considering mxn file starting with a minimum and finishing

```

```

with
    % a minimum, even in interruptions.
    % Vinsp_thorax=[Vinsp_thorax; thorax_vol(thorax_mxn(j,2))-
thorax_vol(thorax_mxn(j-1,2))];
    % Vexp_thorax=[Vexp_thorax; thorax_vol(thorax_mxn(j,2))-
thorax_vol(thorax_mxn(j+1,2))];
    %
    % Vinsp_abdomen=[Vinsp_abdomen; abdomen_vol(abdomen_mxn(j,2))-
abdomen_vol(abdomen_mxn(j-1,2))];
    % Vexp_abdomen=[Vexp_abdomen; abdomen_vol(abdomen_mxn(j,2))-
abdomen_vol(abdomen_mxn(j+1,2))];
    %
    % Vinsp_respi=[Vinsp_respi; respi_vol(respi_mxn(j,2))-
respi_vol(respi_mxn(j-1,2))];
    % Vexp_respi=[Vexp_respi; respi_vol(respi_mxn(j,2))-
respi_vol(respi_mxn(j+1,2))];
    %
    % Vinsp_spiro=[Vinsp_spiro; spiro_vol(spiro_mxn(j,2))-
spiro_vol(spiro_mxn(j-1,2))];
    % Vexp_spiro=[Vexp_spiro; spiro_vol(spiro_mxn(j,2))-
spiro_vol(spiro_mxn(j+1,2))];
    %
    % Vinsp_pnt=[Vinsp_pnt; pnt_vol(pnt_mxn(j,2))-pnt_vol(pnt_mxn(j-1,2))];
    % Vexp_pnt=[Vexp_pnt; pnt_vol(pnt_mxn(j,2))-pnt_vol(pnt_mxn(j+1,2))];
    %
    % creating one vector that contains insp and exp volumes respect
    % minimum and max of total volume
    Vthorax=[Vthorax; thorax_vol(respi_mxn(j,2))-thorax_vol(respi_mxn(j-
1,2))];
    Vthorax=[Vthorax; thorax_vol(respi_mxn(j,2))-
thorax_vol(respi_mxn(j+1,2))];

    Vabdomen=[Vabdomen; abdomen_vol(respi_mxn(j,2))-abdomen_vol(respi_mxn(j-
1,2))];
    Vabdomen=[Vabdomen; abdomen_vol(respi_mxn(j,2))-
abdomen_vol(respi_mxn(j+1,2))];

    %Vrespi=[Vrespi; respi_vol(respi_mxn(j,2))-respi_vol(respi_mxn(j-1,2))];
    %Vrespi=[Vrespi; respi_vol(respi_mxn(j,2))-respi_vol(respi_mxn(j+1,2))];

    Vspiro=[Vspiro; spiro_vol(spiro_mxn(j,2))-spiro_vol(spiro_mxn(j-1,2))];
    Vspiro=[Vspiro; spiro_vol(spiro_mxn(j,2))-spiro_vol(spiro_mxn(j+1,2))];

    Vpnt=[Vpnt; pnt_vol(pnt_mxn(j,2))-pnt_vol(pnt_mxn(j-1,2))];
    Vpnt=[Vpnt; pnt_vol(pnt_mxn(j,2))-pnt_vol(pnt_mxn(j+1,2))];

    j=j+2;

end

% ----- CALIBRATION -----

%SPIROMETER
respivol_cal_spiro = m_spiro*(k_spiro*(thorax_vol) + abdomen_vol);

% Tidal volume values calibration
Vrespi_cal_spiro = m_spiro*(k_spiro*(Vthorax) + Vabdomen);

% mean and standard deviation computings
Vrespi_cal_spiro_mean = mean(Vrespi_cal_spiro);

```

```

Vrespi_cal_spiro_sd = std(Vrespi_cal_spiro);
Vspiro_mean = mean(Vspiro);
Vspiro_sd = std (Vspiro);

% data saving
out1=[m_spiro k_spiro Vspiro_mean Vspiro_sd Vrespi_cal_spiro_mean
Vrespi_cal_spiro_sd];

%PNEUMOTAC
respivol_cal_pnt = m_pnt*(k_pnt*(thorax_vol) + abdomen_vol);

% Tidal volume values calibration
Vrespi_cal_pnt = m_pnt*(k_pnt*(Vthorax) + Vabdomen);

% mean and standard deviation computings
Vrespi_cal_pnt_mean = mean(Vrespi_cal_pnt);
Vrespi_cal_pnt_sd = std(Vrespi_cal_pnt);
Vpnt_mean = mean(Vpnt);
Vpnt_sd = std (Vpnt);

% data saving
out2=[m_pnt k_pnt Vpnt_mean Vpnt_sd Vrespi_cal_pnt_mean Vrespi_cal_pnt_sd];

end

```

2) Functions for the second method of calibration used in the second testing phase:

```

function []=Respisens_Calibration_PDA_Mi_Gennaio(string)

data=load([string '.mat']);
data=data.matldz;
thorax_vol=data(:,1);
abdomen_vol=data(:,2);
respi_vol=data(:,3);
spiro_vol=data(:,4);
pnt_vol=data(:,5);

figure();
title('Select initial and final points for spirometer test');
subplot(3,1,1);
grid on;
hold on;
plot(respi_vol);
title('RESPISENS');
subplot(3,1,2);
plot(spiro_vol);
hold on;
grid on;
title ('SPIROMETER');
subplot(3,1,3);
plot(pnt_vol);
hold on;

```

```
grid on;
title ('PNEUMOTAC');

H3=uicontrol('Style','togglebutton','String','Seleziona','Position',[450 7
60 20],'callback','uiresume');
zoom on;
uiwait;

% select breaths for RESPISENS
x_respi=[];
for i=1:2
    [x,y]=ginput(1);
    x_respi=[x_respi; round(x)];
    subplot(3,1,1);
    plot(x_respi,respi_vol(x_respi),'Or');
end

% select breaths for SPIROMETER
subplot(3,1,2);
x_spiro=[];
for i=1:2
    [x,y]=ginput(1);
    x_spiro=[x_spiro; round(x)];
    plot(x_spiro,spiro_vol(x_spiro),'Or');
end

% select breaths for PNEUMOTAC
subplot(3,1,3);
x_pnt=[];
for i=1:2
    [x,y]=ginput(1);
    x_pnt=[x_pnt; round(x)];
    plot(x_pnt,pnt_vol(x_pnt),'Or');
end

tho_track=thorax_vol(x_respi(1):x_respi(2));
abd_track=abdomen_vol(x_respi(1):x_respi(2));
res_track=respi_vol(x_respi(1):x_respi(2));
spi_track=spiro_vol(x_spiro(1):x_spiro(2));
pnt_track=pnt_vol(x_pnt(1):x_pnt(2));

figure();
subplot(3,1,1);
grid on;
plot(res_track);
title('respisens');
subplot(3,1,2);
plot(spi_track);
grid on;
title ('SPIROMETER');
subplot(3,1,3);
plot(pnt_track);
grid on;
title ('PNEUMOTAC');

spi_interp=interpft(spi_track, length(res_track));
pnt_interp=interpft(pnt_track, length(res_track));
```

```

figure();
subplot(3,1,1);
plot(res_track);
grid on;
title('respisens');
subplot(3,1,2);
plot(spi_interp);
grid on;
title ('SPIROMETER');
subplot(3,1,3);
plot(pnt_interp);
grid on;
title ('PNEUMOTAC');

% res_interp=interpft(res_track, length(spi_track));
%
% figure();
% subplot(3,1,1);
% grid on;
% plot(res_interp);
% title('respisens');
% subplot(3,1,2);
% plot(spi_track);
% grid on;
% title ('SPIROMETER');
% subplot(3,1,3);
% plot(pnt_track);
% grid on;
% title ('PNEUMOTAC');

close all

%%% CALIBRATION BY SPIROMETER
[m_spi,k_spi,q_spi]=LinearLeastSquare_PDA(spi_interp,tho_track,abd_track);

Vrespi_cal_spi = m_spi*(k_spi*(tho_track) + abd_track) + q_spi;

figure();
subplot(2,1,1);
plot(Vrespi_cal_spi);
grid on;
title('respisens Calibrato');
subplot(2,1,2);
plot(spi_interp);
grid on;
title ('SPIROMETER');

%%% CALIBRATION BY PNEUMOTAC
[m_pnt,k_pnt,q_pnt]=LinearLeastSquare_PDA(pnt_interp,tho_track,abd_track);

Vrespi_cal_pnt = m_pnt*(k_pnt*(tho_track) + abd_track) + q_pnt;

figure();
subplot(2,1,1);
plot(Vrespi_cal_pnt);
grid on;
title('respisens Calibrato');
subplot(2,1,2);
plot(pnt_interp);

```

```

grid on;
title ('PNEUMOTAC');

%%% SAVE DATA
data=[Vrespi_cal_spi spi_interp Vrespi_cal_pnt pnt_interp];
matldz=data;

stringa=[string '_PDA.mat'];
eval(['save ',stringa,' matldz;']);

nomefile=[string '_PDAindex.txt'];
fp=fopen(nomefile,'w');
fprintf(fp,'variabile          colonna\n');
fprintf(fp,'RESPISENS-SPI          1\nSPIROMETER
2\nRESPISENS-PNT          3\nPNEUMOTAC          4\n');
fprintf(fp,'\n PARAMETRI USATI:\n\n Fc= 16.000 Hz ');
fclose(fp);

[out]= [m_spi k_spi q_spi m_pnt k_pnt q_pnt];
par=out;
stringa2=[string '_par.mat'];
eval(['save ',stringa2,' par;']);

end

function []=Respisens_Test_PDA_Mi_Gennaio(string,out1,out2)

data=load([string '.mat']);
data=data.matldz;
thorax_vol=data(:,1);
abdomen_vol=data(:,2);
respi_vol=data(:,3);
spiro_vol=data(:,4);
pnt_vol=data(:,5);

m_spi=out1(1);
k_spi=out1(2);
q_spi=out1(3);

m_pnt=out2(1);
k_pnt=out2(2);
q_pnt=out2(3);

figure();
title('Select initial and final points for spirometer test');
subplot(3,1,1);
grid on;
hold on;
plot(respi_vol);
title('RESPISENS');
subplot(3,1,2);
plot(spiro_vol);
hold on;
grid on;
title ('SPIROMETER');
subplot(3,1,3);

```

```

plot(pnt_vol);
hold on;
grid on;
title ('PNEUMOTAC');

H3=uicontrol('Style','togglebutton','String','Seleziona','Position',[450 7
60 20],'callback','uiresume');
zoom on;
uiwait;

% select breaths for RESPISENS
x_respi=[];
for i=1:2
    [x,y]=ginput(1);
    x_respi=[x_respi; round(x)];
    subplot(3,1,1);
    plot(x_respi, respi_vol(x_respi), 'Or');
end

% select breaths for SPIROMETER
subplot(3,1,2);
x_spiro=[];
for i=1:2
    [x,y]=ginput(1);
    x_spiro=[x_spiro; round(x)];
    plot(x_spiro, spiro_vol(x_spiro), 'Or');
end

% select breaths for PNEUMOTAC
subplot(3,1,3);
x_pnt=[];
for i=1:2
    [x,y]=ginput(1);
    x_pnt=[x_pnt; round(x)];
    plot(x_pnt, pnt_vol(x_pnt), 'Or');
end

tho_track=thorax_vol(x_respi(1):x_respi(2));
abd_track=abdomen_vol(x_respi(1):x_respi(2));
res_track=respi_vol(x_respi(1):x_respi(2));
spi_track=spiro_vol(x_spiro(1):x_spiro(2));
pnt_track=pnt_vol(x_pnt(1):x_pnt(2));

figure();
subplot(3,1,1);
grid on;
plot(res_track);
title('respisens');
subplot(3,1,2);
plot(spi_track);
grid on;
title ('SPIROMETER');
subplot(3,1,3);
plot(pnt_track);
grid on;
title ('PNEUMOTAC');

spi_interp=interpft(spi_track, length(res_track));

```

```

pnt_interp=interpft(pnt_track, length(res_track));

figure();
subplot(3,1,1);
plot(res_track);
grid on;
title('respisens');
subplot(3,1,2);
plot(spi_interp);
grid on;
title ('SPIROMETER');
subplot(3,1,3);
plot(pnt_interp);
grid on;
title ('PNEUMOTAC');

close all

%%% CALIBRATION BY SPIROMETER

Vrespi_cal_spi = m_spi*(k_spi*(tho_track) + abd_track) + q_spi;

figure();
subplot(2,1,1);
plot(Vrespi_cal_spi);
grid on;
title('respisens Calibrato');
subplot(2,1,2);
plot(spi_interp);
grid on;
title ('SPIROMETER');

%%% CALIBRATION BY PNEUMOTAC

Vrespi_cal_pnt = m_pnt*(k_pnt*(tho_track) + abd_track) + q_pnt;

figure();
subplot(2,1,1);
plot(Vrespi_cal_pnt);
grid on;
title('respisens Calibrato');
subplot(2,1,2);
plot(pnt_interp);
grid on;
title ('PNEUMOTAC');

%%% SAVE DATA
data=[Vrespi_cal_spi spi_interp Vrespi_cal_pnt pnt_interp];
matldz=data;

stringa=[string '_PDA.mat'];
eval(['save ',stringa,' matldz;']);

nomefile=[string '_PDAindex.txt'];
fp=fopen(nomefile,'w');
fprintf(fp,'variabile          colonna\n');
fprintf(fp,'RESPISENS-SPI          1\nSPIROMETER
2\nRESPISENS-PNT          3\nPNEUMOTAC          4\n');

```

```
fprintf(fp, '\n PARAMETRI USATI:\n\n Fc= 16.000 Hz ');
fclose(fp);
```

```
[out]= [m_spi k_spi q_spi m_pnt k_pnt q_pnt];
par=out;
stringa2=[string '_par.mat'];
eval(['save ',stringa2,' par;']);
end
```

```
function [out1,out2]=Respisens_Volume_Computation_PDA_Mi_Gennaio(string)
```

```
data=load([string '_PDA.mat']);
data=data.matldz;
```

```
p = load([string '_par.mat']);
p = p.par;
m_spi=p(1);
k_spi=p(2);
q_spi=p(3);
m_pnt=p(4);
k_pnt=p(5);
q_pnt=p(6);
```

```
respi_spi_mxn=load([string '_PDA_rsp.mxn']);
spiro_mxn=load([string '_PDA_spi.mxn']);
respi_pnt_mxn=load([string '_PDA_rpn.mxn']);
pnt_mxn=load([string '_PDA_pnt.mxn']);
```

```
respi_spi_vol= data(:,1);
spiro_vol=data(:,2);
respi_pnt_vol= data(:,3);
pnt_vol=data(:,4);
```

```
Vrespi_spi=[];
Vspiro=[];
Vrespi_pnt=[];
Vpnt=[];
```

```
j=2;
for i=1:length(find(respi_spi_mxn(:,1)==-1))
```

```
    if (respi_spi_mxn(j,1)==-1)
        j=j+1;
    end
```

```
    Vrespi_spi=[Vrespi_spi; respi_spi_vol(respi_spi_mxn(j,2))-
respi_spi_vol(respi_spi_mxn(j-1,2))];
    Vrespi_spi=[Vrespi_spi; respi_spi_vol(respi_spi_mxn(j,2))-
respi_spi_vol(respi_spi_mxn(j+1,2))];
```

```
    Vspiro=[Vspiro; spiro_vol(spiro_mxn(j,2))-spiro_vol(spiro_mxn(j-1,2))];
    Vspiro=[Vspiro; spiro_vol(spiro_mxn(j,2))-spiro_vol(spiro_mxn(j+1,2))];
```

```
    Vrespi_pnt=[Vrespi_pnt; respi_pnt_vol(respi_pnt_mxn(j,2))-
respi_pnt_vol(respi_pnt_mxn(j-1,2))];
    Vrespi_pnt=[Vrespi_pnt; respi_pnt_vol(respi_pnt_mxn(j,2))-
respi_pnt_vol(respi_pnt_mxn(j+1,2))];
```

```
Vpnt=[Vpnt; pnt_vol(pnt_mxn(j,2))-pnt_vol(pnt_mxn(j-1,2))];
Vpnt=[Vpnt; pnt_vol(pnt_mxn(j,2))-pnt_vol(pnt_mxn(j+1,2))];

j=j+2;

end

%%% SPIROMETER
Vrespi_spi_mean = mean(Vrespi_spi);
Vrespi_spi_sd = std(Vrespi_spi);
Vspiro_mean = mean(Vspiro);
Vspiro_sd = std (Vspiro);

err = ((Vrespi_spi_mean - Vspiro_mean)/Vspiro_mean)*100;

out1 = [m_spi k_spi q_spi Vspiro_mean Vspiro_sd Vrespi_spi_mean
Vrespi_spi_sd err];

%%% PNEUMOTAC
Vrespi_pnt_mean = mean(Vrespi_pnt);
Vrespi_pnt_sd = std(Vrespi_pnt);
Vpnt_mean = mean(Vpnt);
Vpnt_sd =std (Vpnt);

err = ((Vrespi_pnt_mean - Vpnt_mean)/Vpnt_mean)*100;

out2 = [m_pnt k_pnt q_pnt Vpnt_mean Vpnt_sd Vrespi_pnt_mean Vrespi_pnt_sd
err];
end
```

Appendix C

1) Functions for the first method of calibration used in the validation on COPD patients:

```
function []=Respisens_track(string)

% ----- LOAD DATA -----
% RespiSENS:
[filename,pathname]=uigetfile('*.','Select file from RespiSENS
(_RESPISENS.txt)');
dataRespiS = load([pathname filename]);

Abdomen = dataRespiS(:,1);
Thorax = dataRespiS(:,2);

% SPIROMETER
[filename,pathname]=uigetfile('*.','Select file from SPIROMETER
(_SPIROMETER.txt)');
dataSpir = load([pathname filename]);

Spir_50Hz = dataSpir(:,2);
Spir_16Hz = resample(Spir_50Hz,15,50);
%Spir_16Hz = resample(Spir_50Hz,16,50);

% figure()
% ax(1)=subplot(3,1,1);
% plot(Thorax);
% ylabel('thorax');
% ax(2)=subplot(3,1,2);
% plot(Abdomen);
% ylabel('abdomen');
% ax(3)=subplot(3,1,3);
% plot(Spir_16Hz);
% ylabel('Spirometer');
%
% linkaxes(ax,'x');

% ----- FILTER DATA -----

%FIR, 6th order, 2 Hz cutoff, 16 Hz sample freq
% Wn=fcutoff/(fsamp/2)
%n1 = fir1(6, 0.25, 'low');
n1 = fir1(5, 0.5, 'low');
d1 = 1;

AbdomenFilt = -filtfilt(n1,d1,Abdomen);
ThoraxFilt = -filtfilt(n1,d1,Thorax);
SpirFilt= filtfilt(n1,d1,Spir_16Hz);
SpirVol=detrend((1/16)*cumsum(SpirFilt));

% ----- SELECT DATA -----

figure();
```

```

title('Select initial and final points for spirometer test');
ax(1)=subplot(3,1,1);
grid on;
hold on;
plot(ThoraxFilt);
ylabel('thorax');
ax(2)=subplot(3,1,2);
grid on;
hold on;
plot(AbdomenFilt);
ylabel('abdomen');
subplot(3,1,3);
plot(SpirVol);
hold on;
grid on;
title ('SPIROMETER');

linkaxes(ax,'x');

H3=uicontrol('Style','togglebutton','String','Seleziona','Position',[450 7
60 20],'callback','uiresume');
zoom on;
uiwait;

% select breaths for RESPISENS
x_respi=[];
for i=1:2
    [x,y]=ginput(1);
    x_respi=[x_respi; round(x)];
    subplot(3,1,1);
    plot(x_respi,ThoraxFilt(x_respi),'Or');
    subplot(3,1,2);
    plot(x_respi,AbdomenFilt(x_respi),'Or');
end

% select breaths for SPIROMETER
subplot(3,1,3);
x_spiro=[];
for i=1:2
    [x,y]=ginput(1);
    x_spiro=[x_spiro; round(x)];
    plot(x_spiro,SpirVol(x_spiro),'Or');
end

thorax_vol=ThoraxFilt(x_respi(1):x_respi(2));
abdomen_vol=AbdomenFilt(x_respi(1):x_respi(2));
respi_vol=thorax_vol+abdomen_vol;
spiro_vol=SpirVol(x_spiro(1):x_spiro(2));

close all
figure ();
ax(1)=subplot(2,1,1);
plot(respi_vol);
title('RESPISENS');
ax(2)=subplot(2,1,2);
plot(spiro_vol);
title('SPIROMETER');

H3=uicontrol('Style','togglebutton','String','Continue','Position',[450 7 60
20],'callback','uiresume');

```

```

uiwait;

% pareggio la lunghezza dei due vettori
if length(respi_vol)<length(spiro_vol)
    thorax_vol=[thorax_vol;
thorax_vol(length(thorax_vol))*ones(length(spiro_vol)-
length(thorax_vol),1)];
    abdomen_vol=[abdomen_vol;
abdomen_vol(length(abdomen_vol))*ones(length(spiro_vol)-
length(abdomen_vol),1)];
    respi_vol=[respi_vol;
respi_vol(length(respi_vol))*ones(length(spiro_vol)-length(respi_vol),1)];
else
    spiro_vol=[spiro_vol;
spiro_vol(length(spiro_vol))*ones(length(respi_vol)-length(spiro_vol),1)];
end

dati=[thorax_vol abdomen_vol respi_vol spiro_vol];
matldz=dati;
stringa=[string '.mat'];
eval(['save ',stringa,' matldz;']);

nomefile=[string 'index.txt'];
fp=fopen(nomefile,'w');
fprintf(fp,'variabile          colonna\n');
fprintf(fp,'THORAX              1\nABDOMEN              2\nRESPISENS
          3\nSPIROMETER              4\n');
fprintf(fp,'\n PARAMETRI USATI:\n\n Fc= 16.000 Hz ');
fclose(fp);

close all
end

function [out]=Respisens_Calibration(string)

% ----- LOAD FILES -----

thorax_mxn=load([string '_tho.mxn']);
abdomen_mxn=load([string '_abd.mxn']);
respi_mxn=load([string '_res.mxn']);
spiro_mxn=load([string '_spi.mxn']);
data=load([string '.mat']);
data=data.matldz;
thorax_vol=data(:,1);
abdomen_vol=data(:,2);
respi_vol=data(:,3);
spiro_vol=data(:,4);

% ----- VOLUMES COMPUTING -----

% Volume amplitude computing of Vinsp and exp of every trace, using as mxn
% for respisens only the respi.mxn, not taking into account any eventual
% paradoxycal movements, nor asynchronies.

Vinsp_thorax=[];
Vexp_thorax=[];
Vinsp_abdomen=[];
Vexp_abdomen=[];
Vinsp_respi=[];

```

```

Vexp_respi=[];
Vinsp_spiro=[];
Vexp_spiro=[];
Vthorax=[];
Vabdomen=[];
Vrespi=[];
Vspiro=[];

j=2;
for i=1:length(find(thorax_mxn(:,1)==1))

    if (thorax_mxn(j,1)==-1)
        j=j+1;
    end

    % creating separated vectors for inspiratory volumes and expiratory
    % volumes. Considering mxn file starting with a minimum and finishing
with
    % a minimum, even in interruptions.
    Vinsp_thorax=[Vinsp_thorax; thorax_vol(thorax_mxn(j,2))-
thorax_vol(thorax_mxn(j-1,2))];
    Vexp_thorax=[Vexp_thorax; thorax_vol(thorax_mxn(j,2))-
thorax_vol(thorax_mxn(j+1,2))];

    Vinsp_abdomen=[Vinsp_abdomen; abdomen_vol(abdomen_mxn(j,2))-
abdomen_vol(abdomen_mxn(j-1,2))];
    Vexp_abdomen=[Vexp_abdomen; abdomen_vol(abdomen_mxn(j,2))-
abdomen_vol(abdomen_mxn(j+1,2))];

    %Vinsp_respi=[Vinsp_respi; respi_vol(respi_mxn(j,2))-
respi_vol(respi_mxn(j-1,2))];
    %Vexp_respi=[Vexp_respi; respi_vol(respi_mxn(j,2))-
respi_vol(respi_mxn(j+1,2))];

    Vinsp_spiro=[Vinsp_spiro; spiro_vol(spiro_mxn(j,2))-
spiro_vol(spiro_mxn(j-1,2))];
    Vexp_spiro=[Vexp_spiro; spiro_vol(spiro_mxn(j,2))-
spiro_vol(spiro_mxn(j+1,2))];

    % creating one vector that contains insp and exp volumes respect
    % mininum and max of total volume
    Vthorax=[Vthorax; thorax_vol(respi_mxn(j,2))-thorax_vol(respi_mxn(j-
1,2))];
    Vthorax=[Vthorax; thorax_vol(respi_mxn(j,2))-
thorax_vol(respi_mxn(j+1,2))];

    Vabdomen=[Vabdomen; abdomen_vol(respi_mxn(j,2))-abdomen_vol(respi_mxn(j-
1,2))];
    Vabdomen=[Vabdomen; abdomen_vol(respi_mxn(j,2))-
abdomen_vol(respi_mxn(j+1,2))];

    Vrespi=[Vrespi; respi_vol(respi_mxn(j,2))-respi_vol(respi_mxn(j-1,2))];
    Vrespi=[Vrespi; respi_vol(respi_mxn(j,2))-respi_vol(respi_mxn(j+1,2))];

    Vspiro=[Vspiro; spiro_vol(spiro_mxn(j,2))-spiro_vol(spiro_mxn(j-1,2))];
    Vspiro=[Vspiro; spiro_vol(spiro_mxn(j,2))-spiro_vol(spiro_mxn(j+1,2))];

    j=j+2;

end

```

```

% ----- CALIBRATION -----

% per i dati fino a Fi015 seduto!!!!!!
% % TEMPORANEO!! HO SCAMBIATO THORAX CON ABDOMINAL!!!
% % m and k computing
% [m_insp,k_insp] = LinearLeastSquare(Vinsp_spiro, Vinsp_abdomen,
Vinsp_thorax);
% [m_exp,k_exp] = LinearLeastSquare(Vexp_spiro, Vexp_abdomen, Vexp_thorax);
% [m,k] = LinearLeastSquare(Vspiro, Vabdomen, Vthorax);
%
% % calibration of volume traces
% respivol_inspcal = m_insp*(k_insp*(abdomen_vol) + thorax_vol);
% respivol_expcal = m_exp*(k_exp*(abdomen_vol) + thorax_vol);
% respivol_cal = m*(k*(abdomen_vol) + thorax_vol);
%
% % Tidal volume values calibration
% Vrespi_inspcal = m_insp*(k_insp*(Vabdomen) + Vthorax);
% Vrespi_expcal = m_exp*(k_exp*(Vabdomen) + Vthorax);
% Vrespi_cal = m*(k*(Vabdomen) + Vthorax);

% m and k computing
[m_insp,k_insp] = LinearLeastSquare(Vinsp_spiro, Vinsp_thorax,
Vinsp_abdomen);
[m_exp,k_exp] = LinearLeastSquare(Vexp_spiro, Vexp_thorax, Vexp_abdomen);
[m,k] = LinearLeastSquare(Vspiro, Vthorax, Vabdomen);

% calibration of volume traces
respivol_inspcal = m_insp*(k_insp*(thorax_vol) + abdomen_vol);
respivol_expcal = m_exp*(k_exp*(thorax_vol) + abdomen_vol);
respivol_cal = m*(k*(thorax_vol) + abdomen_vol);

% Tidal volume values calibration
Vrespi_inspcal = m_insp*(k_insp*(Vthorax) + Vabdomen);
Vrespi_expcal = m_exp*(k_exp*(Vthorax) + Vabdomen);
Vrespi_cal = m*(k*(Vthorax) + Vabdomen);

% mean and standard deviation computings
Vrespi_inspcal_mean = mean(Vrespi_inspcal);
Vrespi_inspcal_sd = std(Vrespi_inspcal);
Vrespi_expcal_mean = mean(Vrespi_expcal);
Vrespi_expcal_sd = std(Vrespi_expcal);
Vrespi_cal_mean = mean(Vrespi_cal);
Vrespi_cal_sd = std(Vrespi_cal);
Vspiro_mean = mean(Vspiro);
Vspiro_sd = std (Vspiro);

% data saving
out=[m k Vspiro_mean Vspiro_sd Vrespi_cal_mean Vrespi_cal_sd];

% ----- PLOTTING -----

figure();

ax(1)=subplot(4,1,1);
grid on;
hold on;
plot(respivol_inspcal);
ylabel('inspcal');

ax(2)=subplot(4,1,2);

```

```

grid on;
hold on;
plot(respivol_expcal);
ylabel('expcal');

ax(3)=subplot(4,1,3);
grid on;
hold on;
plot(respivol_cal);
ylabel('cal');

ax(4)=subplot(4,1,4);
grid on;
hold on;
plot(spiro_vol);
ylabel('spiro');

linkaxes (ax,'x');

function [out]=Respisens_Test(string,cal)

m=cal(1);
k=cal(2);

thorax_mxn=load([string '_tho.mxn']);
abdomen_mxn=load([string '_abd.mxn']);
respi_mxn=load([string '_res.mxn']);
spiro_mxn=load([string '_spi.mxn']);
data=load([string '.mat']);
data=data.matldz;
thorax_vol=data(:,1);
abdomen_vol=data(:,2);
respi_vol=data(:,3);
spiro_vol=data(:,4);

% ----- VOLUMES COMPUTING -----

% Volume amplitude computing of Vinsp and exp of every trace, using as mxn
% for respisens only the respi.mxn, not taking into account any eventual
% paradoxycal movements, nor asynchronies.

Vinsp_thorax=[];
Vexp_thorax=[];
Vinsp_abdomen=[];
Vexp_abdomen=[];
Vinsp_respi=[];
Vexp_respi=[];
Vinsp_spiro=[];
Vexp_spiro=[];
Vthorax=[];
Vabdomen=[];
Vrespi=[];
Vspiro=[];

j=2;
for i=1:length(find(thorax_mxn(:,1)==1))

    if (thorax_mxn(j,1)==-1)
        j=j+1;

```

```

end

% creating separated vectors for inspiratory volumes and expiratory
% volumes. Considering mxn file starting with a minimum and finishing
with
% a minimum, even in interruptions.
Vinsp_thorax=[Vinsp_thorax; thorax_vol(thorax_mxn(j,2))-
thorax_vol(thorax_mxn(j-1,2))];
Vexp_thorax=[Vexp_thorax; thorax_vol(thorax_mxn(j,2))-
thorax_vol(thorax_mxn(j+1,2))];

Vinsp_abdomen=[Vinsp_abdomen; abdomen_vol(abdomen_mxn(j,2))-
abdomen_vol(abdomen_mxn(j-1,2))];
Vexp_abdomen=[Vexp_abdomen; abdomen_vol(abdomen_mxn(j,2))-
abdomen_vol(abdomen_mxn(j+1,2))];

%Vinsp_respi=[Vinsp_respi; respi_vol(respi_mxn(j,2))-
respi_vol(respi_mxn(j-1,2))];
%Vexp_respi=[Vexp_respi; respi_vol(respi_mxn(j,2))-
respi_vol(respi_mxn(j+1,2))];

Vinsp_spiro=[Vinsp_spiro; spiro_vol(spiro_mxn(j,2))-
spiro_vol(spiro_mxn(j-1,2))];
Vexp_spiro=[Vexp_spiro; spiro_vol(spiro_mxn(j,2))-
spiro_vol(spiro_mxn(j+1,2))];

% creating one vector that contains insp and exp volumes respect
% minimum and max of total volume
Vthorax=[Vthorax; thorax_vol(respi_mxn(j,2))-thorax_vol(respi_mxn(j-
1,2))];
Vthorax=[Vthorax; thorax_vol(respi_mxn(j,2))-
thorax_vol(respi_mxn(j+1,2))];

Vabdomen=[Vabdomen; abdomen_vol(respi_mxn(j,2))-abdomen_vol(respi_mxn(j-
1,2))];
Vabdomen=[Vabdomen; abdomen_vol(respi_mxn(j,2))-
abdomen_vol(respi_mxn(j+1,2))];

Vrespi=[Vrespi; respi_vol(respi_mxn(j,2))-respi_vol(respi_mxn(j-1,2))];
Vrespi=[Vrespi; respi_vol(respi_mxn(j,2))-respi_vol(respi_mxn(j+1,2))];

Vspiro=[Vspiro; spiro_vol(spiro_mxn(j,2))-spiro_vol(spiro_mxn(j-1,2))];
Vspiro=[Vspiro; spiro_vol(spiro_mxn(j,2))-spiro_vol(spiro_mxn(j+1,2))];

j=j+2;

end

% ----- CALIBRATION -----

respivol_cal = m*(k*(thorax_vol) + abdomen_vol);

% Tidal volume values calibration
Vrespi_cal = m*(k*(Vthorax) + Vabdomen);

% mean and standard deviation computings
Vrespi_cal_mean = mean(Vrespi_cal);
Vrespi_cal_sd = std(Vrespi_cal);
Vspiro_mean = mean(Vspiro);
Vspiro_sd = std (Vspiro);

```

```
% data saving
out=[m k Vspiro_mean Vspiro_sd Vrespi_cal_mean Vrespi_cal_sd];
```

2) Functions for the second method of calibration used in the validation on COPD patients:

```
function []=Respisens_Calibration_PDA(string)

data=load([string '.mat']);
data=data.matldz;
thorax_vol=data(:,1);
abdomen_vol=data(:,2);
respi_vol=data(:,3);
spiro_vol=data(:,4);

figure();
title('Select initial and final points for spirometer test');
subplot(2,1,1);
grid on;
hold on;
plot(respi_vol);
title('RESPISENS');
subplot(2,1,2);
plot(spiro_vol);
hold on;
grid on;
title ('SPIROMETER');

H3=uicontrol('Style','togglebutton','String','Seleziona','Position',[450 7
60 20],'callback','uiresume');
zoom on;
uiwait;

% select breaths for RESPISENS
x_respi=[];
for i=1:2
    [x,y]=ginput(1);
    x_respi=[x_respi; round(x)];
    subplot(2,1,1);
    plot(x_respi,respi_vol(x_respi),'Or');
end

% select breaths for SPIROMETER
subplot(2,1,2);
x_spiro=[];
for i=1:2
    [x,y]=ginput(1);
    x_spiro=[x_spiro; round(x)];
    plot(x_spiro,spiro_vol(x_spiro),'Or');
end

tho_track=thorax_vol(x_respi(1):x_respi(2));
abd_track=abdomen_vol(x_respi(1):x_respi(2));
res_track=respi_vol(x_respi(1):x_respi(2));
spi_track=spiro_vol(x_spiro(1):x_spiro(2));
```

```

figure();
subplot(2,1,1);
grid on;
plot(res_track);
title('respisens');
subplot(2,1,2);
plot(spi_track);
grid on;
title ('SPIROMETER');

spi_interp=interpft(spi_track, length(res_track));

figure();
subplot(2,1,1);
plot(res_track);
grid on;
title('respisens');
subplot(2,1,2);
plot(spi_interp);
grid on;
title ('SPIROMETER');

[m,k,q]=LinearLeastSquare_PDA(spi_interp,tho_track,abd_track);

Vrespi_cal = m*(k*(tho_track) + abd_track) + q;

close all

figure();
subplot(2,1,1);
plot(Vrespi_cal);
grid on;
title('respisens Calibrato');
subplot(2,1,2);
plot(spi_interp);
grid on;
title ('SPIROMETER');

data=[Vrespi_cal spi_interp];
matldz=data;

stringa=[string '_PDA.mat'];
eval(['save ',stringa,' matldz;']);

nomefile=[string '_PDAindex.txt'];
fp=fopen(nomefile,'w');
fprintf(fp,'variabile          colonna\n');
fprintf(fp,'RESPISENS          1\nSPIROMETER          2\n');
fprintf(fp,'\n PARAMETRI USATI:\n\n Fc= 16.000 Hz ');
fclose(fp);

[out]= [m k q];
par=out;
stringa2=[string '_par.mat'];
eval(['save ',stringa2,' par;']);

end

function []=Respisens_Test_PDA(string,out)

```

```

data=load([string '.mat']);
data=data.matldz;
thorax_vol=data(:,1);
abdomen_vol=data(:,2);
respi_vol=data(:,3);
spiro_vol=data(:,4);

m=out(1);
k=out(2);
q=out(3);

figure();
title('Select initial and final points for spirometer test');
subplot(2,1,1);
grid on;
hold on;
plot(respi_vol);
title('RESPISENS');
subplot(2,1,2);
plot(spiro_vol);
hold on;
grid on;
title ('SPIROMETER');

H3=uicontrol('Style','togglebutton','String','Seleziona','Position',[450 7
60 20],'callback','uiresume');
zoom on;
uiwait;

% select breaths for RESPISENS
x_respi=[];
for i=1:2
    [x,y]=ginput(1);
    x_respi=[x_respi; round(x)];
    subplot(2,1,1);
    plot(x_respi,respi_vol(x_respi),'Or');
end

% select breaths for SPIROMETER
subplot(2,1,2);
x_spiro=[];
for i=1:2
    [x,y]=ginput(1);
    x_spiro=[x_spiro; round(x)];
    plot(x_spiro,spiro_vol(x_spiro),'Or');
end

tho_track=thorax_vol(x_respi(1):x_respi(2));
abd_track=abdomen_vol(x_respi(1):x_respi(2));
res_track=respi_vol(x_respi(1):x_respi(2));
spi_track=spiro_vol(x_spiro(1):x_spiro(2));

figure();
subplot(2,1,1);
grid on;
plot(res_track);
title('respisens');
subplot(2,1,2);
plot(spi_track);

```

```

grid on;
title ('SPIROMETER');

spi_interp=interpft(spi_track, length(res_track));

figure();
subplot(2,1,1);
plot(res_track);
grid on;
title('respisens');
subplot(2,1,2);
plot(spi_interp);
grid on;
title ('SPIROMETER');

Vrespi_cal = m*(k*(tho_track) + abd_track) + q;

close all

figure();
subplot(2,1,1);
plot(Vrespi_cal);
grid on;
title('respisens Calibrato');
subplot(2,1,2);
plot(spi_interp);
grid on;
title ('SPIROMETER');

data=[Vrespi_cal spi_interp];
matldz=data;

stringa=[string '_PDA.mat'];
eval(['save ',stringa,' matldz;']);

nomefile=[string '_PDAindex.txt'];
fp=fopen(nomefile,'w');
fprintf(fp,'variabile          colonna\n');
fprintf(fp,'RESPISENS          1\nSPIROMETER          2\n');
fprintf(fp,'\n PARAMETRI USATI:\n\n Fc= 16.000 Hz ');
fclose(fp);

[out2]= [m k q];
par=out2;
stringa2=[string '_par.mat'];
eval(['save ',stringa2,' par;']);

end

function [out]=Respisens_Volume_Computation_PDA(string)

data=load([string '_PDA.mat']);
data=data.matldz;

p = load([string '_par.mat']);
p = p.par;
m=p(1);
k=p(2);

```

```
q=p(3);

respi_mxn=load([string '_PDA_res.mxn']);
spiro_mxn=load([string '_PDA_spi.mxn']);
respi_vol= data(:,1);
spiro_vol=data(:,2);
Vrespi=[];
Vspiro=[];

j=2;
for i=1:length(find(respi_mxn(:,1)==1))

    if (respi_mxn(j,1)==-1)
        j=j+1;
    end

    Vrespi=[Vrespi; respi_vol(respi_mxn(j,2))-respi_vol(respi_mxn(j-1,2))];
    Vrespi=[Vrespi; respi_vol(respi_mxn(j,2))-respi_vol(respi_mxn(j+1,2))];

    Vspiro=[Vspiro; spiro_vol(spiro_mxn(j,2))-spiro_vol(spiro_mxn(j-1,2))];
    Vspiro=[Vspiro; spiro_vol(spiro_mxn(j,2))-spiro_vol(spiro_mxn(j+1,2))];

    j=j+2;

end

Vrespi_mean = mean(Vrespi);
Vrespi_sd = std(Vrespi);
Vspiro_mean = mean(Vspiro);
Vspiro_sd = std (Vspiro);

err = ((Vrespi_mean - Vspiro_mean)/Vspiro_mean)*100;

out = [m k q Vspiro_mean Vspiro_sd Vrespi_mean Vrespi_sd err];

end
```

References

1. Guyton A.C., Hall J.E.: *Textbook of Medical Physiology*, Eleventh Edition, 2006.
2. Kleinstreuer C., Zhang Z.: *Annual Review Fluid Mechanics*, 42:301-334, 2010.
3. West J.B., *Respiratory physiology – the essentials*, 7th edition, 2004.
4. Aliverti A., Brusasco V., Macklem P.T., Pedotti A. *Mechanics of Breathing: Pathophysiology, Diagnosis and Treatment*, 2002.
5. West J.B., *Pulmonary Pathophysiology – the essentials*, 5th edition, 1998.
6. Hanania N.A., Sharafkhaneh A. *COPD: A Guide to Diagnosis and Clinical Management*, 2010.
7. Celli B.R., MacNee W., and committee members. Standards for the diagnosis and treatment of patient with COPD: a summary of the ATS/ERS position paper. *Eur Respir J*, 23: 932-946, 2004.
8. Lucangelo U., Pelosi P., Zin W. A., Aliverti A., *Respiratory System and Artificial Ventilation*, 2008.
9. Aliverti A., Dellacà R., Pelosi P., Chiumello D., Gattinoni L., Pedotti A. Compartmental Analysis of Breathing in the Supine and Prone Positions by Optoelectronic Plethysmography. *Annals of Biomedical Engineering*, 29: 60-70, 2001
10. Stocks J., Sly P.D., Tepper R.S., Morgan W.J, editors. *Infant respiratory function testing*. 1st edition. New York: *John Wiley & Sons, Inc.*; 1996
11. Murphy D. J., Renninger J. P., Schramek D. Respiratory inductive plethysmography as a method for measuring ventilatory parameters in conscious, non-restrained dogs. *Journal of Pharmacological and Toxicological Methods* 62: 47–53, 2010.
12. Brown K., Aun C., Jackson E., Mackersie A., Hatch D., Stocks J. Validation of respiratory inductive plethysmography using the Qualitative Diagnostic Calibration method in anaesthetized infants. *Eur Respir J*, 12: 935–943, 1998.

-
13. Ekkebus S.P. Thesis: Telemonitoring services for home care ventilators, using web services.
 14. Vitacca M., Bianchi L., Guerra A., Fracchia C., Spavanello A., Balbi B., Scalvini S. Tele-assistance in chronic respiratory failure patients: a randomized clinical trial. *Eur Respir J*, 33: 411-418, 2009.
 15. Jaana M., Paré G., Sicotte C. Home Telemonitoring for Respiratory Conditions: A Systematic Review. *The American Journal of Managed Care*. Vol.15, NO.5: 313-320, 2009.
 16. Bolton C.E., Waters C.S., Peirce S., Elwyn G. Insufficient evidence of benefit: a systematic review of home telemonitoring for COPD. *Journal Evaluation Clinical Practice*. 16 Sep 2010.
 - a.
 17. Lawo M., Papadopoulos A., Ciancitto F., Dellaca' R.L., Munaro G., Rosso R. An Open, Ubiquitous and Adaptive Chronic Disease Management Platform. International Workshop on Wearable, Micro, and Nano Technologies for Personalized Health, pHealth, will take place in Oslo, Norway, 24-26 June 2009.
 18. D7.1: CHRONIOUS Wearable
 19. Strömberg T. Error analysis of a natural breathing calibration method for respiratory inductive plethysmography. *Medical & Biological Engineering & Computing* 2001, 39: 310-314.
 20. D7.2: CHRONIOUS Patient Sensing Framework
 21. Sackner M. A., Watson H., Belsito A. S., Feinerman D., Suarez M., Gonzalez G., Bizousky F., Krieger B. Calibration of respiratory inductive plethysmography during natural breathing. *Journal of Applied Physiology January*, Vol. 66, NO. 1: 410-420, 1989.
 22. Scirba F., Criner G.J., Lee S. M., Mohsenifar Z., Shade D., Slivka W., Wise R.A. Six-Minute Walk Distance in Chronic Obstructive Pulmonary Disease. *Am J Respir Crit Care Med*, Vol. 167:1522–1527, 2003.
-

Ringraziamenti

Desidero innanzitutto ringraziare il Professor Giovanni Sparacino per la disponibilità e per il supporto fornitomi durante lo sviluppo del lavoro della tesi.

Un sincero grazie anche all'Ing. Roberto Rosso per avermi dato la possibilità di svolgere lo stage in Tesan e di partecipare attivamente al progetto Chronious. Un grazie ai colleghi in Tesan, in particolare a Giulia, Grazia e Piero che mi hanno dato consigli indispensabili, mi hanno coinvolta nel progetto, nei pranzi e nelle pause caffè.

Ringrazio il Professor Raffaele Dellacà e l'Ing. Leonardo Govoni per gli insegnamenti, i consigli, il supporto e per tutto il tempo che hanno messo a disposizione per seguire il mio lavoro di tesi. Inoltre, voglio ringraziare tutto il Dipartimento di Bioingegneria - TBMLAB, Politecnico di Milano. Grazie per l'aiuto, per il supporto, per le scrivanie rubate e per i tanti dolci mangiati insieme.

Grazie, alla mia famiglia, che ha creduto in me, mi ha sostenuto, incoraggiato, ma soprattutto mi ha sopportato per tutti questi anni. Grazie ad Elisa e Francesco per avermi ospitato a Firenze e avermi aspettato svegli fino a tardi.

Grazie a tutti i miei compagni di Università, in particolare a Isabella, Chiara G., Chiara B., Chiara Z., Francesca, Claudia, Arianna, Filippo e Andrea per l'amicizia, la compagnia, il sostegno e per le tante avventure.

Un grazie di cuore alle mie più care amiche Roberta, Monica, Sara, Sara e Jessica per avermi sostenuta, incoraggiata e perché so che posso sempre contare sul vostro appoggio.

Infine, un grazie speciale ad Andrea per avermi ospitato e sopportato a Milano anche quando ero intrattabile, per l'aiuto che non mi ha fatto mancare e per aver amorevolmente tollerato tutte le ansie e paure di questo periodo.